Pedaling and Braking Forces and Their Effect on Suspension Performance

by:

Kathleen Kramer
Nik Goodell
Cesar Giron

Mechanical Engineering Department
California Polytechnic State University
San Luis Obispo
March 17, 2012

Statement of Disclaimer

Since this project is a result of a class assignment, it has been graded and accepted as fulfillment of the course requirements. Acceptance does not imply technical accuracy or reliability. Any use of information in this report is done at the risk of the user. These risks may include catastrophic failure of the device or infringement of patent or copyright laws. California Polytechnic State University at San Luis Obispo and its staff cannot be held liable for any use or misuse of the project.

Table of Contents

Table of Contents

Table of Contents

Table of Contents

Table of Figures

Table of Figures

Table of Figures

Abstract

The goal of this project is to produce a quantifiable relationship between pedaling and braking forces and suspension behavior. The test results will serve as a benchmark, against which other suspension designs can be compared in an objective, numerical manner. This report details the work completed towards determining this relationship and is primarily focused on design development of the data acquisition system and analysis of braking forces, pedaling forces and suspension response. A 2011 Specialized Stumpjumper FSR Expert Evo was used as the development platform. The system will be used to measure various rear suspension designs for comparison.

1. Project Introduction

Modern mountain bikes have evolved to the point where full suspension is the norm, rather than a novelty, and is considered essential for most serious racing. Bicycle suspension has unique requirements when compared to other suspension systems, such as a motorcycle suspension. The efficiency of energy transfer between the pedals and rear tire is crucial, and the suspension feedback through the pedals plays a large role in the efficiency. The ideal rear suspension would completely isolate the rear wheel movement from pedaling and braking forces while remaining completely active to maintain traction with the ground. Many designs claim to isolate braking and pedaling forces from suspension action. Theoretical calculations and computer models can support these claims, and rider feedback, as well as racing victories, can indicate the effectiveness of the design from a subjective standpoint. Currently, there is no quantitative, empirical data to show the effectiveness of each design. Objective, empirical data that quantifies the relationship between suspension behavior and braking and pedaling forces is needed. Experimental data, collected in a real-world environment, will allow rear suspension designs to be further refined and optimized.

1.1 Sponsor

The sponsor wishes to remain anonymous, per the Non-Disclosure Agreement.

1.2 Objectives

The goal of this project is to quantify the relationship between pedaling forces, braking forces, and rear suspension behavior. Accurate, verifiable results will be produced using scientifically sound testing procedures. Our sponsor requires reliable results so that the collected data can be used to investigate claims about the performance of various suspension designs. The sponsor also requires that a relationship is quantified between suspension response and pedaling forces and suspension response and braking action.

The highest priority requirement, determined by the Quality Function Design (QFD) chart (Appendix A), is collecting data at a sufficient sample rate (not reflected in the QFD chart) to accurately capture the physical response of the measured parameters. Since the bulk of the project involves data collection and analysis, the resolution of instruments and data acquisition systems is a key factor in

capturing useful data. Another important requirement is to keep variables consistent within, and between, each test run in order to obtain comparable data. The next highest priority is to be able collect data through a wireless and mobile system, which makes field testing possible. The weight and set up time requirements were determined to have the lowest priority, but they are still very important requirements to consider for testing.

A list of specifications for the project was developed from the requirements listed in the QFD chart (Appendix A). The specification with the highest risk assessment is the weight of the test apparatus. If the test apparatus adds too much weight to the bike, the bike may function differently than it would without the test apparatus on it. This will affect the reliability of the test results because when a customer is using the bike it will function normally, without the added test apparatus weight. Another specification with a high risk assessment is the amount of time it will take to set up the equipment for testing. To maintain tight control of variables within one specific test, the test should be completed in as little time as possible. The longer the test takes the more likely it is that the weather, or other test conditions, will change, which could affect the trails and rider performance.

Other variables that could affect the test results include:

1. Rider Variables - rider weight, riding position on the bike, riding style, and pedaling style
2. Bike Variables - Tire pressure, tread condition, shock pressure, shock damping, gear selected during tests
3. Trail Variables - Dusty/muddy, wind, hard/soft pack
4. Instrumentation Setup - Alignment of the string potentiometer and other sensors

2. Background

2.1 Suspension Independence

2.1.1 Single Pivot

In its most basic form, a mountain bike's rear suspension is comprised of a swing arm, which is usually the chain stay, as shown below. The chain stay locates the rear axle and is pivoted about a single joint. This design is called a single pivot and has the benefits of being simple and robust. Often, the pivot point is located near the bottom bracket to minimize the moment that the chain forces will create about the pivot.

$$M_{chain} = F_{chain} r_{\perp}$$

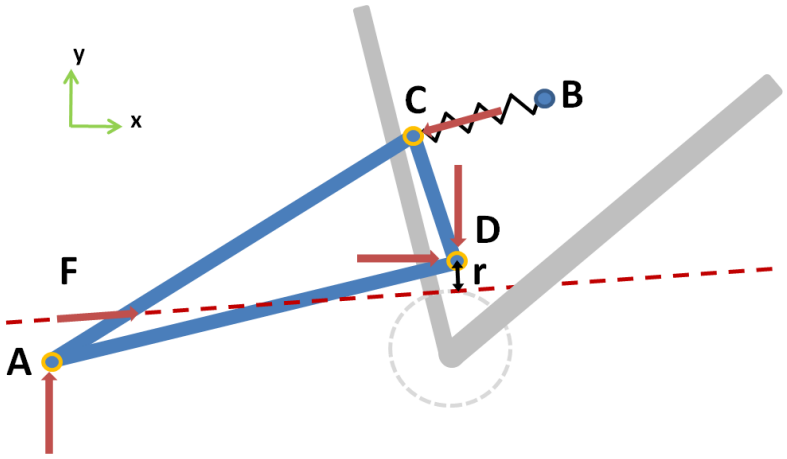

Figure 2.1- The most basic single pivot design has a rear axle at A which travels a circular path around the pivot at D. The chain force, F, creates a moment about the pivot point.

The vector of the chain force (F), applied to the swing arm through the rear sprocket, hub and axle (A), can induce a rotation about the pivot (D). The moment applied to the swing arm is dependent on the magnitude of the chain force (F) and the perpendicular distance (r) from the force vector to the pivot. The force applied to the swing arm from the spring (C) counteracts the moment, acting about the pivot at a perpendicular distance L_{CD}. The only time the chain force is not creating a moment is when the force vector is acting directly through the pivot point; the greater the perpendicular distance (r) the greater the moment. The moment causes the rear axle (A) to pivot about D, changing the distance between the rear sprocket and the front chainring. When the rider reduces force on the pedal the suspension returns to its original equilibrium point until the next pedal stroke causes it to pivot again. This repeated fluctuation in suspension position due to pedaling forces is called pedal bob and can be felt while riding.

Similarly, terrain-induced changes in suspension position will cause a change in chain length, which will change the chain tension if the rider is pedaling. This fluctuation in pedal force is called pedal feedback. In addition, braking forces will also cause a moment about the pivot.

2.1.2 Four Bar Linkage

A four bar linkage system, as shown in **Figure 2.2**, allows for a non-circular rear axle path.

The Specialized FSR (Future Shock Rear) rear suspension incorporates a four bar linkage to control the rear wheel path. A key feature of the FSR design is the "Horst link". As seen in the **Figure 2.2**, the Horst link technology affects the chain stay linkage, with the front pivot located directly behind the bottom bracket and the rear pivot located directly in front of the rear axle. This design creates an instant center of the rear axle path that, theoretically, isolates pedaling forces and braking forces from the suspension travel.

Figure 2.2 -The Specialized FSR suspension and Horst Link. The chain stay pivots are located with the red arrows.

There have been no testing methods which attempt to quantify the relationship between pedaling forces, braking forces and suspension travel in an empirical test. Likewise, there is no established specification for a testing procedure to compare to. The primary tools used today to determine the effectiveness of a suspension design are computer simulations and subjective rider feedback. To measure the relationship empirically, a data acquisition system using a variety of sensors, such as potentiometers to measure suspension position, strain gauges positioned to identify braking forces and pedaling forces, and inductive proximity sensors to measure wheel speed or crank speed, will be used.

2.2 Suspension Dynamics

At a fundamental level the relationship being measured is a cause and effect, where the cause is an applied force or moment and the effect is the movement of the rear wheel. The effect on the movement of the rear wheel could be either an increase or decrease in movement. An ideal suspension would have zero induced movement during pedaling and braking, but it also would not restrict movement so the suspension is still able to react to the terrain and keep the wheel in contact with the ground.

In the case of pedaling, the cause and effect relationship is between the rear wheel and the chain force. A simplified model of this is shown in **Figure 2.3** and the fundamental kinematics behind the relationship in **Figure 2.4**.

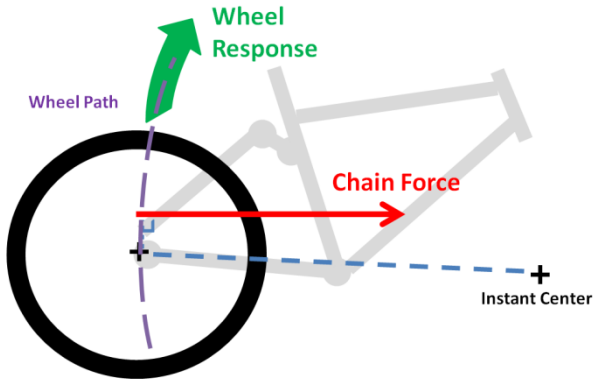

Figure 2.3 - The primary reactions acting at the rear suspension during pedaling.

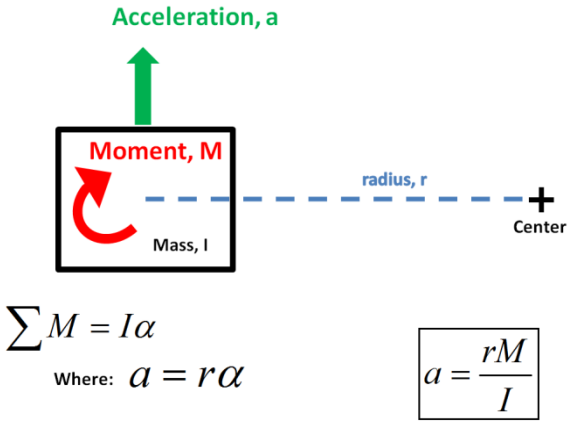

Figure 2.4 - A simplified kinematic model of the system in Figure 2.3

If a relationship is to be found between an applied moment caused by the chain force acting about the instant center and the rear wheel dynamics, it will be found by comparing the chain tension and the rear wheel acceleration. Chain tension is a function of the torque, shown above, and the chainring radius. Acceleration is readily distilled from the position data using the five point forward difference method, discussed later.

Assuming the wheel and suspension to have a constant moment of inertia and radius at every given point of compression, the acceleration of the rear wheel is only a function of the moment applied about the instant center. The moment is a function of the chain tension vector and the perpendicular distance from the instant center. Since the vector direction is determined by which sprocket the chain is on the end result is that there are 2 control variables, one independent variable and one dependent variable. The gear and the suspension position must be known, and then the suspension acceleration can be plotted as a function of pedaling torque. This is a well defined repeatable test that can be used to define a relationship between pedaling forces and suspension action. A perfectly independent system will exhibit zero acceleration of the rear wheel, regardless of input force applied at the pedals. This occurs when the chain tension vector creates no moment about the instant center. Since the chain force is a non-zero value this can only happen when the vector points directly through the instant center, making the perpendicular distance zero.

For braking, the relationship being analyzed is the effect that braking torque applied on the rear suspension has on suspension movement. The simplified model in **Figure 2.5** shows this, and the equivalent kinematic model is shown in **Figure 2.6**.

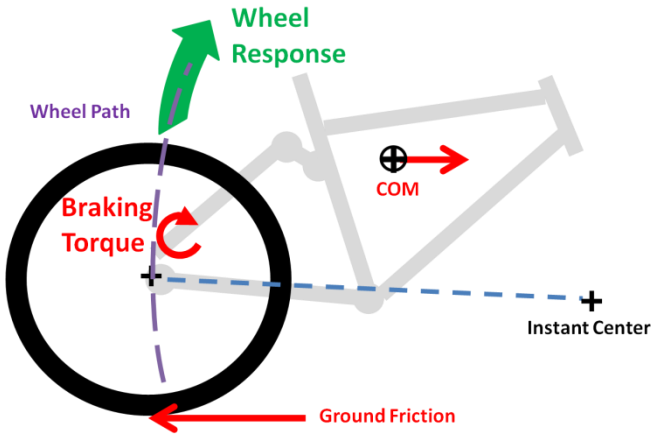

Figure 2.5 - The primary reactions at the rear suspension during braking.

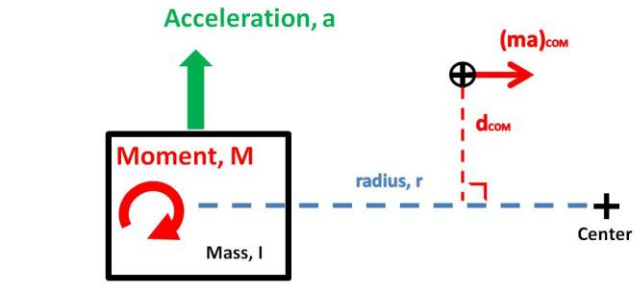

$$\sum M = I\alpha$$

Where: $a = r\alpha$

$$a = \frac{rM + d_{COM}(ma)_{COM}}{I}$$

Figure 2.6 - A Fundamental kinematics for the braking force-suspension movement relationship.

As a bike slows down during braking the center of mass of the bike and rider decelerates, causing a rotational moment on the bike that influences the behavior of the suspension. The deceleration of the center of mass should cause a moment which transfers weight to the front wheel and away from the rear wheel. As weight is removed from the rear wheel it should allow the suspension to decompress. This variable is difficult to accurately measure, isolate or control. Tests will need to be specifically designed to attempt to remove the dynamic effects of the decelerating mass and isolate the relationship between braking forces and suspension response.

2.3 Potentiometers

The position of the suspension linkage relative to the frame has one degree of freedom; therefore, by measuring the position of any one link the position of every other link and pivot can be determined. A three-wire potentiometer is the simplest way to measure position and will output a voltage that is directly proportional to position. Potentiometers are used to measure suspension position in data acquisition systems used on motorcycles, automobiles, and bicycles. The type of potentiometer and mounting location can be varied. Linear potentiometers are easy to set up and are the first choice for measuring linear displacement. When there are pivots, such as those found on any rear suspension swing arm, suspension travel can be measured with a rotary potentiometer. Previous data acquisition systems used on mountain bikes have used rotary potentiometers at pivots, linear potentiometers (**Figure 2.7**), and string potentiometers to measure linear displacement (Specialized).

Figure 2.7 - Data Acquisition system on a K9 bike with a linear potentiometer measuring the shock position. (Levy)

String potentiometers use a cable that is wrapped around a spring-loaded spool. The linear displacement of the cable causes a rotary displacement of the spool, which is measured by the same means as a rotary potentiometer. The string potentiometer changes resistance in a linear fashion for a change in length of the cable. String potentiometers can have many advantages, including: high resolution, flexible mounting options, flexible cable routing options, small package size, and little moving mass. A variety of options are available depending on what features are required.

Previous tests by the sponsor's test engineers have been run using a string potentiometer with a 4-inch stroke and a 60G return acceleration. A high return rate is necessary to ensure the potentiometer will correctly track the suspension as it is compressed. These potentiometers cost approximately $500 and are susceptible to damage if not handled carefully. The reason they were chosen by the sponsor's engineers is that they allow a very flexible mounting platform and can be run around pulleys for setups where frame geometry makes a linear potentiometer difficult or impossible to mount beside the shock. The cable and spool add negligible moving mass to the suspension system and will not have any effect on the dynamic response of the system.

Figure 2.8 - String potentiometer which allows flexible mounting configurations (Celesco)

2.4 Inductive Proximity Sensors

A typical bicycle wheel speed sensor is a Hall Effect sensor, which is triggered once per wheel revolution by a magnet attached to a spoke. The sensor determines an average wheel speed over the last wheel revolution from the period of the triggering events. This is suitable for standard use, but for more accurate measurement of wheel speed, which can measure changes in wheel speed throughout a revolution, a system with higher resolution is needed.

Rather than adding multiple, evenly spaced magnets to the spokes, an inductive proximity sensor can be used to monitor the changing magnetic field of components that already exist on the wheel, such as the brake rotor or the rotor spokes. An inductive proximity sensor works similarly to a Hall Effect sensor. An inductive proximity sensor uses a coil and oscillator to generate a magnetic field near the tip of the sensor. When a metallic object is brought close to the sensor it will cause a damping of the oscillation amplitude. The rise or fall of the oscillation is sensed by a threshold circuit that toggles the output of the sensor.

The wheel speed can be calculated from the frequency of the proximity sensor and the known number of triggering events per revolution. Proximity sensors and Hall Effect sensors are commonly used to measure speed on shafts, pulleys and rotors in industry, and have been used in automotive for functions such as timing ignition pulses in distributors and measuring crankshaft speed. The triggering point is dependent on the type of material being sensed. **Table 2.1** shows the sensitivity of the inductive proximity sensor to different metals. (Fargo Controls) The brake rotors are a stainless steel.

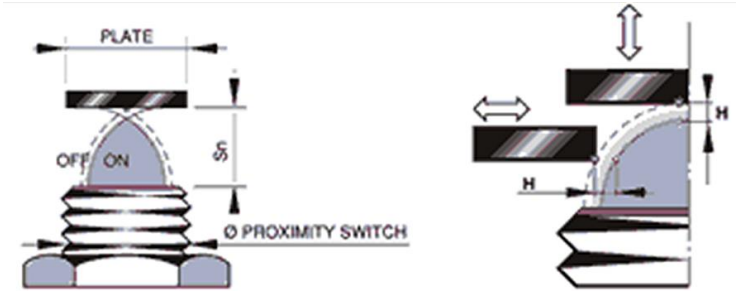

Figure 2.9 – Schematic of a Hall Effect sensor (image from Fargo Controls)

Table 2.1 –Sensitivity when different metals are present. Sn=operating distance, shown in ***Figure 2.9****.*

Fe37 (Iron)	1 x Sn
Stainless steel	0.9 x Sn
Brass - Bronze	0.5 x Sn
Aluminum	0.4 x Sn
Copper	0.4 x Sn

The proximity sensor is capable of triggering thousands of times per second, so it will easily measure the wheel speed. For a 48-slot rotor, the triggering frequency during testing is expected be no greater than 300 Hz.

Figure 2.10 - Inductive Proximity sensor which will be triggered off of the rotor (Fargo Controls)

Figure 2.11 - Rear brake rotor that can be used to measure rotational speed with greater resolution than standard methods (rotor is an Avid G3CS)

2.5 Frequency to Voltage Converter

The inductive proximity sensor outputs a square wave signal with a frequency that is relative to the wheel speed. This frequency will be in the range 0-300Hz. This signal could be recorded directly, as an analog voltage, and post processed to determine the frequency and wheel speed. It could also be converted to an analog voltage, relative to the frequency, and the voltage could be recorded by the data acquisition board. In order to record the square wave and ensure that the rise and fall points are recorded with reasonable accuracy, the DAQ would have to sample at a frequency at least 10 times the frequency of the signal, or 3000Hz. If the frequency is first converted to a voltage by the frequency-to-voltage converter, then the sample rate is determined by the response of the wheel speed signal, which will be maximized when the wheel is locked up during heavy braking (wheel speed declines almost instantly to 0 mph). The sampling rate will need to be high enough to capture lock up behavior.

2.6 Power Meters

Power meters are available for bikes in crankset and rear hub versions. Both operate on the same principal, as well as the same wireless protocol. The power meter uses multiple strain gauges, positioned to measure torque as it is transferred through the hub or crank. Two manufacturers, SRM and Quarq, dominate the market for crankset power meters and one manufacturer, CycleOps, holds the market for rear hub power meters. Since power meters are more commonly used for road bike applications, the market for mountain bike-compatible products is much smaller. The bikes that will be tested for this project are all designed to use double chainring cranksets and 10-speed rear cassettes, rather than the traditional triple chainring cranksets with 9-speed cassettes. This is an emerging trend and the first double chainring crankset power meters became available in March 2011 from SRM; Quarq does not offer any power meters for mountain bike applications. From SRM, there are two crankset power meters that would work; one made by Cannondale and one made by FSA (Full Speed Ahead) (**Figure 2.12**).

Figure 2.12 -Double chainring crank power meter by SRM. (SRM)

For a rear hub power meter there is one option offered by CycleOps; an all mountain hub with 135mm axle spacing and a 160mm non-interchangeable rotor. (**Figure 2.13**)

Figure 2.13 -CycleOps PowerTap rear hub power meter for mountain bikes. (CycleOps)

2.7 ANT Wireless

All of the power meters send data with ANT+ wireless protocol, which is used by various bike computers, heart rate monitors and GPS units. The platform is open to developers, and hardware and development resources are readily available at http://www.thisisant.com. To develop an interface to receive messages from the power meter, an ANT+ antenna and a microcontroller (MCU) is needed. The signal can be processed in the MCU and output to the data acquisition unit on one of the digital output ports. The ANT+ chip is available mounted on an 8051 mixed signal MCU. A developer's kit, the real expense, is needed to program the chip. ANT+ is a controlled protocol with full documentation available to developers. This document (**Table 2.2**) outlines the proper channel configuration to receive information from the power meter, the power meter output, what units the signal is in, and formulas to calculate parameters such as power and cadence or wheel speed. This documentation and much more is available on the ANT website.

Table 2.2 -ANT channel configuration for receiving bike power sensor information

Parameter	Value	Comment
Channel Type	Receive (0x00)	Power sensors require bi-directional communication for calibration and manufacturing purposes.
Network Key	ANT+ Managed Network Key	The ANT+ Managed Network key is governed by the ANT+ Managed Network licensing agreement.
RF Channel Frequency	57	RF Channel 57 (2457 MHz) is used for the ANT+ bike power sensor.
Transmission Type	0 for pairing	The transmission type must be set to 0 for a pairing search. Once the transmission type is learned, the receiving device should remember the type for future searches. To be future compatible, any returned transmission type is valid. Future versions of this spec may allow additional bits to be set in the transmission type.
Device Type	11 (0x0B)	The device type shall be set to 11 (0x0B) when searching to pair to an ANT+ bike power sensor. Please see the ANT Message Protocol and Usage document for more details.
Device Number	1-65535 0 for searching	The transmitting sensor contains a 16-bit number which uniquely identifies its transmissions. Set the Device Number parameter to zero to allow wildcard matching. Once the device number is learned, the receiving device should remember the number for future searches. Please see the ANT Message Protocol and Usage document for more details.
Channel Period	8182 counts	Data is transmitted from the bike power sensor every 8182/32768 seconds (approximately 4.00 Hz)
Search Timeout	(Default = 30 seconds)	The default search timeout is set to 30 seconds in the receiver. This timeout is implementation specific and can be set by the designer to the appropriate value for the system.

2.8 Strain Gauges

2.8.1 Theory

Strain gauges are used to measure the strain of a material, which can be related to the stress and loading on the part through the material properties. The fundamental operation of a strain gauge is based on electrical conductance. A strain gauge is composed of a series of fine wire passes, as shown in **Figure 2.14**, and adheres to the material being strained.

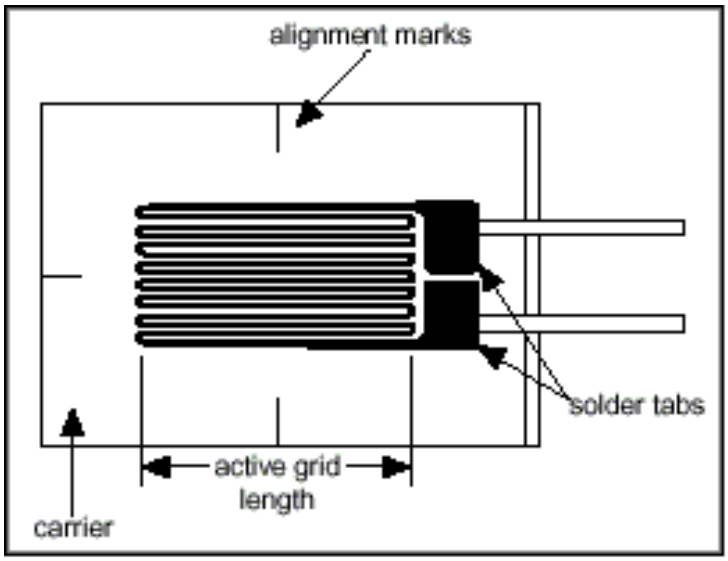

Figure 2.14 - Basic strain gauge design includes multiple passes of fine wire which will change resistance as it is stretched or compressed.

As the material is strained the strain gauge wire is either extended or compressed and it's cross sectional area will change, changing the resistance of the wire. The change in resistance is measured and can be used to determine strain in the part. Some design considerations are the effects of temperature and off-axis strain. A transverse strain will result in a certain change in resistance of the gauge, which can interfere with the parameters of interest. Likewise, changes in temperature will cause expansion of the material and will result in a residual strain, which will skew any readings.

2.8.2 Full Wheatstone Bridge

Though strain can be measured with a single strain gauge, it is often beneficial to configure multiple strain gauges to measure the same strain. A Wheatstone bridge, shown in **Figure 2.15**, enables several strain gauges to be connected in such a way that they will compensate for temperature effects and allow for cancellation of undesired strains. Arranging the gauges in a Wheatstone bridge allows for the change in resistance to be measured from a baseline voltage of 0V, instead of some initial supply voltage. Since the change in resistance will typically result in a voltage change on the order of mV, it is much easier to measure a voltage change when it is referenced from 0V. Multiple gauges can also have the benefit of increasing sensitivity when they are properly configured.

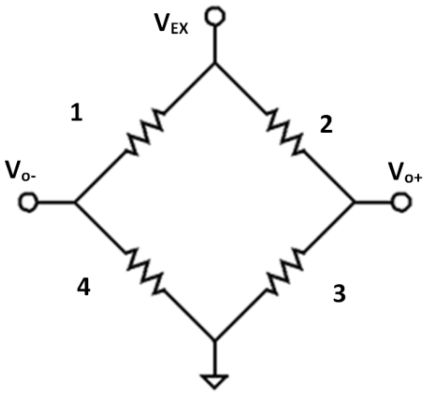

Figure 2.15 - Full Wheatstone Bridge with strain gauges at 1, 2, 3 and 4.

If the gauges are arranged in such a way that a strain on the material causes a tensile strain at 1 and 3 and a compressive strain at 2 and 4, then the sensitivity will be 4 times that of a single gauge. Since a change in temperature will have an equal effect on each gauge, the net voltage read across the output wires V_{O+} and V_{O-} will be zero, eliminating temperature effects.

2.9 DAQ - Collection Systems

The most important component in the data collection system is the data acquisition unit, commonly called a DAQ, DA unit, or data logger. The system must be capable of receiving data from multiple sources at appropriate sample rates and storing the data series for later analysis. There are several factors that are important in a DAQ:

1. Sampling frequency
2. Number of channels
3. Storage capacity
4. Size/Weight
5. Ease of use
6. Cost

The sampling frequency has a large effect on the accuracy of the measured data and all calculations which are based on that data. Acceleration is determined from position data by taking two derivatives. If the position data is not smooth, the slope of it, and its first derivative, will not be smooth and poor acceleration data will result. In addition, higher sample rates allow for more refined noise filtering techniques. This produces data that can be analyzed to produce meaningful relationships. Based on previous suspension testing done by the manufacturer, engineers recommend using a minimum sample rate of 1000 Hz. If accelerometers are used, a sample rate of at least 2000 Hz is recommended. Preliminary tests were performed to identify the necessary sampling rate (results discussed in **Section 3.11**).

The DAQ must be able to monitor every sensor in the system simultaneously and independently. DAQs are available in configurations with anywhere from one to several hundred channels. For the purposes of this project a 4 channel DAQ would be sufficient. The number of channels and the sample rate determines the number of bytes of data recorded per second. The length of the trial run will determine the required storage capacity; increasing the sample rate or the number of channels increases the storage capacity requirements. Since the unit will be used to record data during field tests, the size and weight of the DAQ are important considerations. Ideally, the unit would be mounted on the bike, secured to the frame within the main triangle. Alternately, it could be carried by the rider in a back pack.

3. System Design

3.1 Specifications

- The DAQ channels measuring wheel speed must be capable of accurately measuring speeds up to 30 mph, or signal frequencies of 350 Hz on a common rotor.
- The suspension movement accuracy should be within 1mm at the shock.
- Sensing equipment must not exceed 800 grams of un-sprung weight

3.2 Brake Strain Bridge

3.2.1 Theory

When the brakes are applied the brake pads apply a friction force on the rotor to create a moment which opposes tire rotation. The force is transferred to the caliper, which is mounted to the brake adapter, and finally to the left seat stay. This force is transferred through two bolts and the mating surface of the adapter. It is capable of transferring forces and moments in all three directions. Because the force is from the applied friction force from the spinning rotor the net force applied to the brake adapter is modeled as a tangential force in the rotor plane. Since the lever arm distance from the rotor to the seat stay is small the forces and moment in that direction are assumed small and neglected for design purposes. This leaves only in-plane forces and moment.

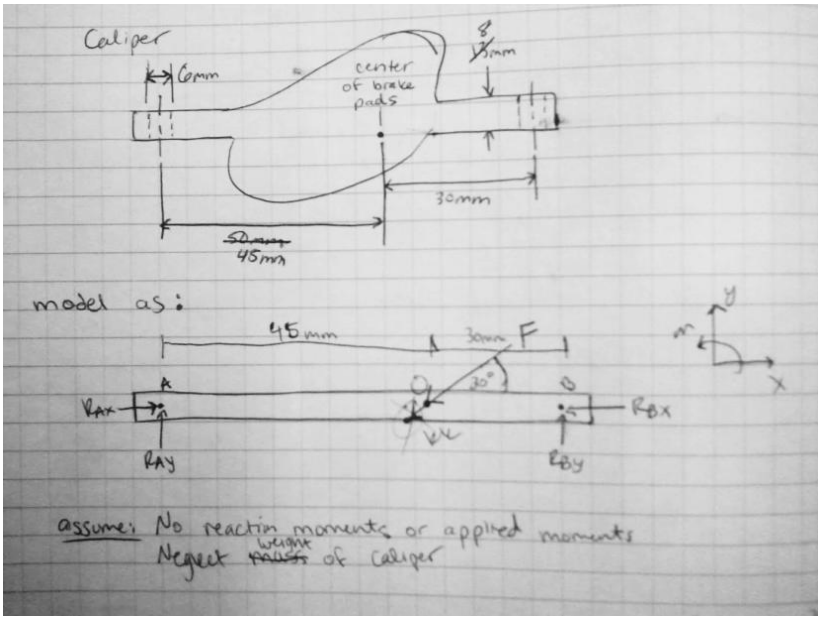

Figure 3.1 –The forces and moment on the caliper were estimated to determine the forces applied to the brake adapter

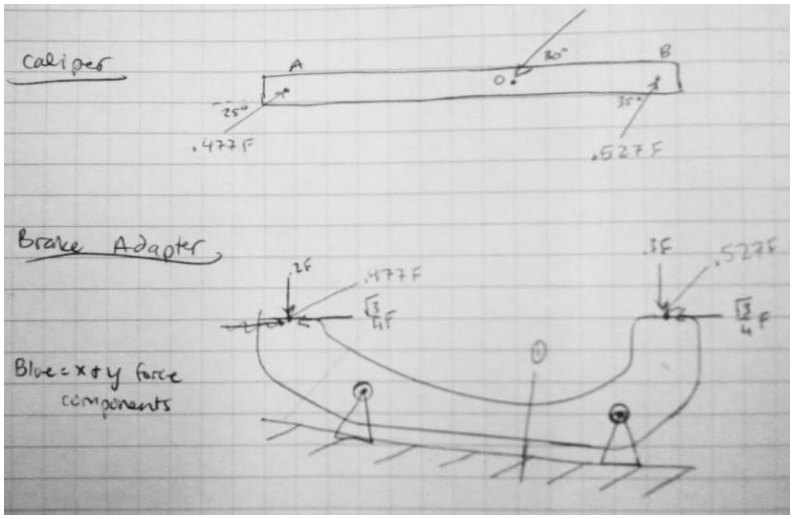

Figure 3.2 - A simplified model helped estimate the loading on the brake adapter

3.2.2 Solid Works Analysis

Using the simplified model, the force vectors acting on the brake adapter were predicted and used to develop loading conditions for a solid model in SolidWorks (**Figure 3.3**).

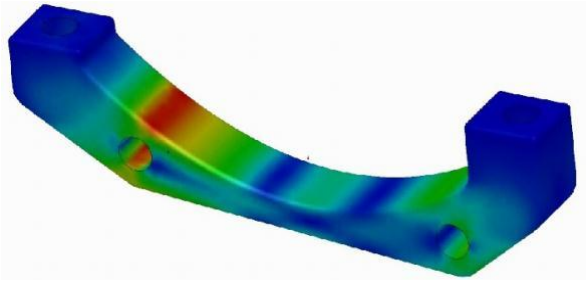

Figure 3.3 -Strain distribution on the unmodified brake adapter. Red areas signify largest values of strain.

The original part was modified in SolidWorks to create a high strain region away from the bolt hole where the part could be gauged more easily. By reducing the cross-sectional area of the brake adapter, a stress concentration was created closer to the center of the adapter (**Figure 3.4**)

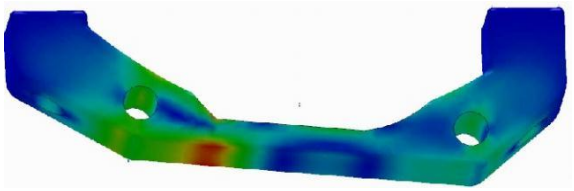

Figure 3.4 -Strain distribution on the modified brake adapter

3.2.3 Wheatstone bridge design

A full Wheatstone bridge was designed to eliminate temperature and tensile strain effects. The gauges are located as shown in **Figure 3.5** on the top and bottom on the brake adapter, which will be subjected to bending with the two bolt holes acting as pivots.

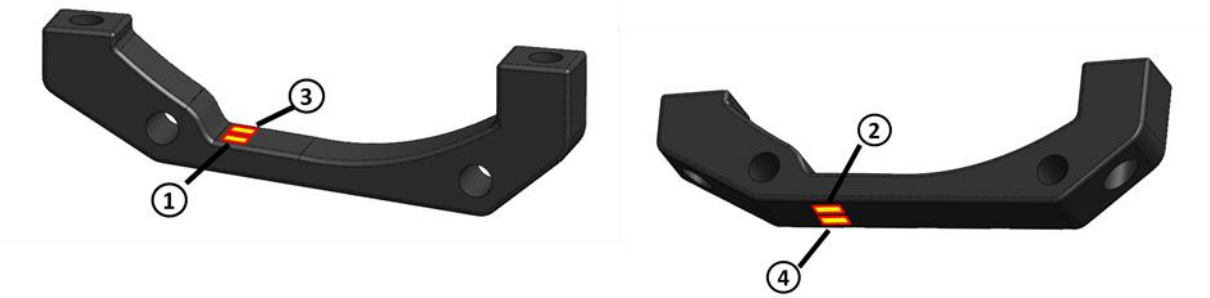

Figure 3.5 - Strain gauge locations on the brake adapter.

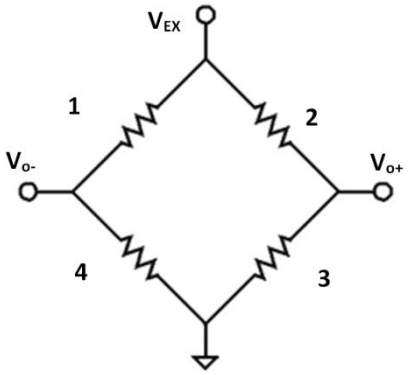

Figure 3.6 - Full Wheatstone bridge for the brake adapter. Temperature and axial strain effects are cancelled by the bridge configuration.

3.2.4 Strain Gauge Selection

Strain gauges with 120 Ω resistance were selected based on the location of the high strain area and the magnitude of the expected strain. Vishay EA-06-240LZ-120/E gauges were chosen for the Wheatstone bridge (see Datasheet Strain Gauges in Appendix D). These gauges were the right size and estimated to be the correct gauge factor to measure the brake adapter strain.

3.3 String Potentiometer

The Celesco MT3A-9L-14-10K-C string potentiometer, shown in **Figure 2.8,** was selected based on recommendations from sponsor engineers (see datasheet String Potentiometer in Appendix D). To make it as universal as possible, the string potentiometer was mounted to an aluminum adapter plate which could be bolted to a standard water bottle cage location.

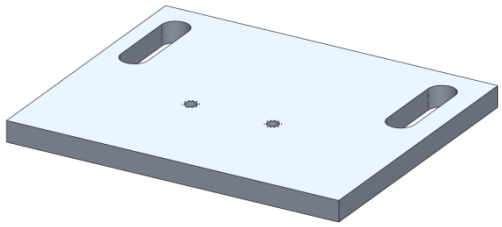

Figure 3.7 - Aluminum adapter plate allows the string potentiometer to be mounted to any bike frame that has standard water bottle cage mounting holes.

Starting from the location of the string potentiometer, the cable is routed around a pulley that will serve to align the string to measure the displacement of a suspension linkage or pivot. The pulley is mounted to an adjustable bracket which allows for proper alignment of the cable.

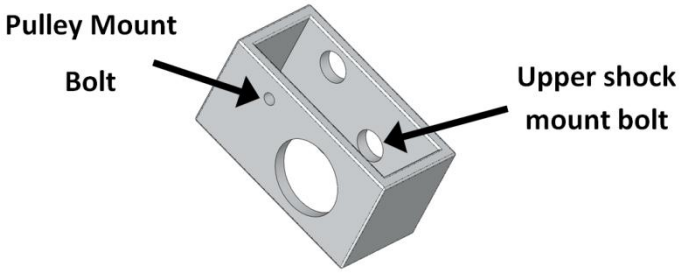

Figure 3.8 – The pulley mount is designed to allow for cable alignment adjustment.

The cable end is clamped securely to a suspension member so the cable will extend and retract as the suspension moves. Based on the geometry of each bike, the change in cable length can be related to the position of various points on the suspension. Not all points will have a linear relationship with the shock compression through the suspension travel.

3.4 Crank Strain Bridge

3.4.1 Theory

Ultimately, it was determined that the ANT+ power meter setup could not be configured to deliver the pedal force data at the frequency required for comparison to suspension data. To collect pedal force data another strain bridge was designed which would measure pedaling forces transferred through the spider to the chain while cancelling or neglecting all other forces. **Figure 3.9** Shows the forces of interest in red and all other forces applied by the bottom bracket and the pedal in blue.

Figure 3.9 - The crank shown with the primary forces acting on it.

The force at the chainring is applied by the chain, which can only support a tensile force. Therefore the forces applied to the chainring in the y and z directions are zero. This means that at the connection to the spider the chainring will apply a reaction which is directly proportional to the chain tension, which is the acting force on the suspension members. Since the bottom bracket can apply reactions to counteract all but the moment about z the sum of the moments gives:

$$\sum M_z = F_{chain} * r_{chainring} - F_{pedal} * r_{crankarm} = 0$$

$$F_{chain} * r_{chainring} = F_{pedal} * r_{crankarm}$$

These equal and opposite moments apply a bending moment to the arms of the spider. By placing strain gauges at the high strain area on the spider arms the strain, relative to the chain force, can be measured. **Figure 3.10** shows the loads of interest and the expected location of the strain gauges. The moment can be applied from either crank arm since they are splined together and both pass the moment to the spider in the same manner.

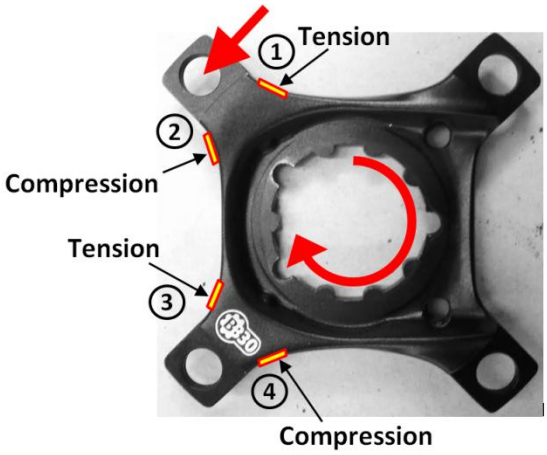

Figure 3.10 - The crank spider with loads applied from the crank arm and the chain tension.

Torque from the left crank arm will apply force to the spider in the same manner, acting through the hub of the right crank arm. The pedal forces from both the left and right crank arms can be captured by gauging the spider. (**Figure 3.11**)

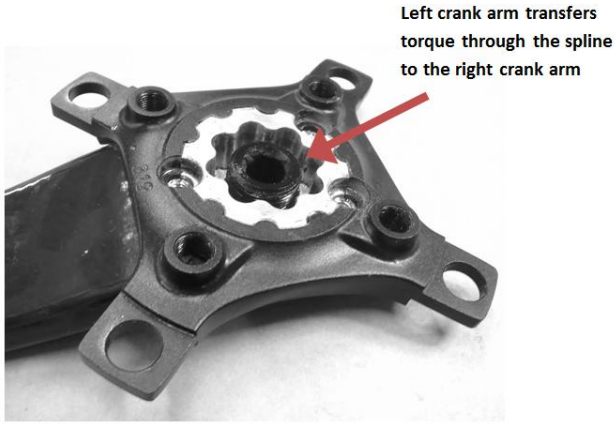

Figure 3.11 - The left crank arm transfers torque to the splined, right crank arm.

3.4.2 Strain Bridge Design

The strain gauges are configured in a full Wheatstone bridge, as shown **Figure 3.12 and 3.10**. This configuration gives a sensitivity factor of 4 and will cancel any radial forces, though no significant forces are expected.

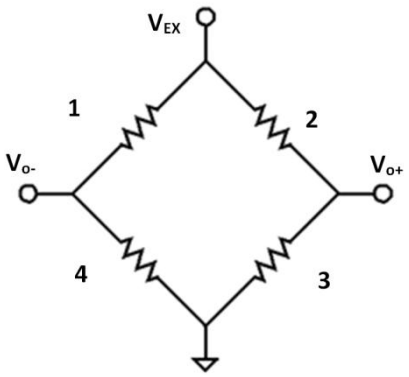

Figure 3.12 - Full Wheatstone bridge design for the crank spider.

3.4.3 Finite Element Analysis of the Crank Spider

Based on the loading determined for the crank spider a finite element model was built to investigate the expected strain and the expected location of the highest strain. This will help achieve optimum placement of strain gauges.

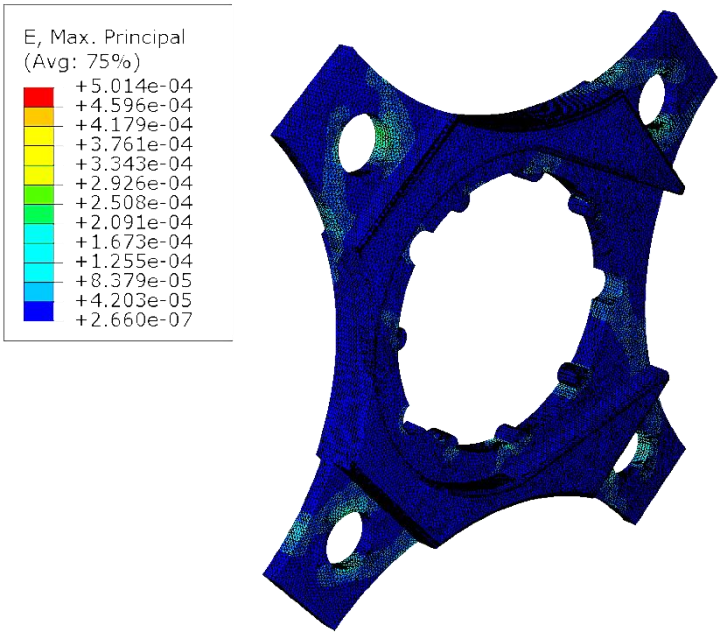

Figure 3.13 - Finite element model of the crank spider

The highest strain in the section of the spider that could be properly gauged was roughly 35 με, when a pedal moment of 15.5 N-m was applied, and was located in the area expected, shown in **Figure 3.10**.

3.4.4 Strain Gauge Selection

Strain gauges were selected based on the strain contours in the gauging area and the magnitude of the expected strain. 350 Ω gauges were chosen to reduce current through the bridge, reducing battery drain and self-heating effects. Vishay EA-06-125AC-350 gauges were chosen for the Wheatstone bridge (see Datasheet Strain Gauges in Appendix D). These gauges were the right size and gauge factor to measure the spider strain.

3.5 Crank Bridge Amplifier

Because the Logomatic V2 does not have a built in bridge amplifier an external one is needed to amplify the mV output of the strain bridge to 0-3.3V for full range. An INA122 instrumentation amplifier was selected to amplify the signal. The circuit is shown in **Figure 3.14,** and the resistor R_G can be interchanged to adjust the gain of the circuit, according to **Table 3.1** or **Equation 3.1**.

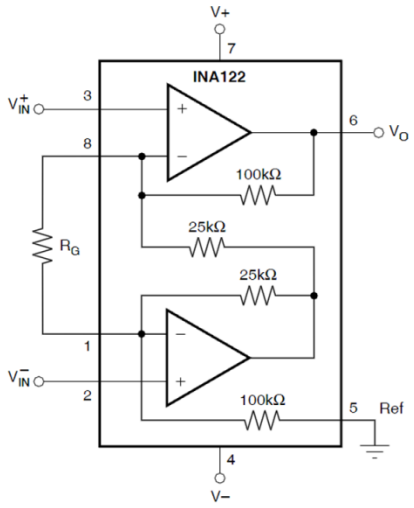

Figure 3.14 – INA122 Bridge Amplifier circuit diagram

$$G = 5 + \frac{200k\Omega}{R_G} \qquad (3.1)$$

Table 3.1 – INA122 Bridge Amplifier resistor values for a desired gain

DESIRED GAIN (V/V)	R_G (Ω)	NEAREST 1% R_G VALUE
5	NC	NC
10	40k	40.2k
20	13.33k	13.3k
50	4444	4420
100	2105	2100
200	1026	1020
500	404	402
1000	201	200
2000	100.3	100
5000	40	40.2
10000	20	20

NC: No Connection.

Initial calibration and testing was done using an R_G value of 220 Ω. It was apparent that the gain was set too high because the signal was being clipped at the maximum of 1023 output units for 3.3V that the 10 bit analog channel could measure (**Figure 3.15**). Also of interest from the initial testing is the low noise to signal ratio of the circuit and the zero offset.

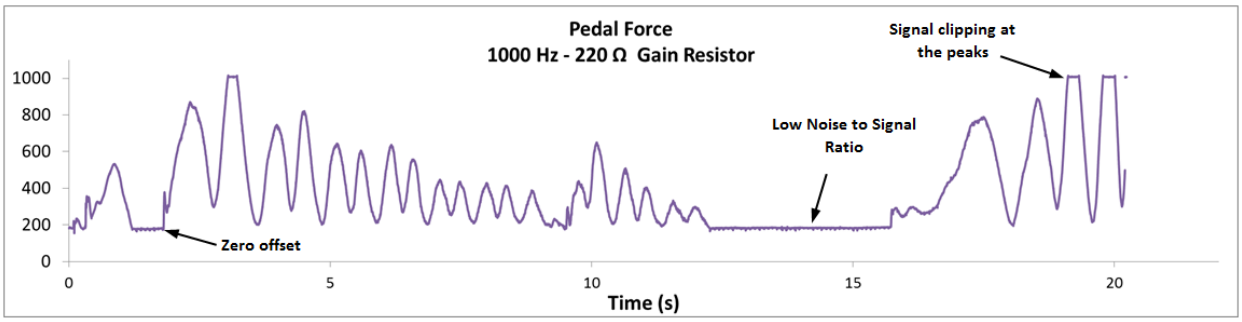

Figure 3.15 - Testing of the initial pedal force setup. The time series shows signal clipping, noise-to-signal ratio and the offset of the circuit, used for circuit refinement.

It was estimated that the gain should be reduced to about 2/3 of the 914 given by the 220 Ω resistor to allow room for higher pedaling forces while maintaining good resolution. The target was to have the maximum pedal forces reaching 900 and the minimum at 0. With a 330 Ω resistor the gain is:

$$G = 5 + \frac{200k\Omega}{330\Omega} = 611$$

The zero offset of the circuit was caused by an unbalanced strain bridge. The resistances were measured across the bridge from the wires at the bridge amplifier and found to be the values shown in **Figure 3.16**. The bridge offset with no loading was 2.2 mV.

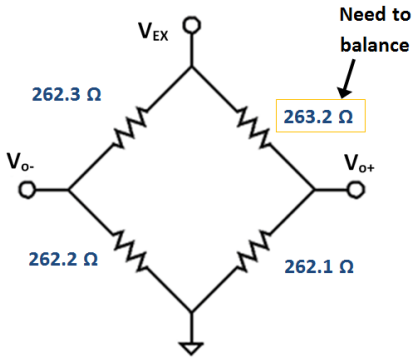

Figure 3.16 - Measured resistances of the spider strain bridge. One resistance was slightly higher than the other legs, causing the zero offset seen in ***Figure 3.15****.*

It was determined that a resistor needed to be connected in parallel across V_{EX} and V_{O+} to reduce the equivalent resistance to 262.2 Ω.

$$R_{Total} = \left[\frac{1}{263.2\ \Omega} + \frac{1}{R_{Bal}}\right]^{-1} = 262.2\ \Omega$$

$$R_{Bal} = 69\ k\Omega$$

A 65 kΩ resistor was added in parallel to achieve an offset of 0 mV from the strain bridge.

3.6 Logomatic V2 Data Collection Board

The crank data is recorded by a SparkFun Logomatic V2 board located on the left crank arm. The board is capable of recording data at 1500 Hz for a single channel (See Datasheet SparkFun Logomatic V2 in Appendix D). It is powered by a polymer lithium ion battery pack and records data to a MicroSD memory card. The amplified signal from the INA122 Bridge Amplifier is recorded on Channel 1 of the Logomatic. 3.3V is drawn off of the board to power the amplifier and the strain bridge.

3.7 Inductive Proximity Sensors

The factors which determine inductive proximity sensor selection are triggering frequency, operating distance and slot width. From the expected maximum frequency of 300 Hz, an operating distance between 1mm and 15mm, and a slot width of 3mm there were many options that would suffice. The final selection was based on the physical dimensions of the inductive proximity sensor and the operating distance. The Fargo S3440 and S3020 (see datasheet in Appendix D) are 8mm sensors with 50mm and 35mm lengths, respectively. Both have an operating distance of 2mm which allows more room for rotor warping or foreign debris than some of the options with smaller operating distances.

3.8 Frequency to Voltage Converter

Since the DAQ can't record at 3000 Hz, the speed sensors require a conversion circuit which will use the frequency as an input and will output a voltage of magnitude relative to the input frequency. This conversion circuit requires ±5V supply, signal amplification, signal conditioning, conversion and ripple filtering. The five functions for both front and rear circuits were built on a breadboard. **Figure 3.17** shows the circuit diagram for each sensor. The frequency to voltage converter and ripple filter were taken from an article from circuitstoday.com.

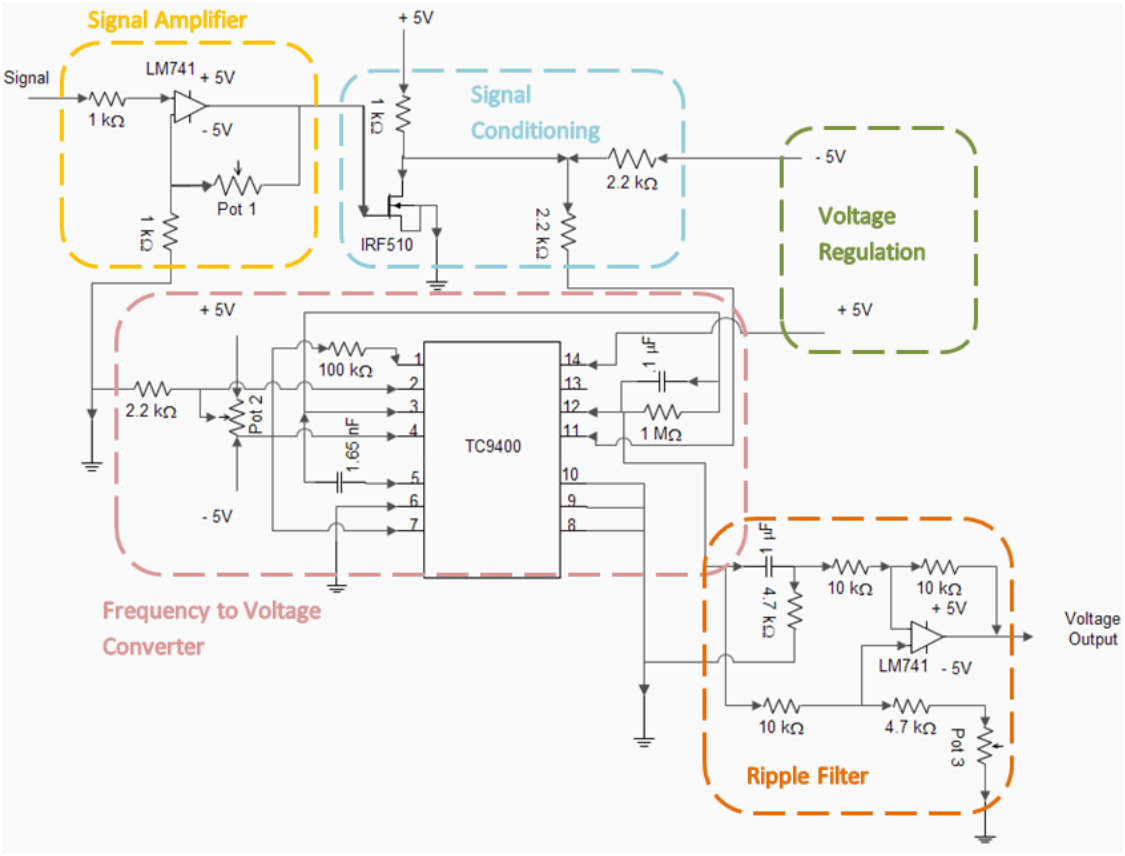

Figure 3.17 - Frequency to Voltage Converter circuit diagram

3.9 Circuit Design

The signal from the sensors produced a 0.25 to 0.7 volt square wave. A function generator was used to replicate the signal for circuit testing. An oscilloscope was used to troubleshoot and to view the effects after adjusting the values of components. In order for the TC9400 to capture the frequency, the signal input needed to be a 5 volt square wave centered at 0 volts. To input the desired signal, a non-inverting amplifier, mosfet, and a voltage divider were added, which are indicated on **Figure 3.17** as the signal amplifier and signal conditioning. A potentiometer, Pot 1, was used in the signal amplifier to adjust the gain to so that the voltage to the mosfet was not 3.0 to 3.3 volts. The potentiometer, Pot 2, of the Frequency to Voltage Converter is adjusted to set the voltage output to zero when the input frequency is

zero. The capacitors of the Frequency to Voltage Converter were adjusted to their current values to amplify the voltage output from pin 12 and to increase the time constant of the converter. Further increasing the 1.65 nF capacitance would increase the voltage output, but reduce the maximum frequency captured. Adjusting the 0.1 uF capacitor would reduce the ripple effect, but limit the response time of the converter. To further reduce the ripple effect from the output voltage, a dedicated ripple filter was added. The potentiometer, Pot 3, was adjusted to increase the gain to further increase the output voltage. The number of slots on the front and rear brake rotors is different, which changes the gain required for each frequency to voltage converter. To compensate for this change, Pot 3 for each circuit was adjusted so that each circuit displaced the same voltage at the same speed.

3.10 Swoop Data Collection Board

The suspension, brake and wheels speed data is recorded by the Swoop board (See Datasheet Swoop in Appendix D) mounted in an enclosure on the frame. The Swoop records the data on an SD card. There are 8 channels configured as follows:

- Ch 0: Bridge amplifier
- Ch 1: Analog Voltage
- Ch 2: Analog Voltage
- Ch 3: Analog Voltage
- Ch 4: Analog Voltage
- Ch 5: Accelerometer x
- Ch 6: Accelerometer y
- Ch 7: Accelerometer z

Four channels are used to record data: Channel 0 is used for the brake strain bridge, Channel 2 is used for rear wheel speed, Channel 3 is used for front wheel speed, and Channel 4 is used for suspension position. The Swoop is configured by editing values in the config.cfg text file on the SD card. As soon as power is connected to the board it will begin recording data as a new CSV file. It was discovered that the first column, which is supposed to be the time series, does not relate to the actual time or to the sampling frequency; it should be ignored.

To protect the board and make it simple and easy to use it is mounted in an enclosure (**Figure 3.18**). The enclosure provides a stable platform for mounting on the bike and allows access for basic operations, such as SD card access and starting and stopping data collection.

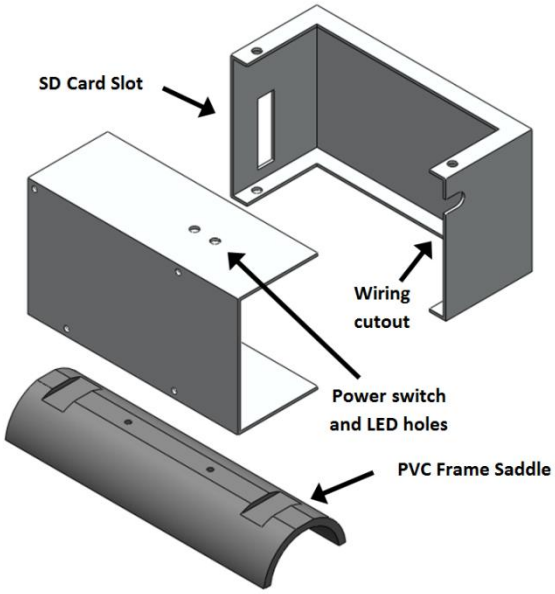

Figure 3.18 - The Swoop is mounted in an enclosure allows operation of basic functions.

The battery is housed within the enclosure and connected by a toggle switch on the box. An LED light indicates the status of the board and a slot in the cover allows the SD card to be removed for transferring data. The box is designed so that the cover can be removed with the box mounted on the bike for access to the battery, board and wiring connections. Access is from the right side of the bike to avoid interference with the string potentiometer.

The Swoop Board is not capable of the sampling rate determined to be ideal during preliminary testing (See Section 3.11) when four channels are active, but it is what was available in the timeframe and budget of this project. Future modifications will incorporate a DAQ capable of recording at higher frequencies.

3.11 Materials and Design

The primary components of the system are:

- Full Wheatstone strain bridges - (2)
- String Potentiometer
- Inductive Proximity sensors - (2)
- Data acquisition unit (2)

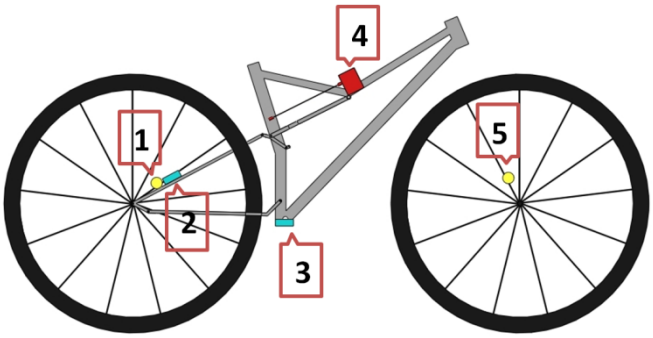

Figure 3.19 -System layout with sensors: Rear wheel speed sensor (1), Brake force strain bridge (2), Pedal force strain bridge (3), String potentiometer (4), and Front wheel speed sensor (5).

The strain gauges were mounted on the aluminum brake adapter (2). Vishay EA-06-240LZ-120/E strain gauges were chosen for size and availability (See Datasheet Strain Gauges in Appendix D). For the crank spider Wheatstone bridge (3) Vishay EA-06-125AC-350 strain gauges were used. The string potentiometer (4) was mounted at the water bottle mount and routed around a pulley to measure shock compression. The string potentiometer selected is a Model #MT3A-9L-14-10K-C6 (see Appendix D for datasheet). This was chosen to allow for the flexibility in mounting that we require for use on multiple bikes and to ensure that the potentiometer will accurately follow the suspension movement over its full travel. Wheel speed is measured using Fargo S3440 and S3020 proximity sensors (1) (5).

The bike being tested is a medium 2011 Specialized Stumpjumper FSR Expert EVO (**Figure 3.20**). The data collected by the DAQ is post processed using Excel and Matlab to develop plots and values that show the relationship of braking and suspension. This will allow the suspension effectiveness to be described numerically under various braking conditions.

Figure 3.20 -2011 Specialized Stumpjumper FSR Expert EVO test bike

3.12 Sampling Rate

Preliminary testing was done in order to determine the sampling rate that would be necessary to collect useful data. This data was intended to help select an appropriate DAQ for this project. Since the data collection system components were not yet installed on the test bike, a Celesco Linear Potentiometer (See Datasheet Linear Potentiometer in Appendix D) was used to measure the position of the front suspension on a 2011 Specialized Stumpjumper hardtail. It was assumed that the front and rear suspension responses are similar, and require similar sampling rates. Data was collected using a Logomatic V2 datalogger from Sparkfun Electronics (See Datasheet SparkFun Logomatic V2 in Appendix D). The Logomatic is capable of sampling at 1500Hz when a single channel is used. Tests were performed with Jacob Publicover riding the bike over a series of 2"x4" boards on smooth pavement to simulate a small bump **(Figure 3.21)**. A variety of tests were performed, varying the speed and spacing of the boards with the rider seated and standing. **Figure 3.22** shows the raw suspension data stored on the board vs. time for Run #3 which was run at ~10mph over three boards spaced 10ft apart with the rider seated.

Figure 3.21 - Preliminary testing was performed over a simple course with controlled features and spacing.

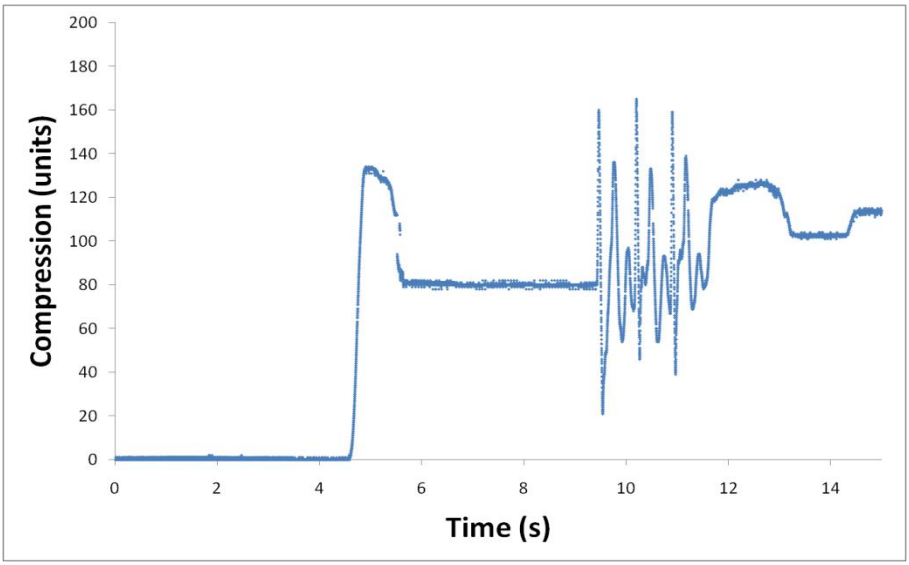

Figure 3.22 - Front suspension position recorded over three 2"x4"'s for Trial 3

In order to investigate the effect of sampling rate, Matlab was used to generate arrays from the data which imitate lower sampling rates. For example a 750 Hz sample rate was imitated by building an array from every other point in the 1500 Hz array. Sample Matlab code for the frequency testing is shown below.

```
% Creating an array for 750 Hz Sample Rate
Sample1500=Data;
for n=1:size1500
    a(n,1)=floor(n/2);
    a(n,2)=n/2;
    if a(n,1)<a(n,2);
    else
        Sample750(a(n,1),1)=1/750*a(n,1);
        Sample750(a(n,1),2)=Sample1500(n,2);
    end
    n=n+1;
end
```

Similar arrays were created all the way down to a frequency of 25 Hz. **Figure 3.23** shows how various sample rates compare to the 1500 Hz data. From this analysis it was determined that a minimum sampling rate 100 Hz should be used to capture suspension data. This sample rate is high enough to collect 7-10 points on an impact curve, enough to get a close approximation of the suspension position, but not enough for velocity or acceleration calculations.

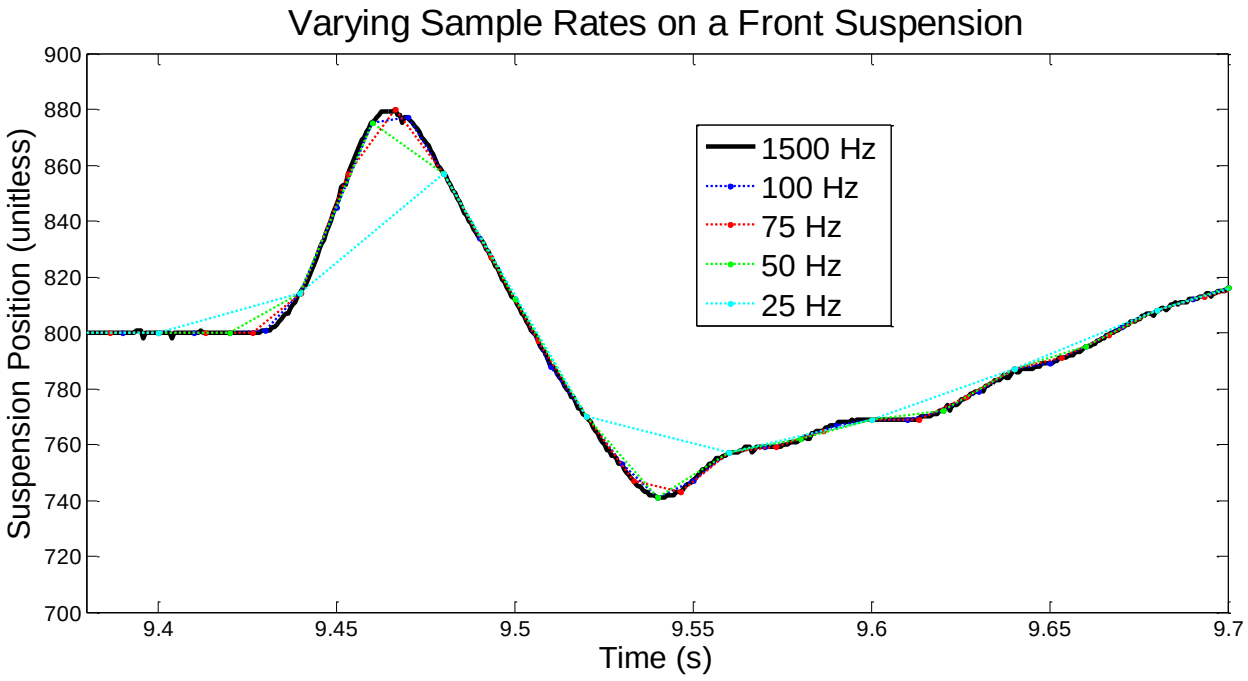

Figure 3.23 -Using Matlab to simulate the effect of lower sampling rates, it was determined that 100Hz is the minimum sample rate necessary for recording accurate suspension response.

3.13 Modifications to Data Collection System for Initial Braking vs. Suspension Testing

Due to the availability of certain components, the design of the data collection system was modified to use a rotary potentiometer in place of the string potentiometer to collect some initial braking vs. suspension data and provide a proof of concept. The string potentiometer and the inductive proximity sensors were back ordered and testing could not be postponed to wait for their arrival. The rotary potentiometer was used at the rocker link to shock pivot, which has the largest change in angle through the suspension stroke. The rotary potentiometer was replaced with the string potentiometer when it arrived. The string potentiometer was used in all pedal testing and later braking tests.

4. Fabrication and Setup

4.1 Brake Strain Bridge

A full bridge was used to cancel temperature and tensile strain effects, capturing only bending strain due to braking forces. The braking bridge has the benefit of being isolated from other loading, such as suspension inputs or chain forces, so the loading of the strain bridge is consistent and predictable. All strains measured will be due to braking forces, and only braking forces, so the bridge can be calibrated experimentally.

4.1.1 Gauge installation

The brake bridge was filed down to reduce the cross-sectional area and increase the strain in the part when braking forces are applied, as shown in the analysis in **Section 3.2**. The surface was prepared following Vishay Instruction Bulletin B-127-14 and the strain gauges were carefully aligned and bonded to the adapter. Solder pads were used to prevent wiring strain from pulling the gauges off of the material.

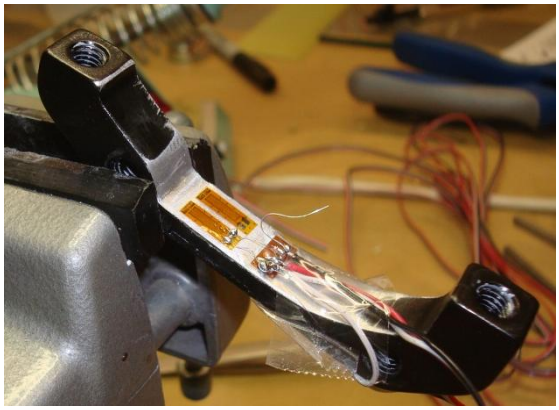

Figure 4.1 -Strain gauges were bonded to the brake adapter at high strain locations following Vishay Instruction Bulletin B-127-14.

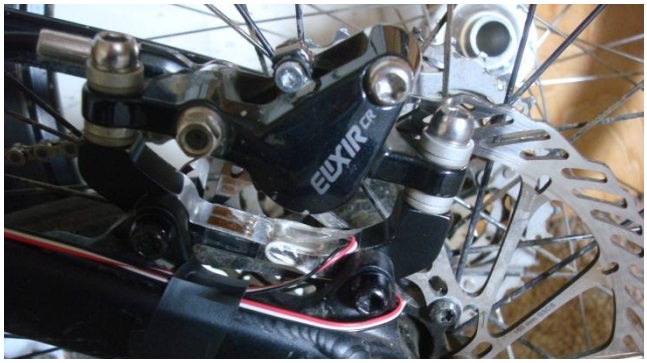

Figure 4.2 - The gauged adapter installed on the bike.

4.1.2 M-Coat F Protective Coating

Since the brake adapter is in a location that could potentially see high exposure to water and dirt and be subjected to impacts from foreign objects it was protected using Vishay M-Coat F. Protection is necessary to ensure that the adhesives are not degraded over time, rendering the calibration inaccurate. To obtain valid results, the strain bridge must measure the braking force consistently over all tests. The first layer of the protective coating is a Teflon base coating to cover the gauges. The Teflon coating is covered by aluminum tape extending beyond the gauges and solder terminals. The edges of the tape are sealed with M-Coat B polyurethane protectant, giving special attention to the locations where the wires exit. The coating was applied following Vishay Instruction Bulletin B-134-4. The coating was finally covered with electrical tape to further prevent wear and tear.

Figure 4.3 - The brake adapter strain bridge is protected with Vishay M-Coat F and electrical tape.

4.1.3 Wiring to the Swoop Board

The wiring is routed from the brake adapter along the seat stay to channel 0 on the Swoop DAQ. The total wiring length is approximately two feet. The wiring is twisted in pairs to prevent signal interference from noise (**Figure 4.4)**.

Figure 4.4 - Twisted pair wiring reduces induced noise between the strain bridge and the Swoop board.

4.2 String Potentiometer

4.2.1 Mounting Plate

To allow for quick mounting on many different bikes, the string potentiometer is mounted to an aluminum plate which can be mounted to any standard water bottle mount. The plate was slotted using an upright mill and tapped with #6-32 threads for mounting the string potentiometer. The slots allow for lateral adjustment of the string potentiometer to align the cable in the same plane as the pulley. The body of the string potentiometer allows for rotational adjustments about two axes. With these adjustments the string can be pointed straight at the pulley as it exits the potentiometer housing to reduce friction and wear as it moves in and out.

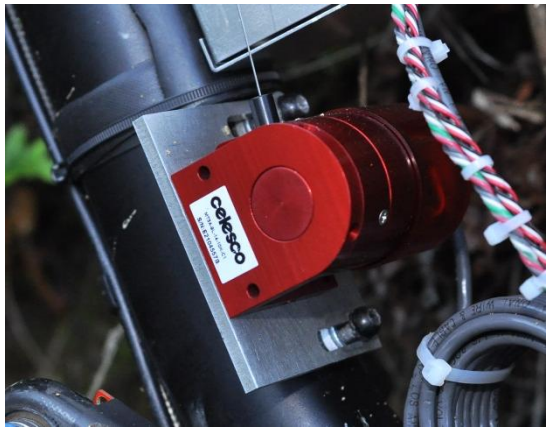

Figure 4.5 - The string potentiometer mounting plate allows for side-to-side adjustment for proper cable alignment on multiple bikes.

4.2.2 Pulley mount

The pulley reroutes the cable to run directly parallel with the axis of the shock, so that the change in length of the string will be 1:1 with the change in length of the shock. To accomplish this, the pulley is mounted to a bracket at the upper shock mount. The pulley is mounted off center so that the bracket can be rotated so that as the cable leaves tangent to the pulley it will travel perfectly parallel to the shock axis.

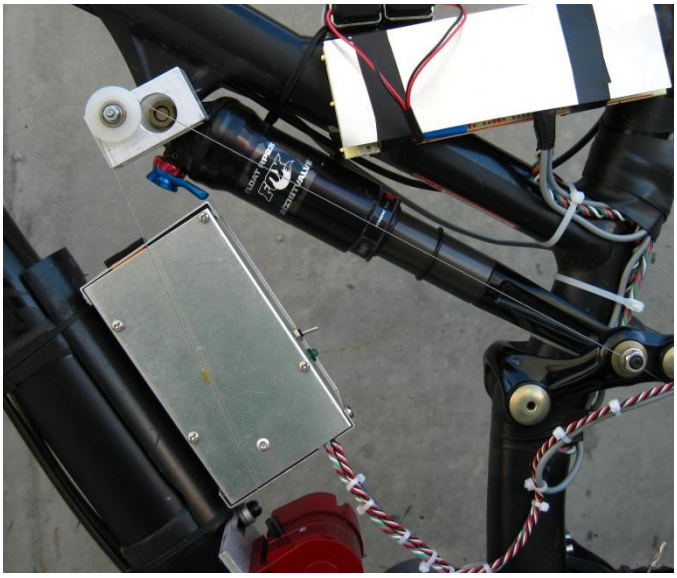

Figure 4.6 - The pulley mount can be rotated about upper shock mount bolt to align the cable along the axis of the shock.

4.2.3 Cable End Clamp

At the lower shock mount, which is attached to the suspension, the cable is clamped by a bolt that is run through the hollow pivot bolt. The pivot bolt was countersunk to allow the head of the 5mm clamp bolt to sit inside the pivot bolt against a shoulder and not interfere with suspension operation. A small hole, just large enough for the cable to pass through, was drilled in the bolt. The clamp bolt is held in place in the pivot bolt with a nut. Then two washers sandwich the cable as it passes through the bolt and the entire assembly is clamped down with another nut.

Figure 4.7 - The cable end clamp mounted in the lower shock pivot.

4.3 Crank Strain Bridge

A full bridge was used to cancel temperature and tensile strain effects, leaving only bending strain due to chain tension, which is directly related to pedaling torque in each gear. The strain bridge has the benefit of being isolated from other loading, such as crank axial or side loading, so the loading of the strain bridge is consistent and predictable. The strain measured by the bridge will be a function of the chain tension and can be calibrated by applying a series of static loading to the crank.

4.3.1 Gauge installation

The spider was prepared by removing paint to expose the bare aluminum in the gauging areas. Gauges were installed in the locations identified in **Section 3.4.1**, following Vishay Instruction Bulletin B-127-14. To prevent the wires from pulling the gauges off, a solder pad was used for all connections.

Figure 4.8 - Gauged spider to measure the strain due to pedaling forces.

4.3.2 M-Coat F Protective Coating

Similar to the brake adapter strain bridge, the crank strain bridge required protection from the elements and foreign debris. The procedure was the same with the exception that a layer of M-Coat FB butyl rubber sealant was added over the wiring for added protection from impacts and to fill gaps and make a weatherproof seal. M-Coat FB butyl rubber sealant was not used on the brake adapter only because of space constraints.

Figure 4.9 - The Teflon tape covers the strain gauges. A section of butyl rubber is used to seal the wire exit first.

Figure 4.10 - Foil tape covers the Teflon tape and helps seal out the elements.

Figure 4.11 - The edges of the foil tape are sealed with M-Coat B polyurethane protectant.

4.3.3 Wiring to the Bridge Amplifier

There is limited space on the right crank arm due to the chainrings and derailleur, so the wires from the strain bridge were routed through the bottom bracket to the left crank arm. The Logomatic V2 datalogger does not have a built-in bridge amplifier so an external one was constructed using an INA122 instrumentation amplifier. The bridge amplifier was built directly onto a DIP socket to minimize the size of the components that had to be carried on the crank arm (**Figure 4.12**).

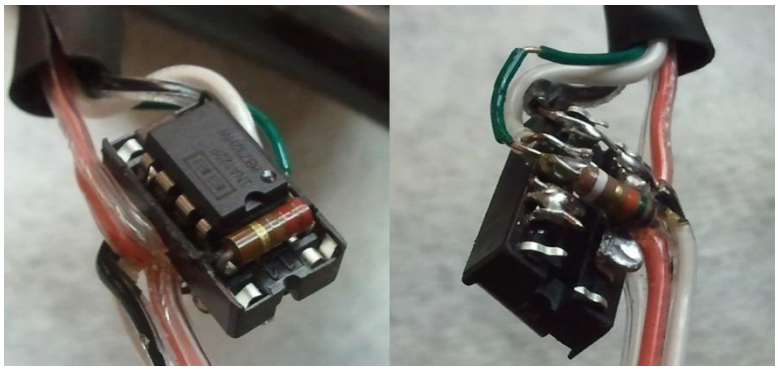

Figure 4.12 - The bridge amplifier circuit is constructed on a DIP socket. The gain resistor is on the top of the circuit (left) and the offset resistor is on the bottom (right).

Once the circuit was finished and tested it was covered in heat shrink to secure the wiring in place and offer elemental protection. A slit was cut to allow gain resistor access, if necessary. The wiring to the strain bridge exits at the top of the DIP socket while the wiring to the Logomatic exits at the bottom (**Figure 4.12)**, forming a compact, inline amplifier that can be secured to the crank arm.

4.4 Logomatic V2 Data Collection Board

The Logomatic V2 is designed to work right out of the box. A text file on the MicroSD card sets the configuration mode and sample frequency of the board (see Datasheet SparkFun Logomatic V2). The board was set to record as an ASCII file on channel 1 at 100 Hz. The Li-Polymer battery pack was connected and secured to the left crank arm, along with the Logomatic, and covered with a layer of butyl rubber to protect them from damage and contamination. The MicroSD card and charging port are accessible at the end of the crank arm. A slit was cut in the rubber for access to the Logomatic power switch.

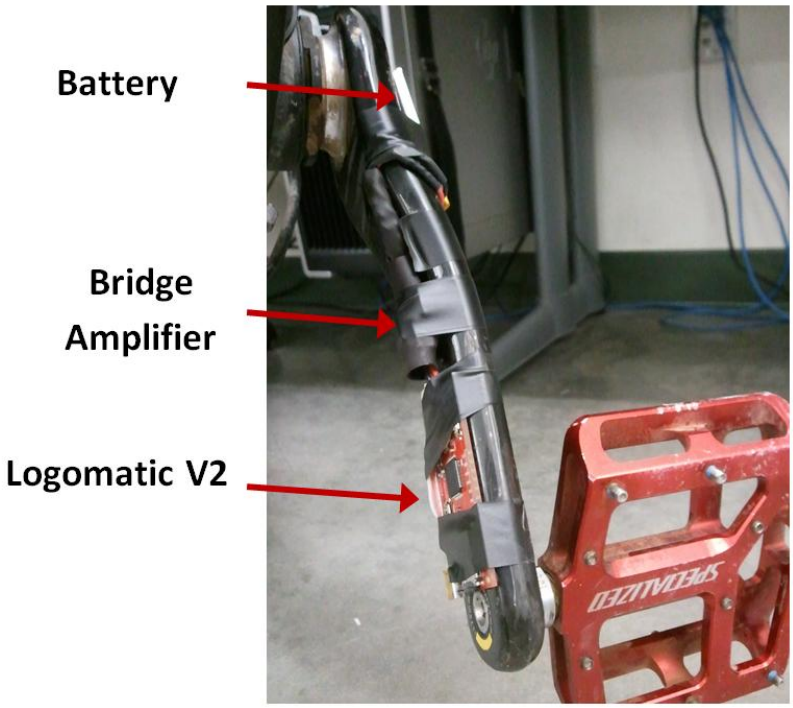

Figure 4.13 - Logomatic V2, Bridge Amplifier and battery pack secured to the left crank arm.

Figure 4.14 - The components on the crank arm protected under a layer of butyl rubber and ready for testing.

4.5 Inductive Proximity Sensors

4.5.1 Design

Mounts were made to position the inductive proximity sensors at the brake rotors. The mounts are made from short sections of 1/16" thick, 90 degree-angled aluminum and provide a rigid mount for the speed sensors so that vibration will not affect the operation of the sensors. The rear mount connects to the bike at the brake adapter/seat stay bolt. The sensor can be adjusted to position it radially and the sensor body is threaded to allow adjustment of the operating distance.

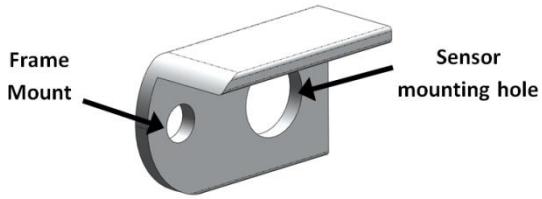

Figure 4.15 - The mounting bracket for the rear wheel speed sensor.

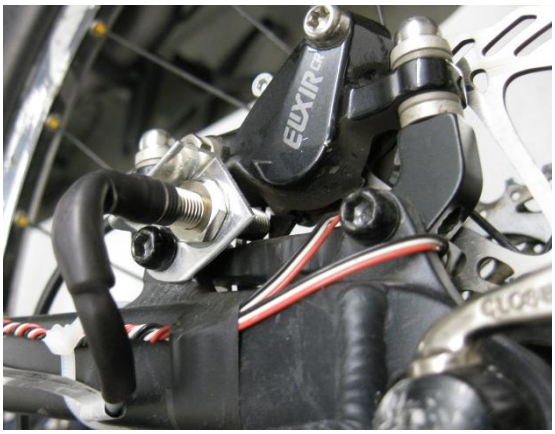

Figure 4.16 - The rear speed sensor mounted at the rear brake adapter.

The front sensor is mounted to the fork bolts under the caliper, making it difficult to align without adjusting the brake. The mount can be pivoted away from the bike to point the sensor radially inward. The sensor body allows for adjustment of operating distance.

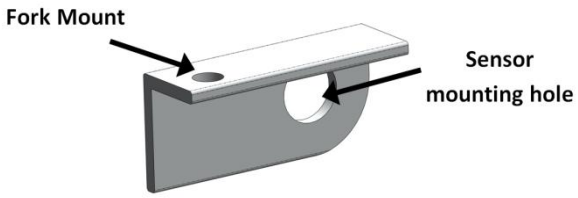

Figure 4.17 - The mounting bracket for the front wheel speed sensor.

Figure 4.18 - The front wheel speed sensor mounted at the fork.

4.5.2 Setup

The sensors have an LED in the tip, where the wire comes out, that indicates the state of the output. This makes setup in the field much easier since the sensor can be adjusted and the output can be verified on the fly. The output signal was also analyzed using an oscilloscope in lab to view the square wave output and the high and low durations. This information was used to design and tune the frequency to voltage converter.

4.6 Frequency to Voltage Converter

Both frequency-to-voltage converters were built on a breadboard, along with the peripheral circuits described in **Section 3.7**. The circuit was adjusted to have a gain for each wheel that would set the maximum expected wheel speed just below the maximum voltage the analog channel would register, 3.3V. The front rotor has 36 slots while the rear rotor has 48 slots, so the gain of the front was set approximately 33% higher than the rear. The frequency generator and oscilloscope proved to be invaluable for setup, adjustment and troubleshooting.

Figure 4.19 - Testing the frequency to voltage converter in lab.

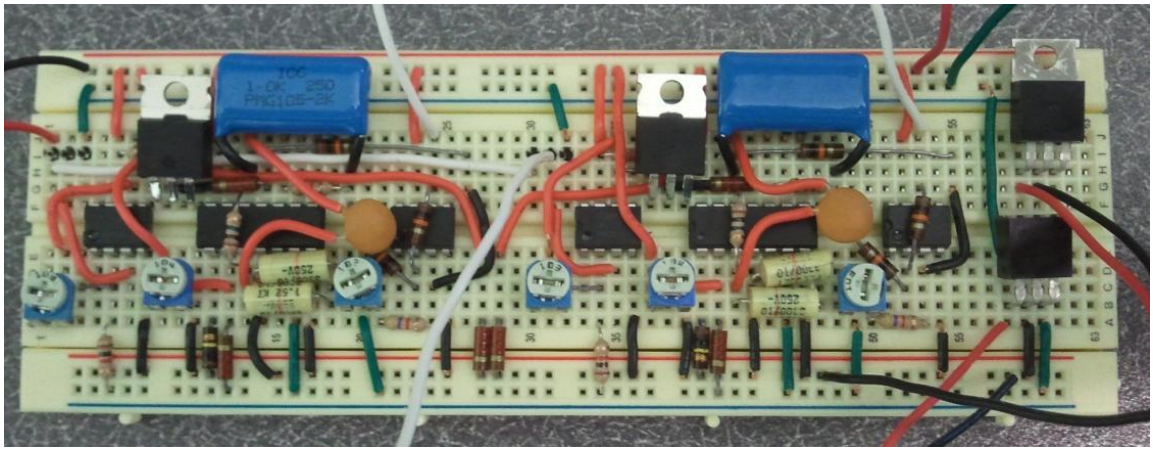

Figure 4.20 - The finished frequency to voltage circuit. The six blue potentiometers are used for tuning the circuit.

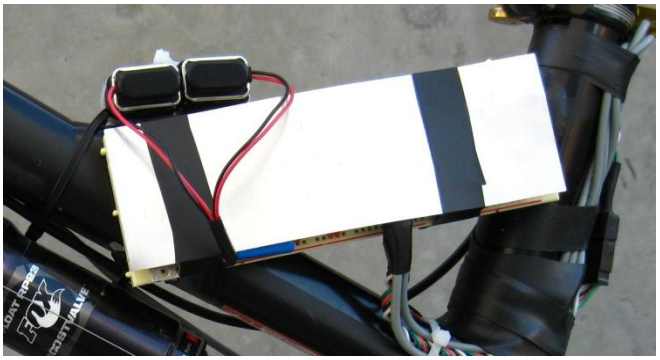

Figure 4.21 - The breadboard was covered with a thin piece of aluminum sheet metal and attached to the frame.

The output wires are run to the Swoop DAQ as a twisted pair to reduce noise. A connecter is used in-line for quick circuit disconnection for testing and switching between bikes.

4.7 Swoop Data Collection Board

4.7.1 Enclosure

The Swoop was mounted in an aluminum housing to protect it and provide a way to secure it to the bike. The housing was purchased from Radio Shack and modified to mount a power switch and LED indicator. A slot was cut to allow access to the SD card and a cutout was made to allow wiring to pass through. A PVC saddle was made and riveted to the box so it can be secured to the down tube of the bike.

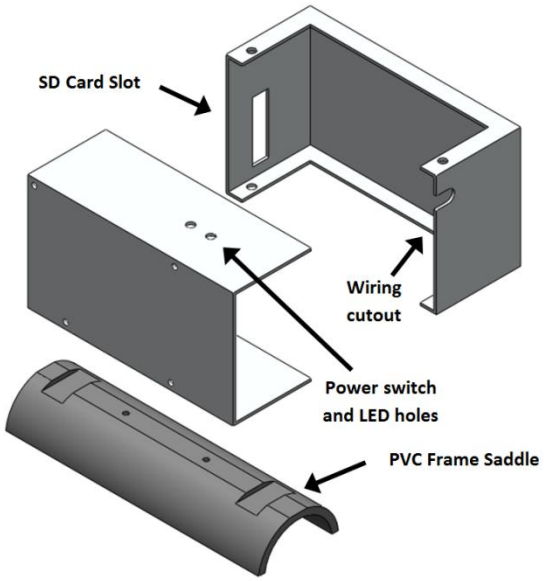

Figure 4.22 - An aluminum housing was modified for the Swoop DAQ.

The board is powered by a 9V battery, also mounted in the enclosure. The Swoop DAQ begins recording as soon as power is turned on, which is controlled by the switch.

Figure 4.23 - The Swoop DAQ enclosure with the cover removed.

4.7.2 Wiring

The board was configured for one strain bridge, on Channel 0, and one analog voltage, on Channel 4. With some minor rewiring, the board was setup to measure analog voltages on Channels 2 and 3 as well. Channels 5, 6 and 7 are dedicated to a three axis accelerometer that was not used.

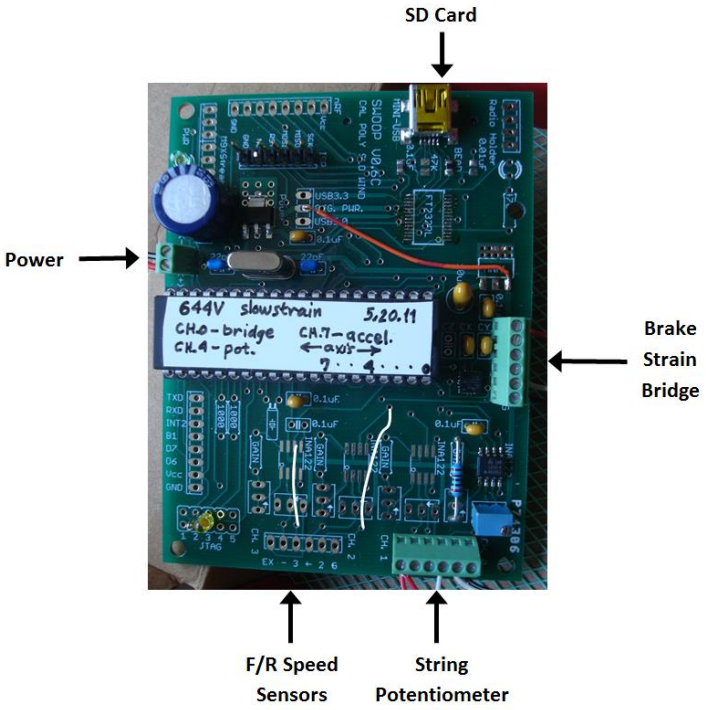

Figure 4.24 - Swoop detail with modifications to enable Ch. 2 and Ch. 3.

4.7.3 Configuration

The Swoop board is configured by editing the config.cfg file on the SD card. The text file reads:

```
40      # Milliseconds per point

on          # Channel 0 is Braking Force
off         # Channel 1 is not active
on          # Channel 2 is Rear wheel speed
on          # Channel 3 is Front Wheel Speed
on          # Channel 4 is Suspension Position
off         # Channel 5 is not active
off         # Channel 6 is not active
off         # Channel 7 is not active
```

Figure 4.25 - The config.cfg file on the Swoop SD card sets the recording parameters.

It was discovered that although the card is setup to sample at 25 Hz the Swoop does not consistently record at that rate. With this configuration the sample rate varied from 20.5 Hz to 24.5 Hz. The maximum sample rate while recording on four channels appears to be 24.5 Hz, regardless of how many milliseconds per point the card is set at.

5. Calibration

Each component used in the data acquisition system required calibration so that the digital values recorded on the SD card could be related to the physical measurement they represented. Experimental calibration was the most accurate method of calibration to obtain a direct relationship between the physical property being measured and the digital value recorded on the DAQ. This method accounts for uncertainties in the linearity of the sensors, the supply voltage, and A/D conversion, and for systematic errors due to resistance in the wiring and the connections. The remaining uncertainty is primarily due to uncertainty in the measurement of the physical property used for calibration and in the resolution of the A/D conversion.

5.1 Rotary Potentiometer

The rotary potentiometer used in initial testing served to highlight potential areas for improvement for reducing uncertainty when selecting sensors. The rotary potentiometer only used 25% of the 0-3.3V range of the DAQ through the full travel of the suspension, leaving room for improvement in resolution.

The potentiometer was calibrated by compressing the shock to various points and recording the value recorded by the DAQ. The air was let out of the shock to allow the suspension to be easily compressed in lab. The travel indicator (a rubber O-ring) and a pair of calipers were used to measure the distance that the shock was compressed at each point (**Figure 5.1**).

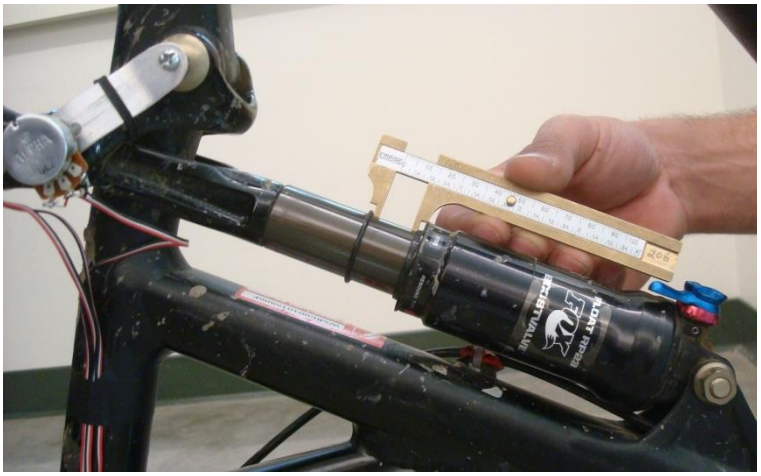

Figure 5.1 - Rotary potentiometer calibration

Calibration data was plotted using Excel and the calibration factor and linearity were determined from a linear fit of the data. Despite the low resolution of the sensor and the non-linear relationship between the rotary pivot point and the linear shock displacement, the calibration data was highly linear, with a squared residual value of 0.999.

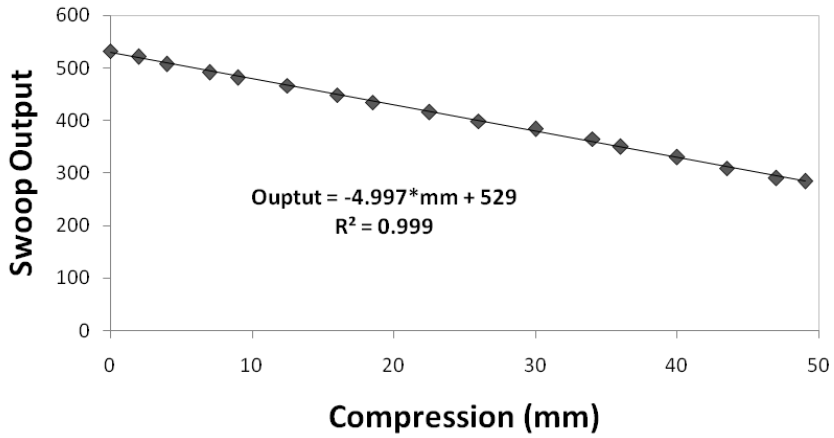

Figure 5.2 - Rotary potentiometer calibration curve

The equation of the trend line is the relationship between the physical property, distance, and the value recorded on the DAQ. From this relationship, the data recorded on the SD card can be converted to meaningful units.

$$Shock\ Compression\ (mm) = -0.200 * (Digital\ value) + 106$$

5.2 String Potentiometer

The rotary potentiometer was replaced with the string potentiometer. The method for calibrating the string potentiometer was identical to that used for the rotary potentiometer.

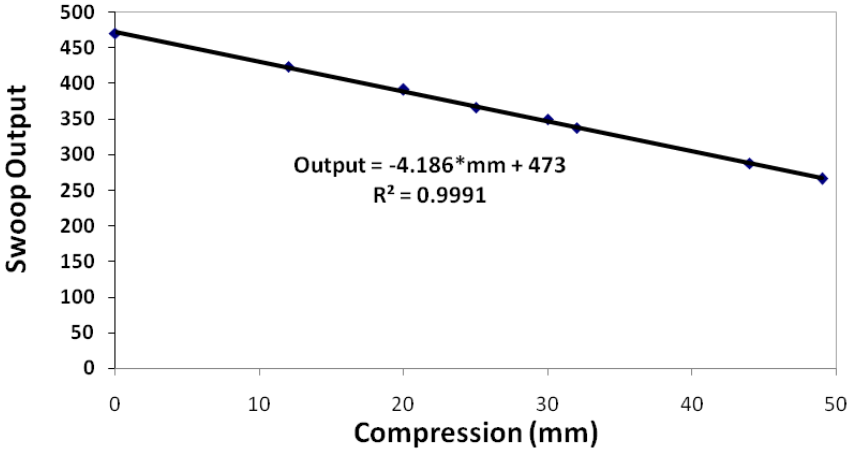

Figure 5.3 - String potentiometer calibration

$$Shock\ Compression\ (mm) = -0.24 * (Digital\ value) + 113$$

The 9 inch stroke range string potentiometer was chosen to provide a flexible platform for mounting on any bike and measuring the displacement of any point on the suspension, up to 9 inches. The current mounting of the string potentiometer results in a resolution that is slightly lower than that of the rotary potentiometer. The resolution could be doubled by running the cable around a pulley at the lower shock pivot and back to the upper pivot. This could be done without any sacrifice in linearity; The pulley mounting at the upper pivot is adjusted to maintain a cable line that is parallel to the shock axis on the upper pass and the lower pass is kept parallel by adjusting the attachment point of the cable end.

5.3 Brake Strain Bridge

To apply a braking force to the strain bridge the rear brake was locked on while weights were hung from a rope wrapped around the rim (**Figure 5.4**). The result is a known force (mass*gravity) applied tangent to the wheel at the horizontal radius of the rim. The applied torque was opposed by the equal and opposite torque applied by the brakes.

Figure 5.4 – Masses hanging from the rim were used to calibrate the brake strain bridge.

By hanging various masses from the wheel and plotting the calculated torque against the value recorded by the DAQ, the calibration curve in **Figure 5.5** was developed. A linear fit of the data produced the relationship between the Swoop data and braking torque.

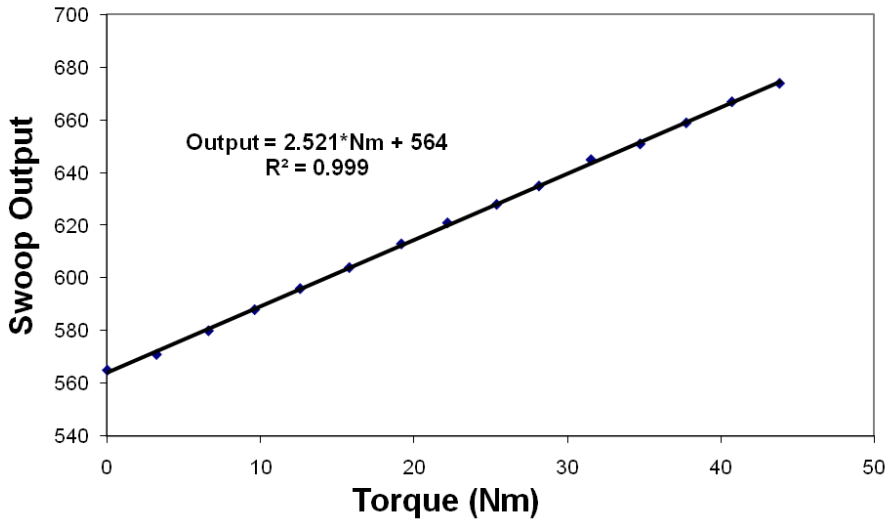

Figure 5.5 - Brake strain bridge calibration curve

$$Braking\ Torque\ (Nm) = \ 0.397 * (Digital\ value) - 224$$

At this time, the full range of measured braking torque was unknown. The resolution of a strain bridge can be compensated for after the fact by increasing the gain of the bridge amplifier. If necessary, this method could be used to improve the resolution of braking force measurements.

5.4 Pedal Strain Bridge

The method for calibrating the strain bridge on the crank spider was similar in concept to the method used for the brake strain bridge calibration. The actual property of interest is chain tension, since that is the magnitude of the force vector that acts on the rear suspension. In each chainring the chain tension has a direct relationship to the crank torque applied. Since the current system was only capable of measuring strain with the chain on the large chain ring, calibration was only performed for that ring. The chain tension is readily determined from the applied torque and the radius of the chain ring.

$$Tension = \frac{Torque}{Radius}$$

With the rear brake locked out, as in the brake strain bridge calibration, weights were hung from the crank arm to apply a torque to the crank (**Figure 5.6**).

Figure 5.6 - Hanging masses from the crank arm to calibrate the pedal strain bridge

To ensure that the masses would apply a force that was both perpendicular and coplanar to the crank arm, the bottom bracket and crank arm were balanced to be horizontal (**Figures 5.7 and 5.8**).

Figure 5.7 - Leveling the bottom bracket before calibration

Figure 5.8 - Leveling the crank arm during calibration

Various masses were hung from the crank and calculated torque was plotted against the output recorded on the crank DAQ. The linear fit of the data produced the relationship between the data on the Logomatic and pedaling torque.

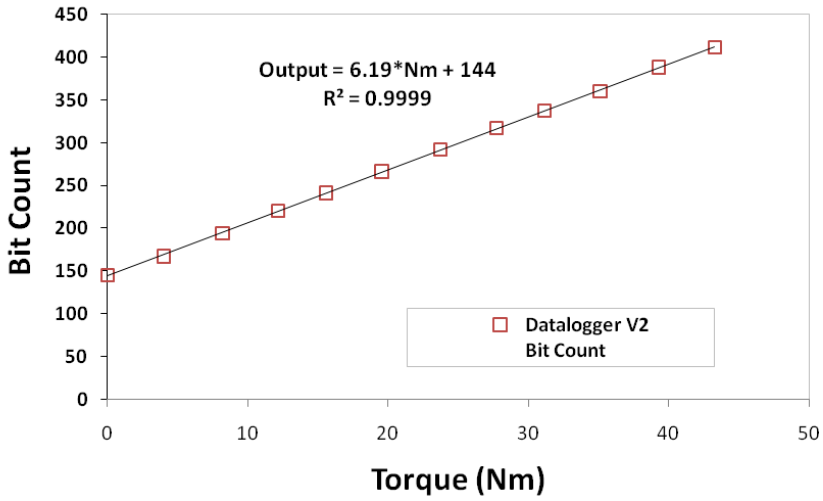

Figure 5.9 - Pedal strain bridge calibration curve

$$Pedaling\ Torque\ (Nm) = 0.161 * (Digital\ value) - 23.26$$

The full range of pedaling torque was also unknown but was initially estimated to be twice body weight, to ensure capture of the data spikes due to the dynamic nature of the loading. After initial trials the amplifier gain and offset were readjusted to maximize resolution within the expected operating range.

5.5 Wheel Speed Sensors

The wheel speed sensors output a square wave signal representing the frequency of rotor slots passing the sensor tip. The frequency to voltage converter was designed to allow for gain and offset adjustments at the signal amplifier and the frequency to voltage conversion. The signal amplifier was tuned in the lab using an HP 5464D Oscilloscope so that it would reliably trigger the MOSFETs which feed the converter a refined square wave with well defined leading and trailing edges. The converter offset did not require adjustment, as a 0 Hz signal resulted in an output of 0 mV. The converter gain was adjusted by running the bike up to a presumed maximum test speed and recording the wheel speed output. To optimize the sample resolution the converter gain was adjusted so that the output at maximum speed would result in an output of 3.1V, or a digital value of about 960 on the SD card. A maximum speed output of 3.1V was set to allow some margin of error in case a test run happened to exceed the setup maximum speed. Each wheel was adjusted independently, with different resistor values, since the rotors had a different number of slots (36 front and 48 rear). **Figure 5.10** shows the original raw data for the maximum speed run with both halves of the converter circuit configured identically. The front wheel indicated speed is roughly 25% lower than the rear wheel indicated speed, consistent with its 25% fewer slots.

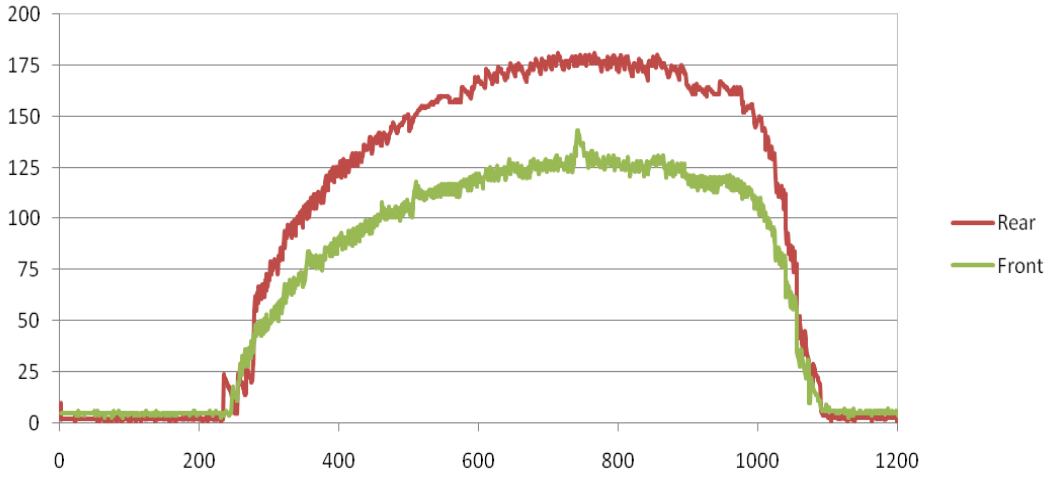

Figure 5.10 - Raw wheel speed before tuning

After the circuit was tuned the maximum speed run produced consistent wheel speeds, as seen in **Figure 5.11**, with 1023 being the maximum that the Swoop board will record; any speed resulting in greater than 1023 (3.3V) will be clipped. This setup maximizes the sampling resolution while preserving a safe margin to eliminate clipping.

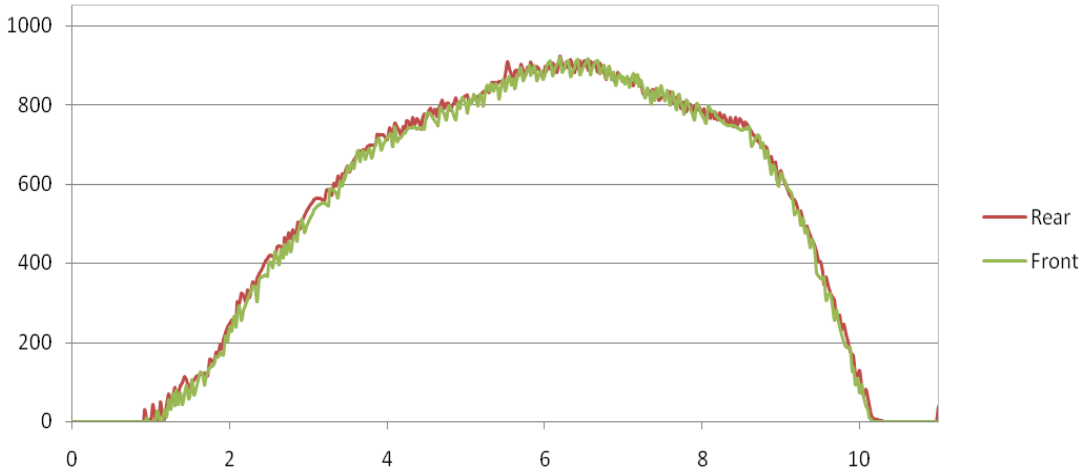

Figure 5.11 - Raw wheel speed data after tuning the frequency to voltage converter

To calibrate the speed sensors the bike was ridden over a known distance and timed from start to stop to obtain an average speed.

$$Avg\ Speed = \frac{distance}{time}$$

The corresponding raw speed data was then averaged, from start to stop, and compared to the actual average speed to obtain the bit-to-MPH conversion factor for each wheel. **Table 5.1** summarizes the results from this calibration. The conversions for the front and rear are 0.0333 and 0.0310 mph/bit, respectively. Therefore a maximum of 1023 bits corresponds to a maximum measurable speed of 31.7 mph before clipping occurs.

Table 5.1 - Wheel speed calibration data

				Avg Raw Data		Conversion	
Trial	Distance (ft)	Time (s)	Avg Speed (mph)	Front (bit)	Rear (bit)	Front (mph/bit)	Rear (mph/bit)
1	226	20.78	7.42	233	231	0.0318	0.0296
2	225	20.86	7.36	230	211	0.0320	0.0298
3	225	19.63	7.81	216	247	0.0362	0.0335
					Average	**0.0333**	**0.0310**

A separate conversion for each wheel is necessary since the two halves of the frequency to voltage conversion do not produce perfectly identical outputs. **Figure 5.12** shows the wheel speed data before and after the conversion factors are applied and demonstrates the effectiveness of the conversion at aligning the wheel speeds.

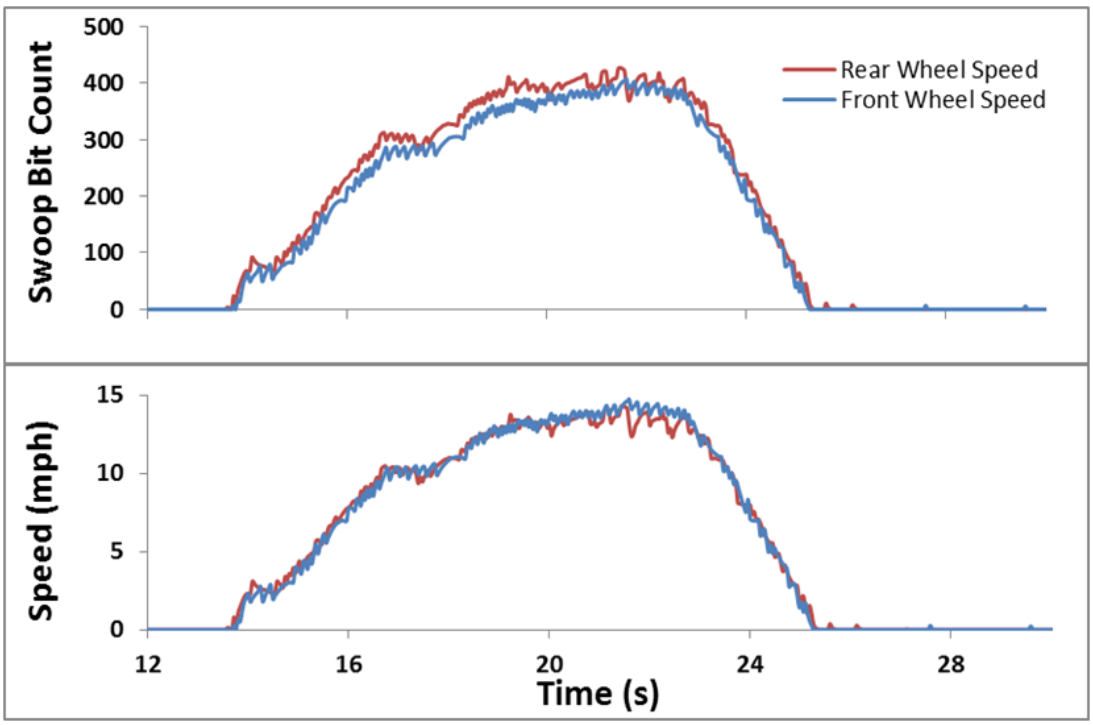

Figure 5.12 - Wheel speed before and after the conversion factors are applied

6. Testing

Braking and pedaling tests were conducted in order to obtain preliminary results and refine the data collection system. Braking and pedaling test data was collected on a trail ride as well as during controlled sidewalk and pavement tests. Many iterations of data collection and hardware and software adjustments resulted in a refined data collection system and preliminary test results to use for comparison with future testing.

6.1 Test methodology

Specific types of terrain were selected for testing with certain test variables. The types of terrain selected for testing were trails, flat pavement and inclined pavement.

Braking and pedaling test data was collected on a ride down a rocky trail off of the San Luis Obispo grade. This test was completed early in the testing phase and proved that the data collection system worked properly during actual trail testing. A trail test was chosen to analyze the bike's behavior in its intended environment. The terrain included rocky and smooth uphill and downhill sections, loose and compact dirt, tight turns, drops, and small jumps. The results were analyzed and it was decided that trail riding has too many variables and that in depth, controlled tests needed to be completed before trail tests were attempted.

Initial braking tests were completed on a sidewalk with a slight downward grade. The terrain provided repeatable conditions with only one suspension disturbance per run. Multiple runs were completed coasting down the paved sidewalk with no braking, continuous light braking, and short intense braking. This was repeated with the additional feature of riding off of the curb in order to cause a relatively large suspension actuation. Skidding was avoided at all times while braking, eliminating an undesired variable. This data provided comparison of suspension behavior in repeatable test conditions while braking and not braking, over smooth ground and off a small drop. The amount of data collected on each run was insufficient for any rigorous statistical analysis.

Baseline pedaling tests were completed on flat pavement with no suspension disturbances. Smooth pavement was chosen to eliminate as many suspension input variables as possible. During testing the rider remained seated and tried to pedal as smoothly as possible, aiming to eliminate pedal bob. Five gear ratios were tested by pedaling around a newly paved Cal Poly parking lot, seven laps per gear ratio, in order to obtain a statistically sufficient amount of data. This test provided data to serve as a base comparison to pedaling data collected while riding over bumpy terrain. Additional pedaling tests were completed on a paved hill in order to test lower gear ratios.

The test methodology was refined and simplified in response to feedback obtained during subsequent data analysis. It was clear that initial attempts were far too ambitious and baseline testing needed to be done with the tightest control of variables possible. System testing under real world conditions will need to be the final step, only after thorough baseline testing is complete in laboratory setting.

6.2 System Configuration

Before beginning each test the bike was set up specifically for the test rider. **Table 6.1** below lists the value of each parameter for both test riders.

Table 6.1: Parameter specifications set before testing for each test rider

Parameter	Nik Goodell	Kathleen Kramer
Shock Pressure	200 PSI	170 PSI
Fork Compression Pressure	90 PSI	80 PSI
Fork Rebound Pressure	90 PSI	80 PSI
Front Tire Pressure	34 PSI	34 PSI
Rear Tire Pressure	34 PSI	34PSI
Command Post Position	Full height	¾ height

6.3 Procedure

A specific procedure was performed each time data was collected in order to ensure that the data could be properly post-processed. In order to compare data collected from each instrument, the time dependent arrays from each data acquisition board had to be correctly aligned. This was accomplished by holding the rear brake and sharply stomping on the pedal 3 times, creating 3 spikes of data on the pedaling force and braking force channels that would correspond exactly in time. Matlab code was written to find the first large data peak from the pedaling channel and braking channel and set each corresponding time stamp to 0 seconds, thereby aligning the two time dependent data arrays. The three data spikes at the end of each data series ensure the data is aligned properly over the whole time series, since the sampling frequency of the Swoop data acquisition board tended to vary between tests. After turning the data acquisition boards on, the operator waits 3 seconds before applying the pedal thrusts in order to allow the boards to self-zero. The following is the procedure followed before and after collecting data:

1. Turn on the Swoop and Logomatic V2 data acquisition boards, ensuring that power is supplied to both strain bridges, the string potentiometer, and both inductive proximity sensors.
2. Wait 3 seconds, holding the bike still without actuating braking or pedaling.
3. Apply and hold the rear brake.
4. Stomp on pedal sharply and cleanly 3 times.
5. Let go of the rear brake.
6. Wait 3 seconds, holding the bike still without actuating braking or pedaling.
7. Carry out data collection.
8. When finished, stop and dismount the bike.
9. Wait 3 seconds, holding the bike still without actuating braking or pedaling.
9. Apply and hold the rear brake.
10. Stomp on pedal sharply and cleanly 3 times.
11. Let go of the rear brake.
12. Wait 3 seconds, holding the bike still without actuating braking or pedaling.
13. Turn both data acquisition boards off.

7. Results

While a final quantifiable relationship has not yet been defined, the results gathered during this phase of the project were an invaluable step towards achieving that goal. The data collected was used to constantly refine the data collection system, as well as the analysis and test methodology, in order to pave the way for continued work that will ultimately identify the desired relationship.

7.1 Braking Forces vs. Suspension

Braking tests were performed first and helped identify the relationships and trends that would be useful for quantifying independence. As data was collected and analyzed the testing procedure and Matlab code were refined to close in on a method for identifying the relationship between braking force and suspension action. This turned out to be an iterative process; tests were performed based on theory, data was analyzed to look for trends, theory was revised based on observations of the trends, and so-on.

7.1.1 Controlled Tests: Changing One Independent Variable

Baseline testing was performed on a controlled section of street, allowing for repeatability. These tests were short runs, about 20 seconds each, with slightly different test parameters for each run. The idea was to alter one independent variable on each run in the hopes that a trend could be seen in the data, such as reduced suspension response in all runs where brakes were applied, regardless of speed. This testing produced results showing interesting correlations from a qualitative perspective, but nothing statistically significant that could be used for developing a quantitative relationship. The amount of data from a single run was too little. At any given braking torque range there was only about 5-10 data points. **Figure 7.1** shows an example of the raw time series from one run. **Appendix F** shows the test parameters and complete results from these tests.

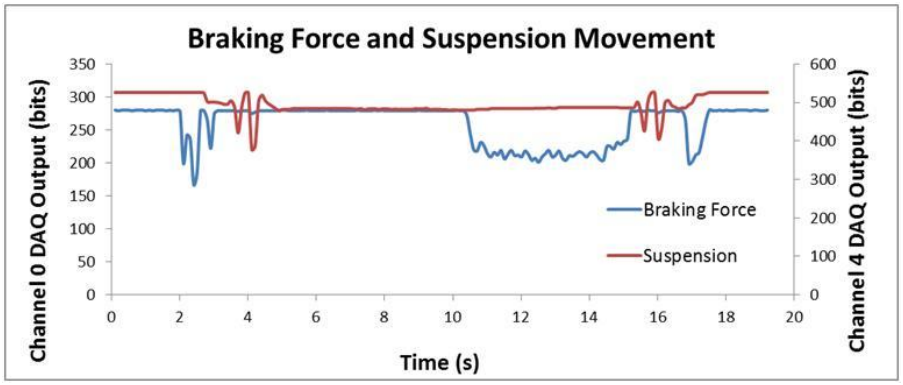

Figure 7.1 – Time series of raw data as recorded by the data acquisition board

The most notable observation drawn from these tests, which is consistent with later testing, was that the suspension actually compresses or 'squats' slightly under rear braking. This was counterintuitive since it was expected that the weight transfer to the front wheel and the moment about the rear wheel, caused by the deceleration of the center of mass during braking, would cause the rear suspension to

unload instead of squat. This indicated that it was likely that a relationship would be found between braking and suspension but, unless the dynamic effects of the rider and bike could be removed from the equation, it could not be solely attributed to the rear suspension design.

7.1.2 Trail Tests: Collecting a Large Quantity of Data

The next round of testing was performed under real world riding conditions to get an idea of what trends might be visible and to determine if the response to braking could be isolated from undesired external inputs using statistical methods. The theory is that if the suspension response from the trail only, not related to braking forces, could be assumed random then, with enough data, statistical methods could be used to identify any suspension response that did not appear to be randomly distributed. By comparing data for the same run with brakes applied (independent variable) and with no brakes applied (control) the difference in suspension action could be presumably attributed to the braking force being applied. As discussed earlier, dynamic considerations complicate this simplification of the problem. However, since bikes are always subjected to similar dynamic forces during braking, the comparison can still provide valuable insight into the performance of the suspension design under typical operating conditions. **Figure 7.2** shows braking torque and suspension position data during a 3 minute run on a downhill section of trail in San Luis Obispo. The time series of the run is useful for identifying any logical inconsistencies, such as brake force data indicating heavy braking while travelling backwards. These inconsistencies are important to keep in mind while working with the data in Matlab. It is probable that such unlikely data will be rejected when developing numerical relationships.

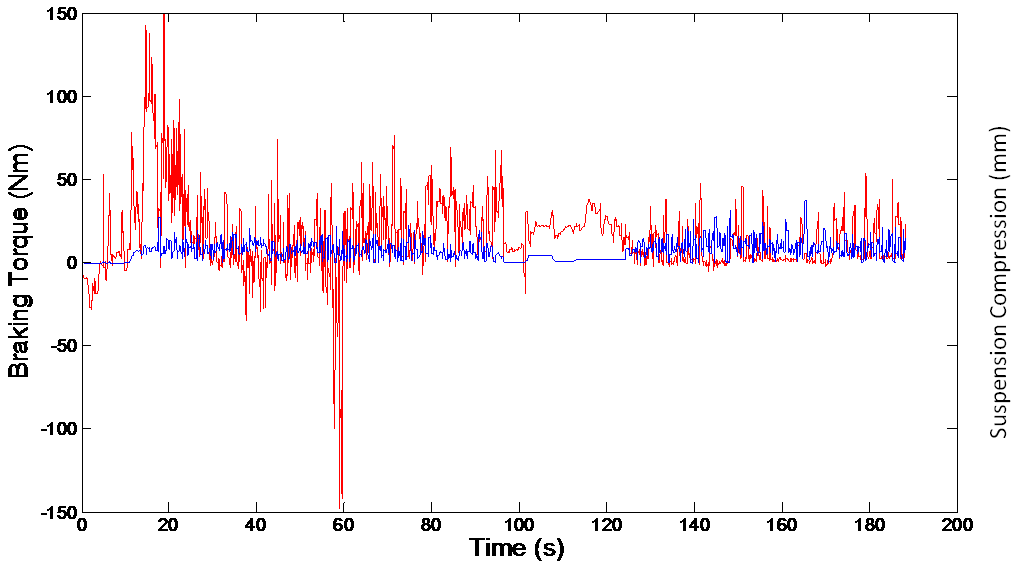

Figure 7.2 – Braking (blue) and suspension (red) data during a trail decent. Data has been converted to physical units using calibration values.

The calibration constants were applied to the raw data in Matlab. This produced a braking torque series, in Nm, and a suspension position series, in mm. All other series' are derived from these.

7.1.3 Braking Torque vs. Suspension Position

A scatter plot of braking torque and suspension position (**Figure 7.3**) shows every data point collected from the morning glory test run.

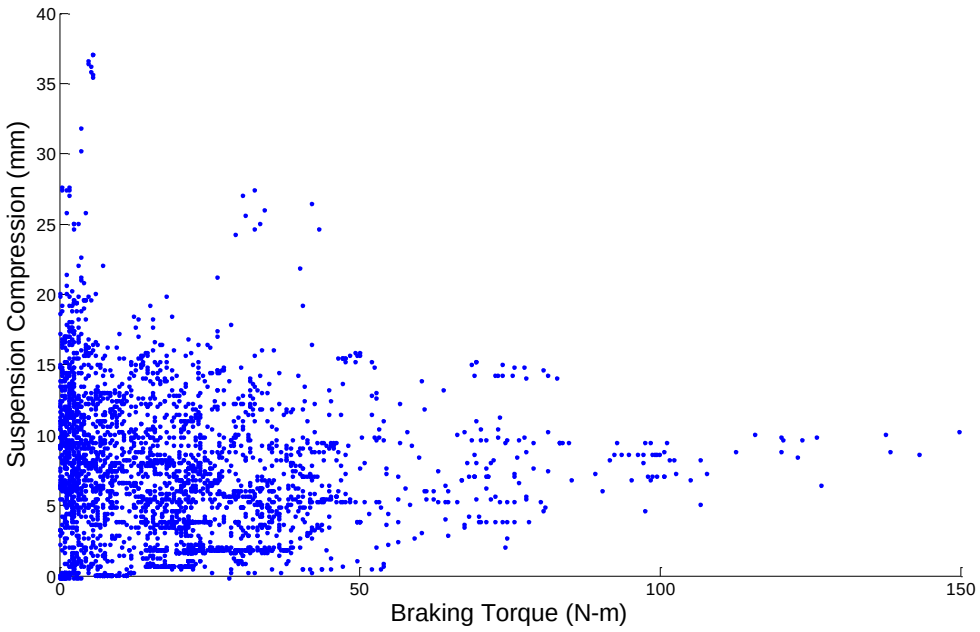

Figure 7.3 - Scatter plot of suspension position at various braking torques.

Several qualitative observations were noticed. First, the data appears to exhibit a positive, roughly liner, correlation between braking torque and suspension compression; the harder the brakes were applied the more the suspension compressed, similar to the way a spring compresses proportionately to the applied force. This is consistent with earlier test results that demonstrate a tendency to squat under braking. The correlation suggests that a practical relationship between the braking forces and the suspension compression, including dynamic effects, could be determined in the same way a spring constant is determined. On flat, smooth pavement, with a constantly applied braking torque and fixed rider position, there should be one point of compression at which the rider weight, braking torque, spring force and dynamic deceleration forces are in equilibrium. In a series of experimental data, this point of compression is the average suspension position at a given torque range. A visual estimate of the braking torque-suspension compression relationship (**Figure 7.3)** is about 1mm of compression for every 40 Nm of applied braking torque.

Second, the quantity of data points at high braking torque is much lower, with very few data points over 110 N-m. The reason becomes clear when analyzing the braking response curves from the strain gauges. Only the peak values of braking torque rise above 100 N-m, with the limit for sustained braking torque at roughly 60 N-m. This is believed to represent the braking threshold for static friction between the tire and ground. Torque above 60 N-m will typically cause the rear tire to lose traction and skid, thus producing kinetic friction and lowering the opposing force from the rear wheel. Braking torque

spikes above 60 N-m are possible due to the angular momentum of the wheel itself. Even if the wheel were brought up to speed in a bench test with no contact to the ground, a sharp application of the brake would likely produce a spike that exceeds 60 N-m, as the impulse needed to decelerate the rotating mass to zero in a very short amount of time requires a large force input.

Finally, the distribution of the data is much narrower at higher braking torques, with the minimum and maximum values spanning a smaller range of suspension positions than at lower braking torque. This is perhaps most critical to the project. The implication is that, besides the squat induced during braking, the brakes may be limiting the suspension's ability to respond to terrain inputs, which should show up as a random distribution of points at various compression positions. This is further investigated by looking at the suspension velocity over the torque range.

Looking at position data gives an idea of the absolute compression of the suspension as well as the range of movement recorded at various braking inputs. A look at velocity data can indicate the speed at which the suspension is able to move at various braking inputs. If braking forces were locking up the suspension and causing brake jack it would appear as much lower velocity. The velocity series, determined using a three point forward difference technique, was plotted against braking torque to produce **Figure 7.4**.

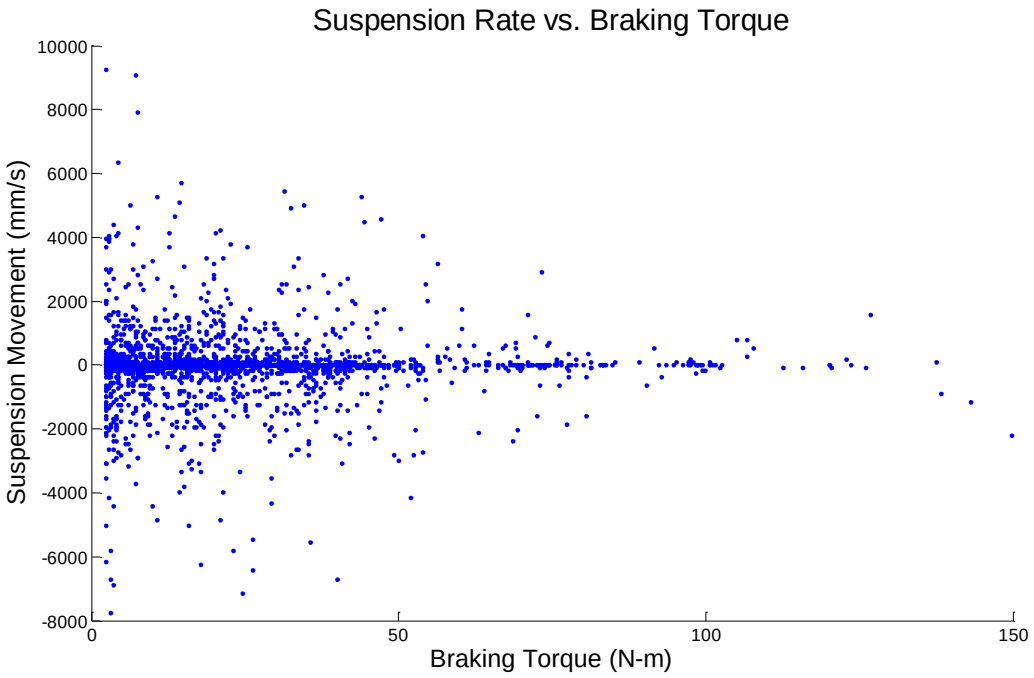

Figure 7.4 - The rate of suspension position change at various braking torque can indicate how the suspension is performing through the braking range.

The data collected seemed to suggest that under heavy braking the suspension experienced a reduced range of suspension rates. To provide a basis for statistical analysis the data was averaged into bins and plotted to produce a curve fit (**Figure 7.5**).

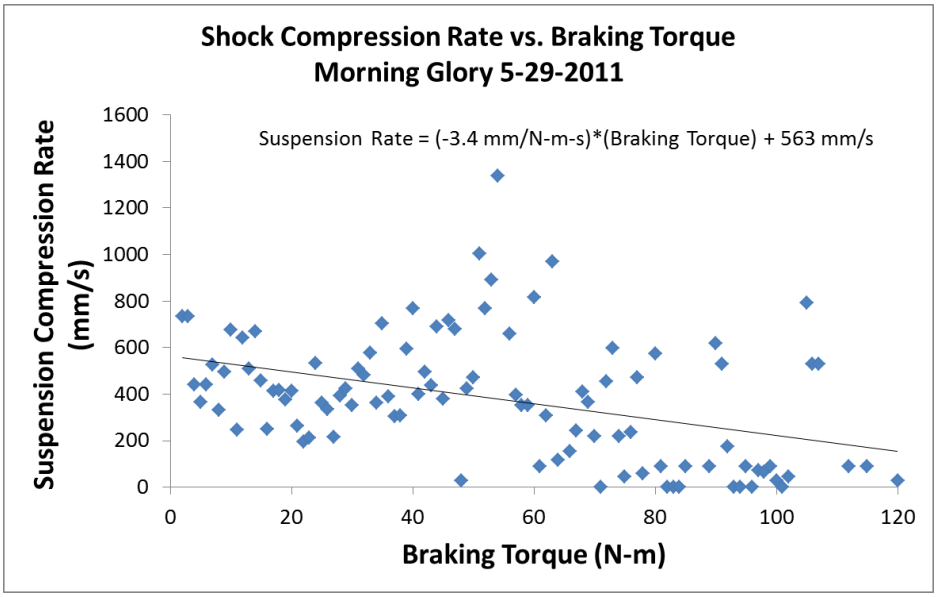

Figure 7.5 - To develop the suspension to braking torque relationship the data is binned and averaged so that regressions analysis can be performed.

The liner fit indicates a negative correlation of about 340 mm/s for every 100 N-m. This results in an average suspension rate that is 40% slower at 100 N-m braking torque than it is under no braking load. Further testing will attempt to verify and determine the cause but the apparent reduction cannot yet be attributed to braking forces. Of perhaps greater importance is the maximum and minimum compression rates that the suspension is capable of during braking, since they reflect the ability of the suspension to respond to impulses from the terrain. In order to properly compare the values at different torques there should be an equal number of samples across the spectrum of braking torque, so the values displayed in **Figure 7.5** are not sufficient for a direct comparison. Instead, the data in each bin was analyzed to determine a standard deviation as well as an average. The 3rd standard deviation was used to represent the maximum compression rate at each braking torque (**Figure 7.6**). Bins with fewer than 10 sample points were ignored. Ideally, the minimum number of samples in any bin would be no less than 20 to maintain statistical significance using the Student T test.

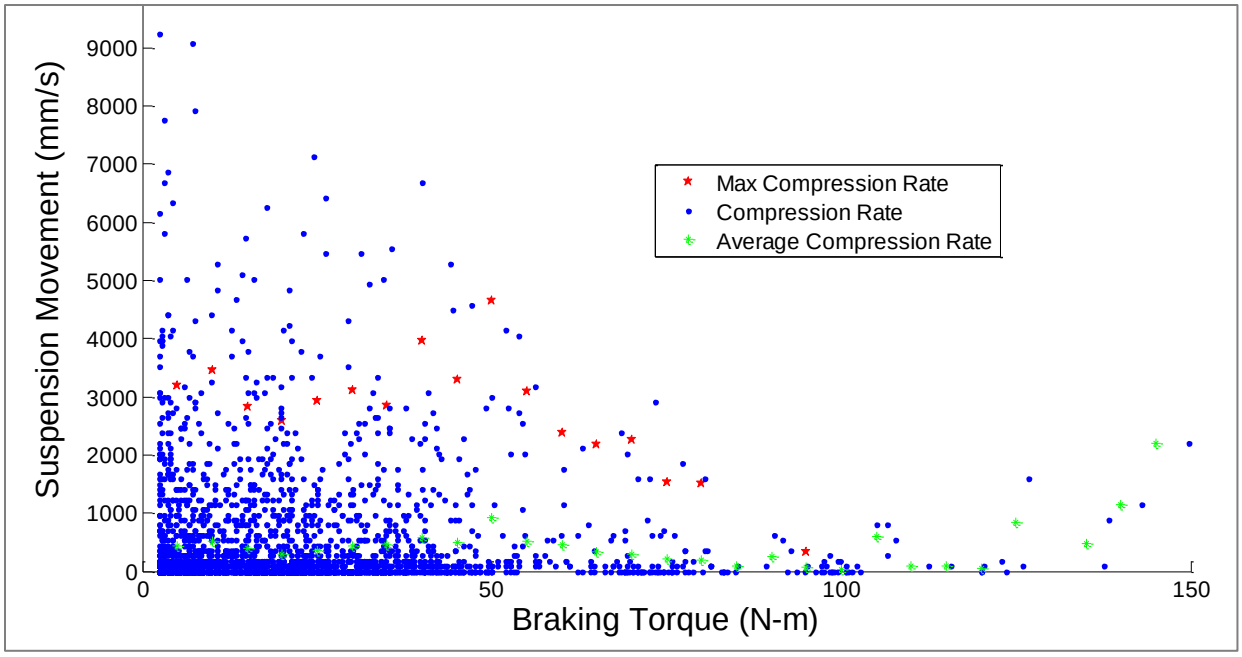

Figure 7.6 - Statistical methods are used to identify maximum and average compression rates in bins of various sample sizes.

Both the average and the maximum scatter plots seem to have a fairly constant trend until braking reaches 60 N-m, where they begin to slope in a negative correlation. As mentioned previously, this may represent a significant threshold for the braking-suspension relationship and the point where the wheel begins to lock up. This point also marks a noticeable decline in the number of sample points recorded by the data acquisition system (**Figure 7.7**).

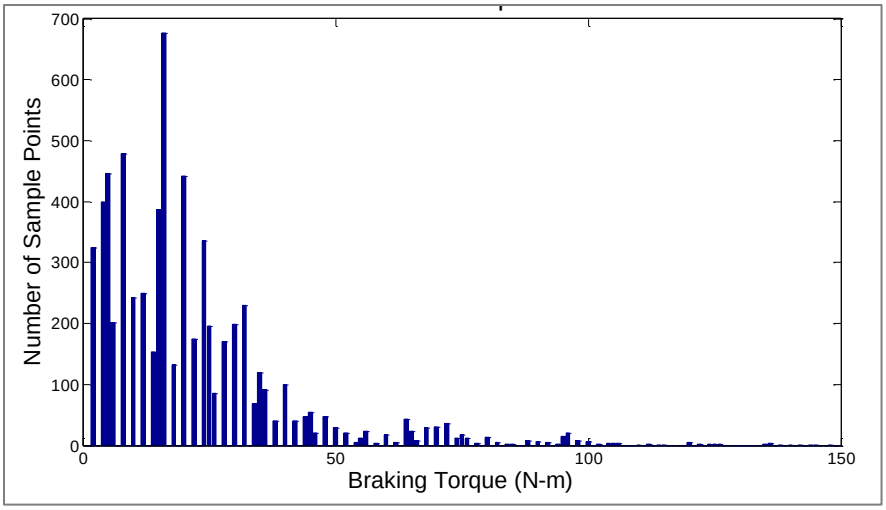

Figure 7.7 - The quantity of data points drops dramatically through the range of braking torque, possibly indicating the limit of traction.

If 60 N-m truly is the limit for traction then at higher torques a negative trail input (dip) would reduce normal force on the wheel, break traction, and plot any resulting suspension response at a lower braking torque. Likewise, a positive trail input (bump) would increase normal force and similarly effect braking torque, though it would be more likely for positive trail inputs to register in the higher torque ranges, potentially skewing the data in a positive correlation. To eliminate this possibility, baseline tests will be performed on smooth pavement to isolate the compression equilibrium point for an applied braking torque and each test rider. Next, testing will be performed on the trail test-course to identify the braking threshold. With these two factors identified for the test rider, trail testing can determine if there is a reduction in dynamic suspension response at higher braking torque. Data gathered while the wheel is locked up is not necessarily applicable to the development of the relationship the applied wheel forces are different when sliding over a rock as opposed to rolling over it.

7.2 Pedaling Forces vs. Suspension

Testing was performed to develop the instrumentation for the pedaling force to suspension response relationship. The tests were designed to isolate chain tension as the primary external force acting on the suspension members. By attempting to hold speed constant during the tests the moment caused by the acceleration of the center of mass is mitigated. Tests were performed with the rider seated and pedaling at a steady cadence to reduce the effect of rider movements on the suspension. To investigate the relationship without any trail inputs, testing was performed on smooth pavement. Choosing this terrain eliminates many variables, making chain tension due to pedaling force the one independent variable.

7.2.1 Flat Pavement Pedaling in Various Gears

Tests were performed in 3^{rd} – 10^{th} gears in a parking lot with a very slight grade. Each test consisted of 7 laps in a single gear. At the beginning and end of each run the rear brake was held and the pedals were pumped 3 times to allow for synchronization during post processing. This data was distilled in Matlab to produce similar comparisons as those in the braking testing. While the position and velocity relationships did not show any definitive relationships, the acceleration to suspension comparison was promising. This comparison is used to identify a cause and effect relationship between the rear wheel and the chain force. A simplified model of this is shown in **Figure 7.8** and is related to the fundamental kinematics behind the relationship in **Figure 7.9**.

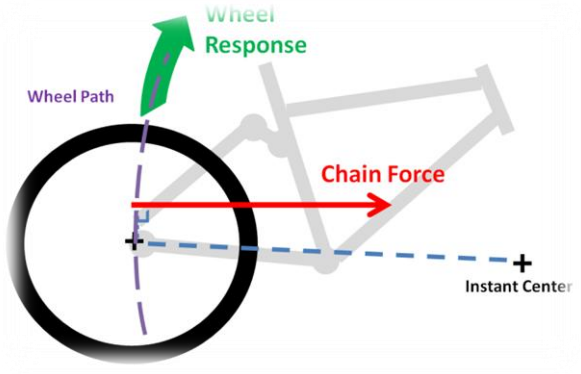

Figure 7.8 - Primary reactions at the rear suspension

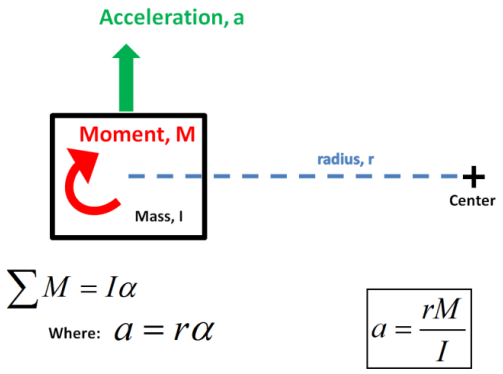

Figure 7.9 - A simplified kinematic model showing of Figure 7.8

The location of the instant center changes as the suspension moves through its travel. There is typically one point in the suspension travel for each gear where the chainline points directly through the instant center and therefore does not produce a moment on the suspension. Theoretically, this point in the suspension travel is the one point where the pedaling forces and suspension are truly independent. Everywhere else in the suspension travel there is a linkage position that is dependent on the suspension position. This leaves, at a minimum, 2 independent variables and one dependent variable that must be measured to develop a pedal force to suspension response relationship. For each point or, practically speaking, for each discrete range in the suspension travel, a relationship is developed for acceleration vs. pedal torque. When plotted this produces a 3D surface map with suspension position and pedaling torque axes in the horizontal plane and acceleration data vertically. Each of the horizontal axes is divided into discrete bins, creating a grid, and statistical analysis is performed for the data within each grid square to identify average acceleration, maximum acceleration, acceleration range, and standard deviation for uncertainty analysis. The data collected during these development tests was plotted in 2D, with only the pedal torque being considered as the independent variable. This limits the measured relationship to the specific rider and bike setup used during the tests, since a heavier rider or less shock pressure would set the suspension further into the travel and produce a different pedal force to suspension acceleration relationship. A sampling of these 2D trends is shown in the figures below for Gears 3 and 8. The full results can be found in **Appendix F**.

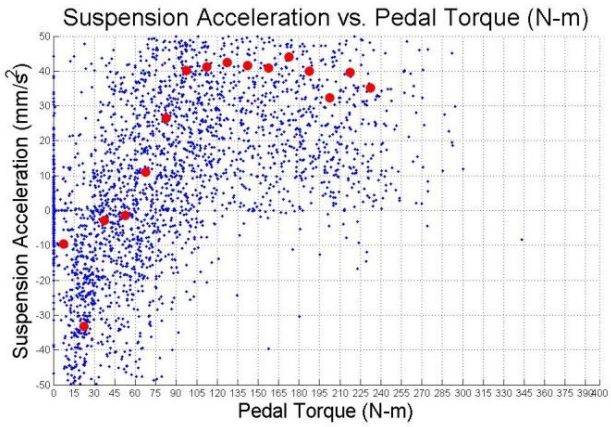

Figure 7.10 - Acceleration of the rear suspension vs. pedal torque input in Gear 3.

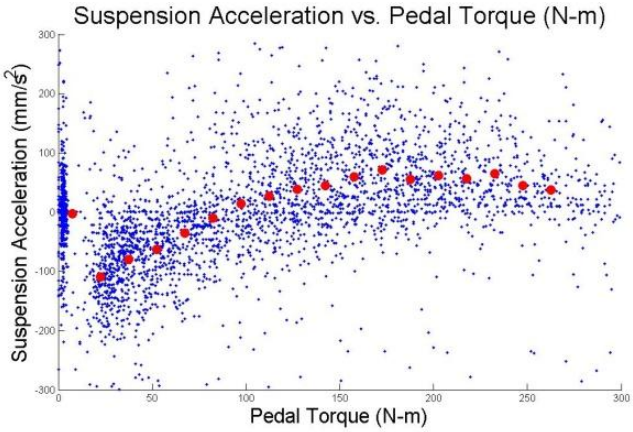

Figure 7.11 - Acceleration of the rear suspension vs. pedal torque in Gear 8.

Both tests were performed on level pavement. The curve for Gear 8 is much smoother because the higher gear allowed for a more consistent cadence and didn't forward surges, even under higher pedal forces. Gear 3 was low enough that high pedal torques caused the bike to surge forward, inducing undesirable and inconsistent results in the upper pedal torque ranges. This highlights the importance of maintaining a steady cadence and eliminating any acceleration of the center of mass that can cause a suspension response. The relationship map will not be complete until the suspension position is also tracked. In theory, any trend should intersect at zero since as pedaling torque approaches zero the suspension should not experience any acceleration. The 3D map should readily identify the neutral suspension position in each gear as the line where the surface intersects the zero acceleration plane.

7.2.2 Uphill Pavement Pedaling in Various Gears

To attempt to collect data and produce a trend for the lower gears tests were repeated on a steep paved hill, with about a 10% grade. When analyzed, the data from these runs produced no identifiable trends; the distribution appeared to be a random. This is either indicative of suspension independence or is a result of too small of a sample size. Additional tests will clarify which explanation is true.

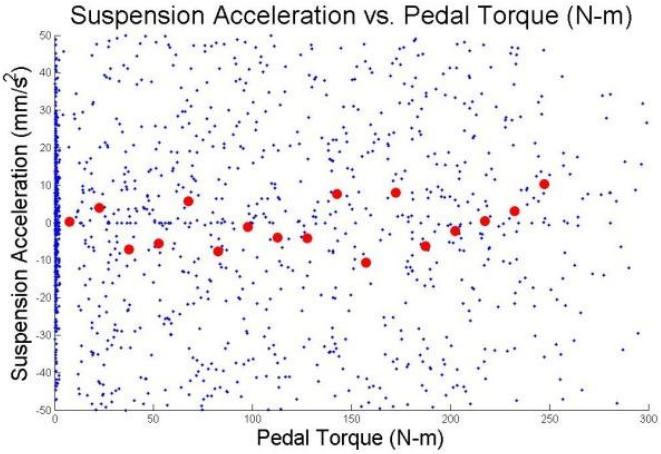

Figure 7.12 - Data taken during uphill testing in Gear 4 appears to be a random distribution.

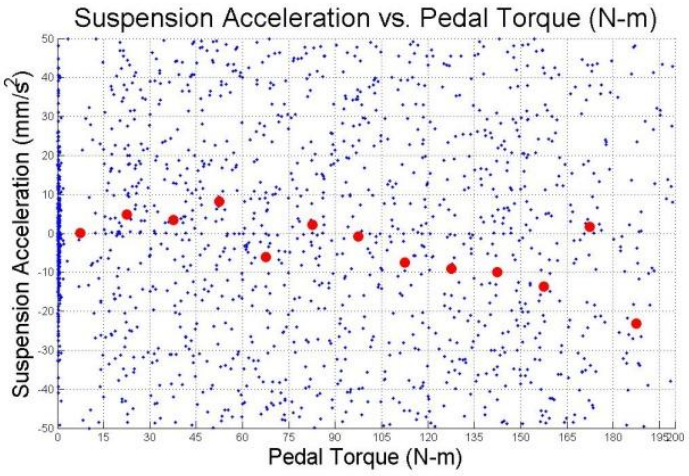

Figure 7.13 - Data taken in identical testing for Gear 5 also appears to be randomly distributed.

With the small sample size for each of these runs there is no apparent trend like there was in previous tests. **Figure 7.12** and **Figure 7.13** above show a textbook case of randomly distributed data, with a squared residual value below 0.2.

8. Future Work

Now that Senior Project class is done, Chris D'Elia, Greg Hermansen, and Dr. Mello (project advisor) will continue work on the project as individual study. For the Winter 2012 quarter, Kathleen Kramer will work with Chris and Greg to transfer information about the project.

8.1 Project Status to Date

At the completion of the Senior Project several primary objectives were completed. A data acquisition system was created, tested, and refined. This process included instrument selection, installation, calibration, and ensuring accurate capture of instrument signals. Once it was proven that the data acquisition worked properly, a Matlab program was written to post process the collected data. The program synced the two time dependant arrays, filtered the data, and output the required graphs for comparison. Lastly, initial braking and pedaling tests were conducted. A full set of pedaling results were produced for one gear, including the ultimate metric for comparison, suspension acceleration per unit pedaling force.

8.2 Project Re-definition:

In a meeting with the sponsor on February 10, 2012, the scope of the project was reduced to only include analysis of braking forces and their effect on suspension behavior. The test apparatus will no longer collect pedaling force data, although it still can be collected if desired.

8.3 Next steps

8.3.1 DAQ

Since pedaling forces will no longer be collected, only one data acquisition board is needed. Chris will replace the Swoop Board with a Logomatic V2 board that will collect all required data. This eliminates the need for syncing the timing of the two data acquisition boards in Matlab. Chris will also replace the current frequency-to-voltage converter with a smaller board that will fit inside the aluminum housing box.

8.3.2 Metric for Comparison

A single value must be produced from the collected and analyzed data to rate how effectively the rear suspension geometry isolates braking forces from suspension behavior. This metric will be used to compare different rear suspension designs. At the end of Senior Project a metric of "rear suspension acceleration per unit braking force" was chosen. The previously determined metric needs to be studied to determine if it is the most appropriate metric to use as a base comparison.

8.3.3 Bench Testing

A bench test will be created to obtain initial results for the effect of braking forces on rear suspension behavior. One idea for a bench test set up includes using a treadmill to simulate rear wheel movement on the ground. The front end of the bike will be secured so that the rear wheel rests on the

treadmill belt and is free to move when the treadmill does. Weights will be secured to the saddle to simulate rider weight. This set up would allow for controllable, repeatable rear wheel speeds. Disturbances may be added by securing protrusions to the treadmill belt. Once the bench test is refined a test method will be developed.

8.3.4 Outdoor Testing

Once the bench testing method has been refined and can produce verifiable results, an outdoor test will be developed. The bench testing results will serve as a basis for outdoor testing since test variables will be harder to control during outdoor testing. Outdoor testing should produce results that follow the same trends as the bench testing results.

8.3.5 Test Method

A test method must be written to ensure repeatable testing procedures that will produce results that can be compared between multiple bikes. Developing the test method will be an on-going task and will be finalized when the bench tests and outdoor tests are finalized.

8.3.6 Final Testing and Comparison of Results

After the bench and outdoor tests are refined, and a final test method is completed, official testing of bikes can begin. Results will be obtained for the 2011 Specialized Stumpjumper EVO first and then the test apparatus will be moved to other bikes. All of the testing will culminate to produce one metric for each bike. This metric will be compared between all bikes to rank the effectiveness of each rear suspension design at isolating braking forces from suspension behavior.

9. References

1. Circuits Today. “Frequency to Voltage converter circuit based on the TC9400 IC.” Circuits Today, December 6, 2011. http://www.circuitstoday.com/frequency-to-voltage-converter.

2. Fargo Controls Inc. “Inductive Sensor Operating Principles”, December 5, 2011. http://www.fargocontrols.com/sensors/inductive_op.html.

3. Jeff Baltes, Cory Sutela, and Rob Redfield. “Development of a Freeride Mountain Bike Suspension Fork.” Sports Technology 1, no. 2-3 (2008): 152-165.

4. Ken Sasaki, Peter Ejvinsson, José Rubio, and Gergely Kovacs. “Path Analysis.” Path Analysis, 2001. http://www.rdrop.com/~/twest/mtb/pathAnalysis/.

5. Michael Stanfill. “Physics of Bicycle Suspension - About”, 2010. http://ffden-2.phys.uaf.edu/211_fall2010.web.dir/Michael_Stanfill/About.html.

6. Mike Levy. “Luis Arraiz - K9 Designer and Suspension Guru - Pinkbike.com.” Pink Bike, February 17, 2011. http://www.pinkbike.com/news/luis-arraiz-interview-2011.html.

7. Radek Burkat. “Different Strokes - Decoding the marketing hype of rear-suspension designs by Radek - Pinkbike.com.” Pink Bike, February 3, 2006. http://radek.pinkbike.com/blog/mike-ferrentino-different-strokes.html.

8. Sam Pickman. “Interview with Sam Pickman, Test Engineer”, March 3, 2011.

9. Specialized Bicycle Components. “Specialized Suspension Sciences.” Specialized, December 5, 2011. http://cdn.specialized.com/bc/microsite/suspension/suspension.html.

10. SRM. “SRM Power Meters”, December 5, 2011. http://www.srm.de/us/home.

11. “This is ANT, the Wireless Sensor Network Solution”, December 5, 2011. http://www.thisisant.com/.

12. Vishay Micro-Measurements. “Instruction Bulletin B-134-4”. Vishay Micro-Measurements, February 4, 2005.

13. “Vishay Precision Group - Micro-Measurements - Home Page”, December 5, 2011. http://www.vishaypg.com/micro-measurements/.

Appendix

Appendix A – QFD, List of Tasks, Gantt Chart, and Indented Bill of Materials

Table A.1 - Quality Function Design (QFD) chart

Engineering Requirements

Customer Requirements	weighting (1 to 5)			<5% weight increase	< 30 min step up time		Sample rate/ resolution	resolution: degrees	resolution: Watts (%)	resolution: Newtons		wireless/mobile		
reliable data	5			3			9	9	9	9				
chain tension	5						9							
brake action	5									9				
pedal action	5									9				
input power	5								9					
output power	5								9					
suspension position	5						9	9						
geometry changes	5						9	9						
test in field	5			3	9							9		
test in lab	2			3								1		
data communication	5			9	1							3		
light weight apparatus	5			9								9		
adaptable test apparatus	5				9		9	9	9	9		9		
Units														
Targets														
Benchmark #1														
Benchmark #2														
Importance Scoring		0	0	126	95	0	225	180	180	180	0	152	0	0
Importance Rating (%)		0	0	56	42	0	100	80	80	80	0	68	0	0

Table A.2 - List of specifications developed from QFD requirements

Specification	Parameter	Requirement	Tolerance	Risk
1	Set up time	Less than 30 minutes	10 minutes	High
2	Weight	Less than 7.5% increase	0.2 %	High
3	Suspension position measurement resolution	0.5 mm	0.1 mm	Medium
4	Angle measurement resolution	1 degree	0.1 degree	Medium
5	Power measurement resolution	2 watts	0.1 watt	Medium

Table A.3 - List of tasks, their required completion date, and their completion status.

Task	Due Date	Completed?
Skype with Sam	Every Thursday, 10:00 AM	On going
Project Introduction Letter	1/11/2011	Yes
Visit the sponsor	1/20/2011	Yes
Project Requirements Document	2/3/2011	Yes
Brainstorm solutions	2/10/2011	Yes
Visit the sponsor	2/16/2011	Yes
Concept Design Review	3/1/2011	Yes
Concept Model	Week of March 8, 2011	Yes
Conceptual Design Report	3/10/2011	Yes
Figure out DAQ	5/1/2011	Yes
Obtain preliminary bikes	3/25/2011	Yes
Acquire Instrumentation	6/6/2011	Yes
Have bikes instrumented	7/26/2011	Yes
Finish Testing round 1	11/7/2011	Yes
Print Expo Poster	11/28/2011	Yes
Senior Project Expo	12/1/2011	Yes
Finish Final Report	12/5/2011	Yes
Present to sponsor	12/8/2011	Yes

Table A.4 - Gantt chart of the tasks listed in Table A3 of the appendix.

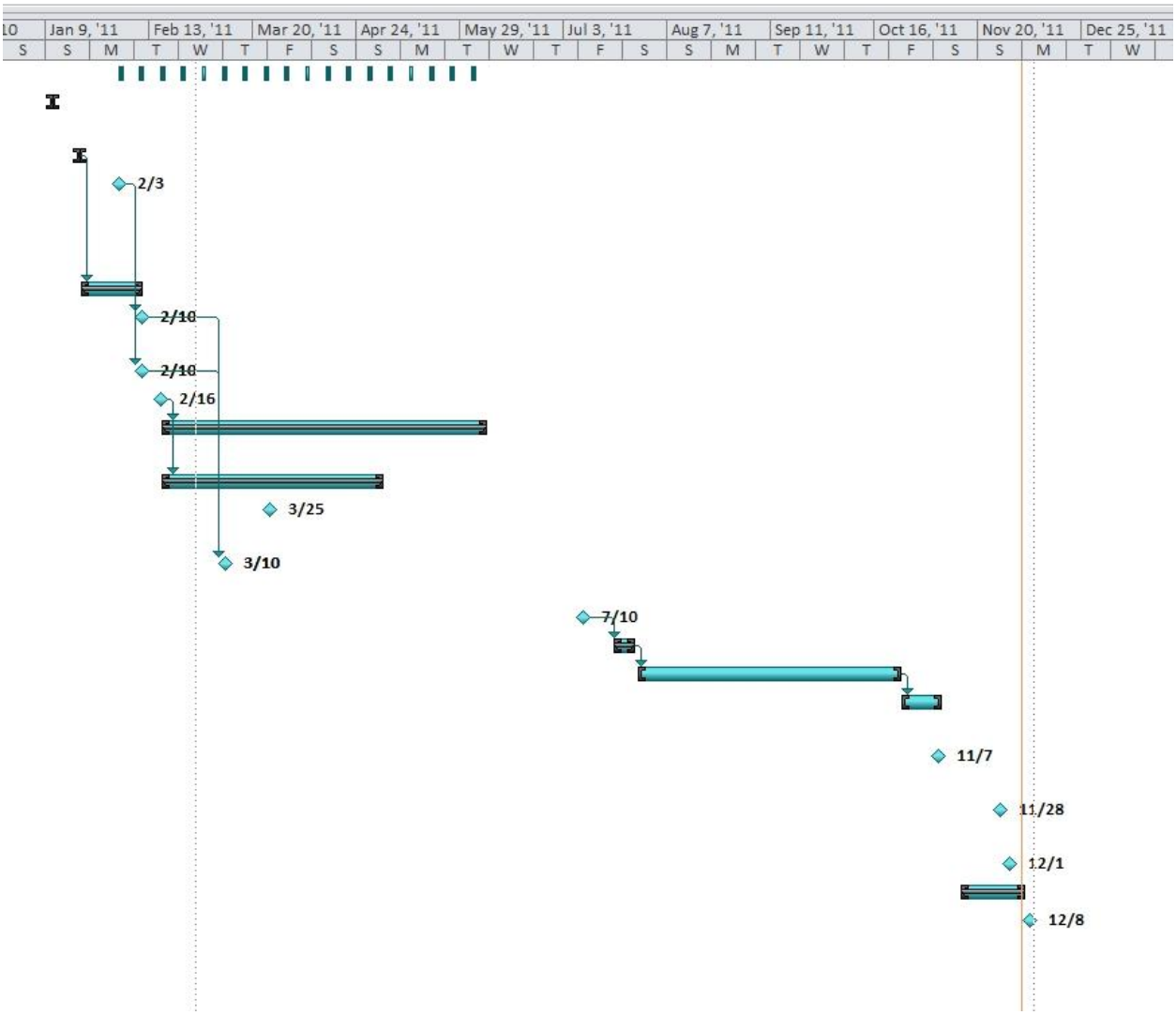

Table A.5 - Indented Bill of Materials for FSR Sensor Array.

Indented Bill of Material (BOM)

FSR Sensor Array

Assembly Level	Part Number	Description			Vendor	Qty	Cost	Ttl Cost
		Level 0	Level 1	Level 2				
0	100000	Final Assy			------			
1	101000		Board and Housing Assembly		------			
2	101001			Metal box	RadioShack	1	$5.00	$5.00
2	101002			Swoop Board	Calpoly	1	$30.00	$30.00
2	101003			9V battery	Energizer	1	$1.00	$1.00
2	101004			Screws	CrownBolt	4	$0.25	$1.00
1	101005		Suspension Movement Sensor Assy		------			
2	101006			String Potentiometer	Celesco	1	$600.00	$600.00
2	101007			Pulley	SDP	1	$11.30	$11.30
2	101008			Nut	CrownBolt	1	$0.02	$0.02
2	101009			Mounting Braket	N/A	2	$5.00	$10.00
2	101010			Bolt	CrownBolt	1	$0.03	$0.03
1	101011		Wheel Speedometer Assembly		------			
2	101012			Hall Effect Sensor	Celesco	2	$0.03	$0.06
2	101013			Mounting Braket	N/A	2	$5.00	$10.00
2	101014			Bolt	CrownBolt	4	$0.25	$1.00
2	101015			Nut	CrownBolt	4	$0.25	$1.00
1	101016		Pedal Forces Sensor Assembly		------			
2	101017			Strain Gauges	MM	4	$0.21	$0.84
2	101018			Op Amp	RadioShack	1	$1.19	$1.19
2	101019			Resistor	RadioShack	1	$0.24	$0.24
2	101020			Battery	UnionBattery	1	$11.95	$11.95
2	101021			Sparkfun micro-computer	Sparkfun	1	$75.00	$75.00
1	101022		Braking Forces Sensor Assembly		------			
2	101023			Strain Gauges	MM	1	$0.21	$0.21
2	101024			Modified Brake Adaptor	Specialized	1	$20.00	$20.00
1	101025		Speedometer Circuit Assembly		------			
2	101026			Resistors	RadioShack	26	$0.24	$6.24
2	101027			Capacitors	RadioShack	6	$0.95	$5.70
2	101028			Potentiometers	RadioShack	5	$1.69	$8.45
2	101029			Beadboard	RadioShack	1	$14.99	$14.99
2	101030			Voltage Regulator	RadioShack	2	$1.79	$3.58
2	101031			Op Amp	RadioShack	4	$1.19	$4.76
2	101032			Mosfet	RadioShack	2	$2.19	$4.38
2	101033			TC9400 IC	Microchip	2	$8.71	$17.42
2	101034			9V battery	Energizer	2	$1.00	$2.00
Total Parts						**85**		**$847.35**

Appendix B – Raw Calibration Data

Strain Gauges / Braking Torque

Table B.1 - (Below) Recorded actual masses of the masses used for calibration.

mass#	mass (kg)
1	1.103
2	1.167
3	1.095
4	1.131
5	1.085
6	2.46
7	2.403
8	4.504
9	4.58
10	11.152

Table B.2 - (Right) Strain at each mass, recorded by P3

mass #s	mass (kg)	strain
1	1.103	41
6	2.46	90
3-6	3.555	127
8	4.504	159
3-8	5.599	194
6-8	6.964	239
1-6-8	8.067	276
8-9	9.084	310
1-8-9	10.187	347
10	11.152	378
4-10	12.283	416
6-10	13.612	464
4-7-10	14.686	501
9-10	15.732	535
5-9-10	16.817	574
7-9-10	18.135	621
5-7-9-10	19.22	664
8-9-10	20.236	702
5-8-9-10	21.321	746
7-8-9-10	22.639	800
5-7-8-9-10	23.724	855
6-7-8-9-10	25.099	903
5-6-7-8-9-10	26.184	946
6-7-8-9-10	25.099	915
7-8-9-10	22.639	832
8-9-10	20.236	759
8-9-10	20.236	657
5-6-7-8-9-10	26.184	845
6-7-8-9-10	25.099	810
7-8-9-10	22.639	725
8-9-10	20.236	658
7-8-10	18.059	584
9-10	15.732	508
6-10	13.612	443
10	11.152	364
8-9	9.084	299
6-8	6.964	230
8	4.504	150
6	2.46	81
1	1.103	34
10	11.152	361

Figure B.1 - Method for applying a known torque to the wheel, which is counteracted by the braking torque, involved hanging known masses from a rope wrapped around the rim. This creates a force that acts tangentially at a known radius for all trials.

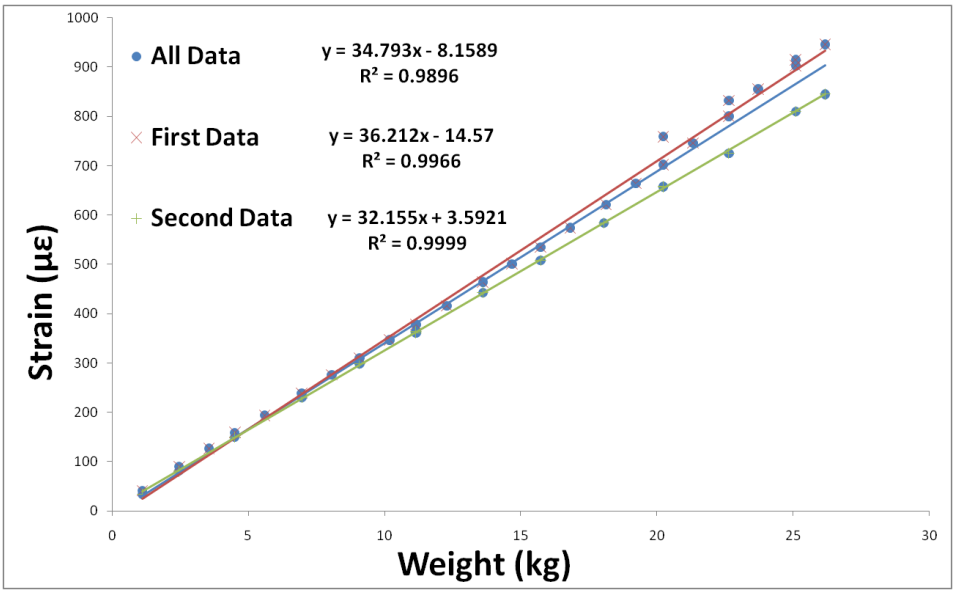

Figure B.2 - Strain recorded by the P3 box with various masses hung from the wheel

Table B.3 – A/D counts recorded as each mass was applied to the wheel and the corresponding torque in N-m.

mass #s	A-D	mass (kg)	Torque (N-m)
0	565	0.0	0.0
2	571	1.2	3.2
7	580	2.4	6.6
7,3	588	3.5	9.6
9	596	4.6	12.6
9,2	604	5.7	15.8
9,7	613	7.0	19.2
9,7,3	621	8.1	22.2
9,7,3,2	628	9.2	25.4
9,8,2	635	10.3	28.2
9,8,7	645	11.5	31.6
9,8,7,2	651	12.7	34.8
9,8,7,2,3	659	13.7	37.8
9,8,7,2,3,5	667	14.8	40.7
9,8,7,2,3,4,5	674	16.0	43.9

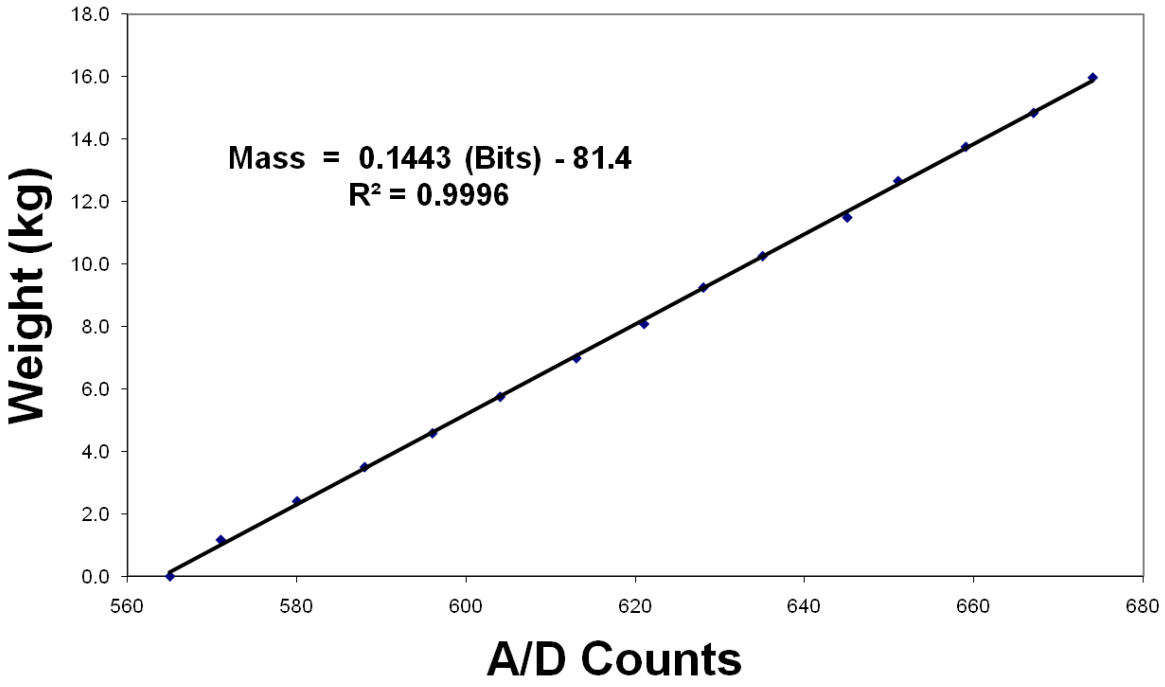

Figure B.3 - Calibration from A/D counts, recorded by the Swoop board, to the known mass applied. This can easily be converted to torque using the mass, gravity and the known radius

Rotary Potentiometer / Suspension Position

Figure B.4 - Calibration from A/D counts, recorded by the Swoop board, to the measured compression of the shock in mm.

Table B.4 – A/D counts recorded at each shock compression position and the fit for the first, second and third order. Interestingly the linear fit was the closest fit to the actual data in all cases

File Name	Bit Count	Compression (mm)	Linear Fit Prediction	2nd Order Fit Prediction	3rd Order Fit Prediction
Data_001.txt	532	0	-0.5	10.3	-15.9
Data_002.txt	521	2	1.7	12.1	-13.2
Data_003.txt	507	4	4.5	14.4	-9.8
Data_004.txt	491	7	7.6	17.1	-5.7
Data_005.txt	482	9	9.4	18.5	-3.4
Data_006.txt	467	12.5	12.4	21.0	0.5
Data_007.txt	449	16	16.0	24.0	5.2
Data_008.txt	435	18.5	18.8	26.3	8.9
Data_009.txt	416	22.5	22.6	29.5	13.8
Data_010.txt	399	26	26.0	32.4	18.2
Data_011.txt	384	30	29.0	34.9	22.0
Data_012.txt	365	34	32.8	38.1	26.7
Data_013.txt	350	36	35.8	40.7	30.3
Data_014.txt	330	40	39.8	44.1	35.0
Data_015.txt	309	43.5	44.0	47.7	39.6
Data_016.txt	291	47	47.6	50.8	43.3
Data_017.txt	284	49	49.0	52.0	44.6

Appendix C – List of Vendor contact information and pricing

Specialized Bicycle Components

15130 Concord Circle
Morgan Hill, CA 95037
(877) 808-8154
(408) 779-6229
http://www.specialized.com

CycleOps

5253 Verona Road
Madison, WI 53711
Phone: (800) 783-7257
http://www.cycleops.com

Nu Horizons Electronics Corp.

70 Maxess Road
Melville, NY 11747
Phone: (631) 396-5000
Fax: (631) 396-5050
1-888-747-NUHO (6846)
http://www.nuhorizons.com

ANT Wireless

#201, 100 Grande Blvd.
Cochrane, Alberta Canada
T4C 0S4
Phone: (403) 932-9292
Fax: (403) 932-4196
Email: info@thisisant.com
http://www.thisisant.com

Micro-Measurements/Vishay

Vishay Precision Group
3 Great Valley Parkway
Suite 150
Malvern, PA 19355
Phone: +1-484-321-5300
Fax: +1-484-321-5301
Email: corporate@vishaypg.com
http://www.vishaypg.com

Dr. John Ridgely

Associate Professor of Mechanical Engineering
California Polytechnic State University
San Luis Obispo, California 93407
(805) 756-1303
jridgely@calpoly.edu
http://www.calpoly.edu/~jridgely/

Radio Shack

#01-3510
481 MADONNA RD STE A
SAN LUIS OBISPO, CA 93405
Phone: (805) 544-5400
http://www.radioshack.com

Celesco

20630 Plummer Street
Chatsworth, CA 91311
Tel: 1.818.701.2750
• 800.423.5483 [US only]
Fax: +1.818.701.2799
email: info@celesco.com
http://www.celesco.com/

Appendix D - Component Specifications and Datasheets

Datasheet Strain Gauges

Brake bridge strain gauges

Crank spider bridge strain gauges

Datasheet Vishay M-Coat F Protective Coating

M-Coat F

Vishay Micro-Measurements

Protective Coating

FEATURES

- Excellent for outdoor applications
- No cure required
- Versatile

DESCRIPTION

Kit of selected materials easily applied in various combinations. Provides environmental and mechanical protection. Particularly well-suited to field applications where conditions are not ideal. Typical applications include pipelines, tunnels, bridges, reinforcement bars in concrete structures, heavy machinery, ships, aircraft, motor vehicles, and pressure vessels.

CHARACTERISTICS

Cure Requirements:
No mixing or curing required.

Operating Temperature Range:
Short Term: –70° to +250°F [–55° to +120°C].
Long Term: –20° to +175°F [–30° to +80°C].

Shelf Life:
1 year at +75°F [+24°C].

PACKAGING OPTIONS

Kit:
12 pieces (3-3/4 in square x 1/8 in T [95 x 3.2 mm]) each:
• M-Coat FB Butyl Rubber Sealant
• M-Coat FN Neoprene Rubber Sheets

1 roll (0.003 in x 2 in x 20 ft [0.08 mm x 50 mm x 6 m])
M-Coat FA Aluminum Foil Tape

2 brush-cap bottles (1/2 oz [15 ml] ea)
M-Coat B Air-Drying Nitrile Rubber Coating

M-Coat FT Teflon® Tape

Bulk:
M-Coat FB-2 Butyl Rubber Sealant — 25 pieces

M-Coat FN-2 Neoprene Rubber Sheets — 25 pieces

M-Coat FA-2 Aluminum Foil Tape — 20-ft [6-m] roll

M-Coat B Air-Drying Nitrile Rubber Coating —
4 brush-cap bottles (1 oz [30 ml] ea)

M-Coat FT Teflon® Tape
1-x-20-x-0.003-in [25-x-500-0.08-mm] — 10 pieces

Teflon is a Registered Trademark of DuPont.

Datasheet Inductive Proximity Sensor

FARGO CONTROLS, INC.

Inductive

8 mm Diameter DC 3 Wire

FEATURES:

- Stainless steel case
- Short circuit & reverse polarity protection
- Protection degree IP67: dust tight and protection from the effects of immersion
- LED function indicator
- +100° C high temperature version available upon request
- 3.5, 5, 7.5 and 10 meter cable lengths available upon request

		MODEL		
Output Function	NPN, NO	S3440	S3014E	S3740
	NPN, NC	S3441	S3015E	S3741
	PNP, NO	S3442	S3016E	S3742
	PNP, NC	S3443	S3017E	S3743
Dimensions: mm 1 mm = .03937" CE		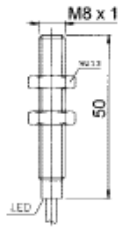	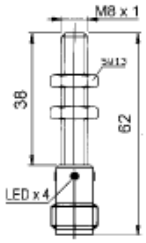	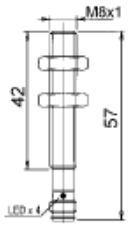
Operating Distance (Sn)		2 mm		
External Diameter		M 8 x 1		
Power Supply		10 - 30 Vdc		
Max Switching Current		200 mA max		
Power Drain (24Vdc)		< 12 mA		
Voltage Drop		< 1.8 V		
Short Circuit Protection		Yes		
Operating Frequency		2 kHz		
Repeatability (%Sn)		≤ 3%		
Hysteresis (%Sn)		< 10%		
Case		Stainless Steel		
Flush Mounting		Yes		
Protection Degree		IP 67		
Operating Temperature		- 25 to +70 °C*		
Output Connection		Cable PVC, L=2m	Connector C	Connector C1

* +100° C high temperature version available upon request

WIRING:

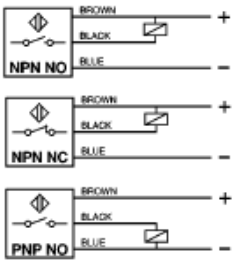

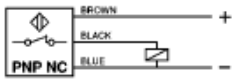

CONNECTOR:

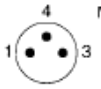

Male connector C1
1= brown/+
3= blue/-
4= black/output NO-NC

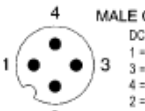

MALE CONNECTOR C
DC 3 wire
1 = brown +
3 = blue -
4 = black output NO-NC*
2 = white output NC

* In the 3 wire sensors with type C connector and NC output the pins 2 & 4 are internally wired together

FARGO CONTROLS, INC.

Inductive

8 mm Diameter DC 3Wire "Short Series"

FEATURES:

- Stainless steel case
- Short circuit & reverse polarity protection
- Protection degree IP67: dust tight and protection from the effects of immersion
- LED function indicator
- +100° C high temperature version available upon request
- 3.5, 5, 7.5 and 10 meter cable lengths available upon request

		MODEL			
Output Function	NPN, NO	S3020	S3650	S3024	S3654
	NPN, NC	S3021	S3651	S3025	S3655
	PNP, NO	S3022	S3652	S3026	S3656
	PNP, NC	S3023	S3653	S3027	S3657
Dimensions: mm 1 mm = .03937" 		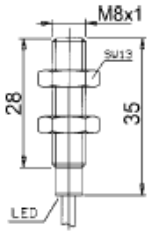	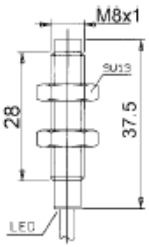	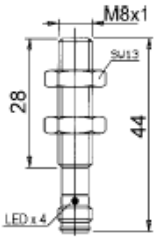	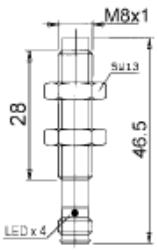
Operating Distance (Sn)		**2mm**	**3 mm**	**2 mm**	**3 mm**
External Diameter		M8 x 1			
Power Supply		6 - 30 Vdc			
Max Switching Current		200 mA			
Power Drain (24Vdc)		< 12 mA			
Voltage Drop		< 1.8			
Short Circuit Protection		Yes			
Operating Frequency		2 kHz			
Repeatability (%Sn)		≤ 3%			
Hysteresis (%Sn)		< 10%			
Case		Stainless Steel			
Flush Mounting		Yes	No	Yes	No
Protection Degree		IP 67			
Operating Temperature		- 25 to +70 °C *			
Output Connection		Cable PVC: L = 2 m		Connector C1	

* +100° C high temperature version available upon request

MATING CONNECTORS:

ID#	Type	Description
S3494	C	right angle w/ 2 meter cable
S3495	C	right angle w/ 5 meter cable
S3497	C	straight w/ 2 meter cable
S3498	C	straight w/ 5 meter cable
S3480	C1	right angle w/ 5 meter cable
S3481	C1	straight w/ 5 meter cable

MOUNTING FOR NON-FLUSH SENSORS:

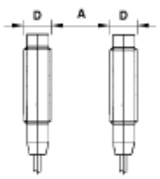

Side by side mounting
A ≥ 2D

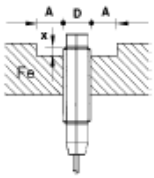

Non flush mounting
A ≥ 2D X ≥ 0mm

Datasheet Rotary Potentiometer

Potentiometer Specs	
Model	271-1721
Type	Audio-Taper
Resistance	Up to 10K ohm
Power Rating	.05 W
Tolerance	20%
Max Voltage	250 VDC
Built-in Devices	1-11/16” long x 1-1/4” diameter shaft
Recommended Through hole use	5/16” diameter
Misc.	Nut and washer included

Datasheet Linear Potentiometer

Linear Potentiometer

Miniature • Extended Temperature Range

Ranges: 0-.5 to 0-6 inches [0-12,5 to 0-150 mm]

1.25K – 10K ohms • IP67

MLP

Specification Summary:

GENERAL

Full Stroke Ranges ..... 0-0.5 to 0-6 in. (0-12.5 to 0-150 mm)
Output Signal..... voltage divider (potentiometer)
Linearity..... ± 0.5% full stroke
Repeatability ..... .0.01 mm
Resolution..... essentially infinite
Life Expectancy..... > 25 million cycles
Operating Speed ..... 400 inches (10 M) per second max.
Enclosure Material ..... aluminum
Sensor..... conductive plastic linear potentiometer
Weight ..... 1.6 oz. (46 g) max., *see ordering information*

ELECTRICAL

Input Resistance..... 1.25K to 10K ohms (±20%), *see ordering information*
Recommended Maximum Input Voltage ..... 42 VDC
Recommended Operating Wiper Current..... < 10µA
Electrical Cable ..... 24 AWG Raychem 55M wire with VITON sleeve
Electrical Cable Length ..... 19 inches (500mm)

ENVIRONMENTAL

Enclosure Design IP67
Operating Temperature, *Continuous* ..... -22° to 300°F (-30° to 150°C)
Operating Temperature, *Short Term* ..... 350°F (175°C)
Vibration ..... up to 10 G's to 2000 Hz maximum

Celesco's miniature MLP series linear potentiometers offer unrivaled performance in an amazingly small size. Though small, the MLP is environmentally robust (IP67), operates over a broad temperature range (-22° to 300°F) and is long lasting (>25 million cycles).

These features make our miniature MLP linear potentiometer the perfect solution for many applications including industrial, medical, automotive and motion control.

Ordering Information:

Item Number:	MLP-12	MLP-25	MLP-50	MLP-75	MLP-100	MLP-125	MLP-150
measurement range, in. [mm]:	0.5 [12.5]	1 [25]	2 [50]	3 [75]	4 [100]	5 [125]	6 [150]
resistance, ohms (±20%):	1.25K	2.5K	5.0K	7.5K	6.5K	8.0K	10.0K
linearity, %:	± 0.5%	± 0.5%	± 0.5%	± 0.5%	± 0.5%	± 0.5%	± 0.5%
weight, oz. [grams]:	.8 [24]	.9 [26]	1 [29]	1.2 [33]	1.3 [37]	1.5 [43]	1.6 [46]

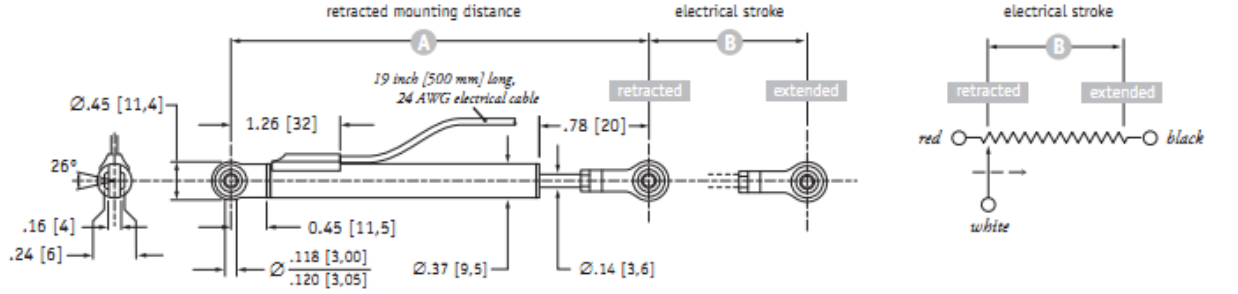

Measurement Range	0.5 12.5	1 25	2 50	3 75	4 100	5 125	6 150	in mm
A	3.3 82.5	3.7 95	4.7 120	5.7 145	7.0 178	8.0 203	9.0 228	± 0.08 in adjustment ± 2 mm adjustment
B	0.49 12.5	0.98 25.0	1.97 50.0	2.95 75.0	3.94 100.0	4.92 125.0	5.91 150.0	in mm

All Dimensions are in INCHES [MM] • Tolerances are 0.03 in. [0.5 mm] unless otherwise noted

version: 1.0 last updated: January 15, 2007

celesco
celesco.com • info@celesco.com
Celesco Transducer Products, Inc.
20630 Plummer Street • Chatsworth, CA 91311
tel: 800.423.5483 • +1.818.701.2750 • fax: +1.818.701.2799

Datasheet String Potentiometer

Precision Potentiometric Output Ranges: 0-3, 0-9, 0-15, 0-30 inches Test Applications • Wet Environments

MT3A-9L-14-10K-

MT3A

CE

Specification Summary:

GENERAL

Full Stroke Ranges ..... 0-3, 0-9, 0-15, 0-30 inches, min., *see ordering information*
Output Signal ..... voltage divider (potentiometer)
Accuracy ..... ±1.1 to 0.25% full stroke, *see ordering information*
Repeatability ..... ± 0.02% full stroke
Resolution ..... essentially infinite
Measuring Cable ..... Ø.019-in. nylon-coated stainless steel
Enclosure Material ..... anodized aluminum
Sensor Cover ..... polycarbonate
Sensor ..... conductive plastic-hybrid potentiometer
Weight ..... 0.5 lb. max.

ELECTRICAL

Input Resistance ..... 10K ohms (± 10%)
Power Rating, Watts ..... 2.0 at 70° C (derated to 0 @ 125°C)
Recommended Maximum Input Voltage ..... 30V (AC or DC)
Output Signal Change Over Measurement Range ..... 94% ±4% of input voltage

MECHANICAL

Measuring Cable Tension Options ..... *see ordering information*
Maximum Measuring Cable Acceleration ..... *see ordering information*

ENVIRONMENTAL

Enclosure ..... NEMA 4 / IP67
Operating Temperature ..... -40° to 250°F (-40° to 125°C)

The MT3A is the solution for high-acceleration test applications in potentially wet environments. Just like the MT2A, the MT3A comes in 4 different full-stroke ranges, has a high-tension heavy-duty measuring cable designed for the demands of flight and automotive crash tests and comes with an easy to use 2-axis 360° rotation mounting bracket for installation in hard to fit areas.

For extreme high impact applications, the MT3A is now available with a rugged all aluminum sensor cover!

Outline Drawing

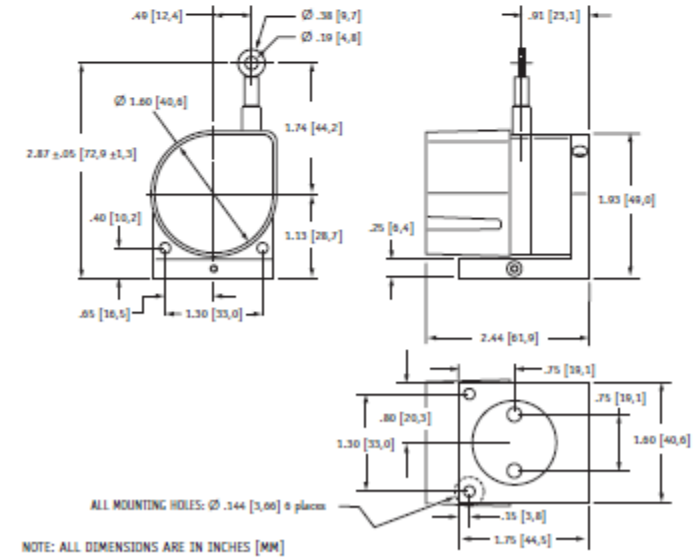

Output Signal

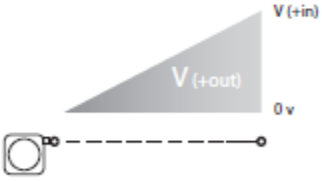

Schematic

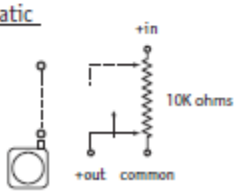

celesco
celesco.com • info@celesco.com

Celesco Transducer Products, Inc.
20630 Plummer Street • Chatsworth, CA 91311
tel: 800.423.5483 • +1.818.701.2750 • fax: +1.818.701.2799

Ordering Information:

Model Number:

MT3A - 9 L - 14 - 10K - C

order code: ① Ⓐ Ⓑ Ⓒ

Sample Model Number:

MT3A - 9E - 33 - 10K - C1A

① range: 9 inches
Ⓐ measuring cable termination: eyelet
Ⓑ measuring cable tension: 33 oz. (±6 oz.)
Ⓒ electrical connection: 15-ft cable w/end-mountad strain relief/aluminum cover

Full Stroke Range:

① order code:

	3	9	15	30
full stroke range, min:	3 inches	9 inches	15 inches	30 inches
potentiometer cycle-life:	2.5 x 10^6	8.3 x 10^5	5.0 x 10^5	2.5 x 10^5
accuracy (% of full stroke):	1.1 %	.25%	.25%	.25%

Measuring Cable Termination:

Ⓐ order code:

E — Eyelet

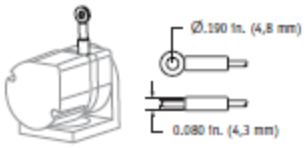

L — Leader Cable (24 in. long)

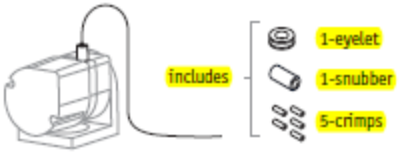

Measuring Cable Tension:

Ⓑ order code:

	9	14	33
tension:	9 (±2) oz.	14 (±4) oz.	33 (±6) oz.
max. cable acceleration:	17 G's	50 G's	90 G's

Electrical Connection/ Sensor Cover:

Ⓒ order code:

	C1	C1A	C4	C4A	C2	C2A	C5	C5A
sensor cover:	polycarbonate	aluminum	polycarbonate	aluminum	polycarbonate	aluminum	polycarbonate	aluminum
electrical cable length:	15 ft (4.5 m)		30 ft (9 m)		15 ft (4.5 m)		30 ft (9 m)	

end-mount strain relief

side-mount strain relief

Ⓒ order code:

	C3	C3A	C6	C6A	BC	BCA
sensor cover:	polycarbonate	aluminum	polycarbonate	aluminum	polycarbonate	aluminum
electrical cable length:	15 ft (4.5 m)		30 ft (9 m)		n/a	n/a

top-mount strain relief

blank cover*

Signal Connection Color Code

color	signal
Red	+In
Black	common
Green	+out

24 gauge, shielded

** **blank cover** option is for customers who want to provide their own connector or strain relief. This cover comes without electrical wiring access holes so customer can drill to their requirements.*

version:8.0 last updated: October 14, 2010

Datasheet Idler Pulley

sdp INCH

Grooved Idler Pulleys

■ MOLDED OR STEEL WITH STEEL BALL BEARINGS ■ HEAVY-DUTY

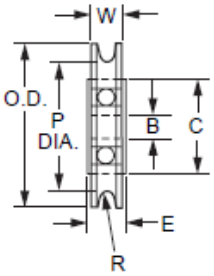

Fig. 1

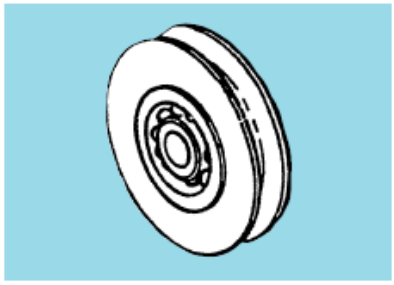

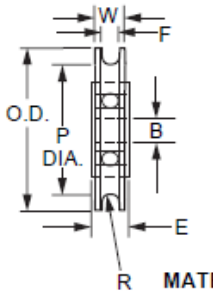

Fig. 2

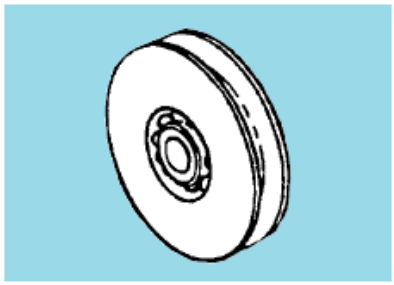

MATERIAL: **Pulley** - Nylon
Bearing - Steel, Ball – Precision Machined

2 BELTS AND CHAIN DRIVES

• Fig. 1 MOLDED PULLEYS

Catalog Number	P. Dia. ±.020	O.D. ±.020	B Bore +.005 -.001	W Width ±.010	E Length ±.010	C Dia.	R Radius Ref.	For Max. Cable Dia.	Load Rating lbs. @ 500 rpm
A 6Z 9-00804	.437	.500	.125	.125	.156	.375	.025	3/64	10
A 6Z 9-01004	.500	.625				.375	.015	1/32	
A 6Z 9-01204	.625	.750		.156	.156	.375	.025	3/64	10
*A 6Z 9-01604	.813	1.000			.171	.500			35
A 6Z 9-01706	.885	1.070	.187	.219	.250	.687	.025	3/64	35
A 6Z 9-01708			.250						
A 6Z 9-02006	1.063	1.250	.187	.219	.250	.687	.035	1/16	45
A 6Z 9-02008			.250						
A 6Z 9-02408	1.250	1.500	.250	.281	.312	1.000	.050	3/32	80
A 6Z 9-02412			.375						70
A 6Z 9-02808	1.373	1.750	.250	.281	.312	1.000	.065	1/8	80
A 6Z 9-02812			.375						70

* Supplied with a shielded bearing and a bore tolerance of ± .0005.

MATERIAL: **Pulley** - Steel, Case-Hardened Races, Machined Raceways
Bearing - Balls – Precision Steel
Finish - Zinc Plated

• Fig. 2 STEEL PULLEYS

Catalog Number	P. Dia. ±.005	O.D. +.000 -.010	B Bore +.005 -.000	W Width ±.005	E Length ±.005	F ±.005	R Radius	For Max. Cable Dia.	Load Rating lbs. @ 50 rpm
A 6C 9-00804	.375	.500	.125	.156	.188	.096	.025	3/64	36
A 6C 9-01606	.750	1.000	.187	.312	.375	.165	.065	1/8	145
A 6C 9-01706	.875	1.063	.187	.250	.282	.190	.050	3/32	175
A 6C 9-02008	.875	1.250	.250	.375	.438	.250	.095	3/16	175
A 6C 9-02812	1.250	1.750	.375	.438	.500	.315	.125	1/4	290
A 6C 9-03212	1.500	2.000							410

2–241

Datasheet INA122 Bridge Amplifier

BURR-BROWN®

INA122

Single Supply, *Micro*Power INSTRUMENTATION AMPLIFIER

FEATURES

- LOW QUIESCENT CURRENT: 60µA
- WIDE POWER SUPPLY RANGE
  Single Supply: 2.2V to 36V
  Dual Supply: –0.9/+1.3V to ±18V
- COMMON-MODE RANGE TO (V–)–0.1V
- RAIL-TO-RAIL OUTPUT SWING
- LOW OFFSET VOLTAGE: 250µV max
- LOW OFFSET DRIFT: 3µV/°C max
- LOW NOISE: 60nV/√Hz
- LOW INPUT BIAS CURRENT: 25nA max
- 8-PIN DIP AND SO-8 SURFACE-MOUNT

APPLICATIONS

- PORTABLE, BATTERY OPERATED SYSTEMS
- INDUSTRIAL SENSOR AMPLIFIER:
  Bridge, RTD, Thermocouple
- PHYSIOLOGICAL AMPLIFIER:
  ECG, EEG, EMG
- MULTI-CHANNEL DATA ACQUISITION

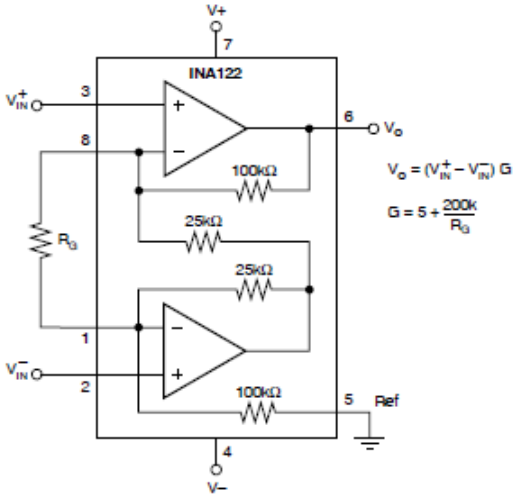

$V_O = (V_{IN}^+ - V_{IN}^-)\,G$

$G = 5 + \frac{200k}{R_G}$

DESCRIPTION

The INA122 is a precision instrumentation amplifier for accurate, low noise differential signal acquisition. Its two-op-amp design provides excellent performance with very low quiescent current, and is ideal for portable instrumentation and data acquisition systems.

The INA122 can be operated with single power supplies from 2.2V to 36V and quiescent current is a mere 60µA. It can also be operated from dual supplies. By utilizing an input level-shift network, input common-mode range extends to 0.1V below negative rail (single supply ground).

A single external resistor sets gain from 5V/V to 10000V/V. Laser trimming provides very low offset voltage (250µV max), offset voltage drift (3µV/°C max) and excellent common-mode rejection.

Package options include 8-pin plastic DIP and SO-8 surface-mount packages. Both are specified for the –40°C to +85°C extended industrial temperature range.

International Airport Industrial Park • Mailing Address: PO Box 11400, Tucson, AZ 85734 • Street Address: 6730 S. Tucson Blvd., Tucson, AZ 85706 • Tel: (520) 746-1111 • Twx: 910-952-1111
Internet: http://www.burr-brown.com/ • FAXLine: (800) 548-6133 (US/Canada Only) • Cable: BBRCORP • Telex: 066-6491 • FAX: (520) 889-1510 • Immediate Product Info: (800) 548-6132

PDS-1388B

Printed in U.S.A. October, 1997

SPECIFICATIONS

At T_A = +25°C, V_S = +5V, R_L = 20kΩ connected to V_S/2, unless otherwise noted.

PARAMETER	CONDITIONS	INA122P, U			INA122PA, UA			UNITS
		MIN	TYP	MAX	MIN	TYP	MAX	
INPUT								
Offset Voltage, RTI			±100	±250		±150	±500	µV
vs Temperature			±1	±3		*	±5	µV/°C
vs Power Supply (PSRR)	V_S = +2.2V to +36V		10	30		*	100	µV/V
Input Impedance			10^{10} ‖ 3			*		Ω ‖ pF
Safe Input Voltage	R_S = 0	(V–)–0.3		(V+)+0.3	*		*	V
	R_S = 10kΩ	(V–)–40		(V+)+40	*		*	V
Common-Mode Voltage Range		0		3.4	*		*	V
Common-Mode Rejection	V_{CM} = 0V to 3.4V	83	96		76	90		dB
INPUT BIAS CURRENT			–10	–25		*	–50	nA
vs Temperature			±40			*		pA/°C
Offset Current			±1	±2		*	±5	nA
vs Temperature			±40			*		pA/°C
GAIN			G = 5 to 10k			*		V/V
Gain Equation			$G = 5 + 200k\Omega/R_G$			*		V/V
Gain Error	G = 5		±0.05	±0.1		*	±0.15	%
vs Temperature	G = 5		5	10		*	*	ppm/°C
Gain Error	G = 100		±0.3	±0.5		*	±1	%
vs Temperature	G = 100		±25	±100		*	*	ppm/°C
Nonlinearity	G = 100, V_O = –14.85V to +14.9V		±0.005	±0.012		*	±0.024	%
NOISE (RTI)								
Voltage Noise, f = 1kHz			60			*		$nV/\sqrt{Hz}$
f = 100Hz			100			*		$nV/\sqrt{Hz}$
f = 10Hz			110			*		$nV/\sqrt{Hz}$
f_B = 0.1Hz to 10Hz			2			*		µVp-p
Current Noise, f = 1kHz			80			*		$fA/\sqrt{Hz}$
f_B = 0.1Hz to 10Hz			2			*		pAp-p
OUTPUT								
Voltage, Positive	V_S = ±15V	(V+)–0.1	(V+)–0.05		*	*		V
Negative	V_S = ±15V	(V–)+0.15	(V–)+0.1		*	*		V
Short-Circuit Current	Short-Circuit to Ground		+3/–30			*		mA
Capacitive Load Drive			1			*		nF
FREQUENCY RESPONSE								
Bandwidth, –3dB	G = 5		120			*		kHz
	G = 100		5			*		kHz
	G = 500		0.9			*		kHz
Slew Rate			+0.08/–0.16			*		V/µs
Settling Time, 0.01%	G = 5		350			*		µs
	G = 100		450			*		µs
	G = 500		1.8			*		ms
Overload Recovery	50% Input Overload		3			*		µs
POWER SUPPLY								
Voltage Range, Single Supply		+2.2	+5	+36	*	*	*	V
Dual Supplies		–0.9/+1.3		±18	*	*	*	V
Current	I_O = 0		60	85		*	*	µA
TEMPERATURE RANGE								
Specification		–40		+85	*		*	°C
Operation		–55		+85	*		*	°C
Storage		–55		+125	*		*	°C
Thermal Resistance, θ_{JA}								
8-Pin DIP			150			*		°C/W
SO-8 Surface-Mount			150			*		°C/W

* Specification same as INA122P, INA122U.

PIN CONFIGURATION

Top View — 8-Pin DIP, SO-8

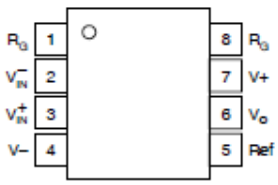

ABSOLUTE MAXIMUM RATINGS(1)

Supply Voltage, V+ to V–	36V
Signal Input Terminals, Voltage(2)	(V–)–0.3V to (V+)+0.3V
Current(2)	5mA
Output Short Circuit	Continuous
Operating Temperature	–40°C to +125°C
Storage Temperature	–55°C to +125°C
Lead Temperature (soldering, 10s)	+300°C

NOTES: (1) Stresses above these ratings may cause permanent damage. (2) Input terminals are internally diode-clamped to the power supply rails. Input signals that can exceed the supply rails by more than 0.3V should be current-limited to 5mA or less.

PACKAGE INFORMATION

PRODUCT	PACKAGE	PACKAGE DRAWING NUMBER(1)
INA122PA INA122P	8-Pin DIP 8-Pin DIP	006 006
INA122UA INA122U	SO-8 Surface Mount SO-8 Surface Mount	182 182

NOTE: (1) For detailed drawing and dimension table, see end of data sheet, or Appendix C of Burr-Brown IC Data Book.

ELECTROSTATIC DISCHARGE SENSITIVITY

This integrated circuit can be damaged by ESD. Burr-Brown recommends that all integrated circuits be handled with appropriate precautions. Failure to observe proper handling and installation procedures can cause damage.

ESD damage can range from subtle performance degradation to complete device failure. Precision integrated circuits may be more susceptible to damage because very small parametric changes could cause the device not to meet its published specifications.

TYPICAL PERFORMANCE CURVES

At T_A = +25°C and V_S = ±5V, unless otherwise noted.

GAIN vs FREQUENCY

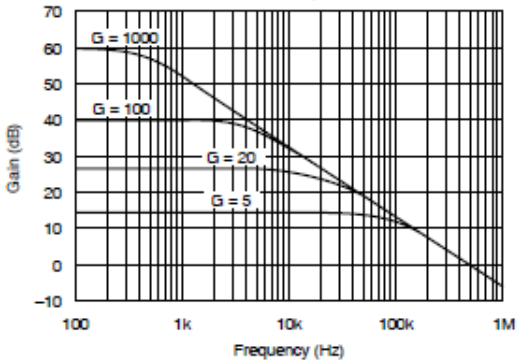

COMMON-MODE REJECTION vs FREQUENCY

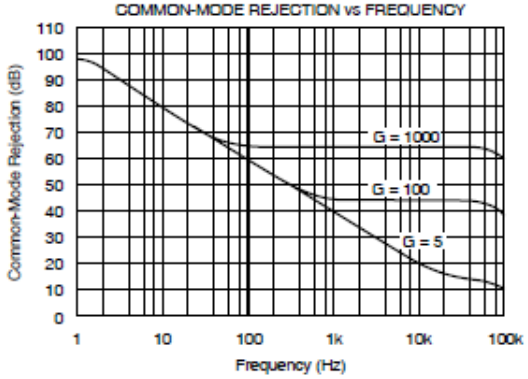

POSITIVE POWER SUPPLY REJECTION vs FREQUENCY

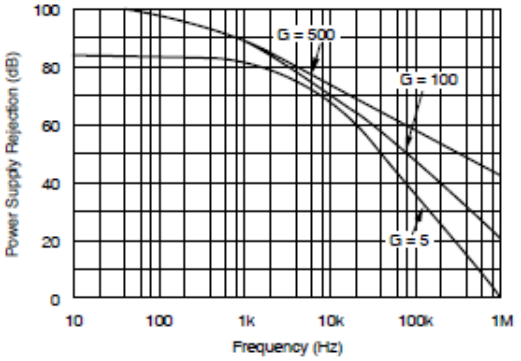

NEGATIVE POWER SUPPLY REJECTION vs FREQUENCY

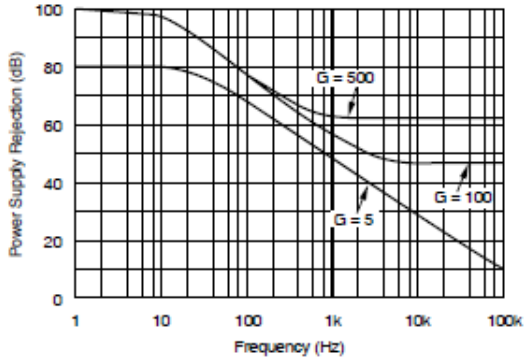

INPUT COMMON-MODE RANGE vs OUTPUT VOLTAGE, V_S = ±15V, G = 5

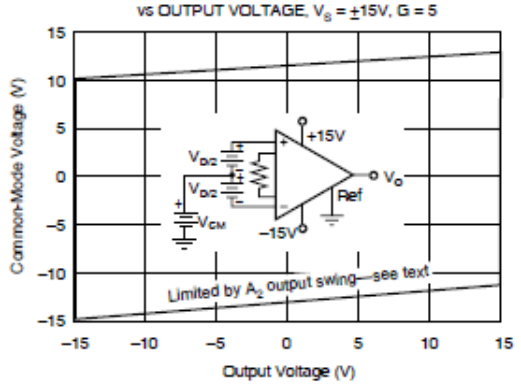

INPUT COMMON-MODE VOLTAGE vs OUTPUT VOLTAGE, V_S = ±5V, G = 5

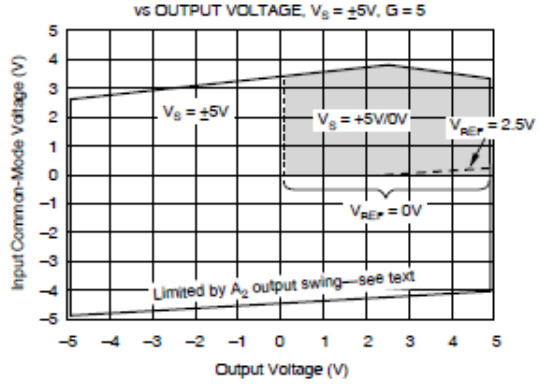

TYPICAL PERFORMANCE CURVES (CONT)

At T_A = +25°C and V_S = ±5V, unless otherwise noted.

VOLTAGE and CURRENT NOISE DENSITY vs FREQUENCY (RTI)

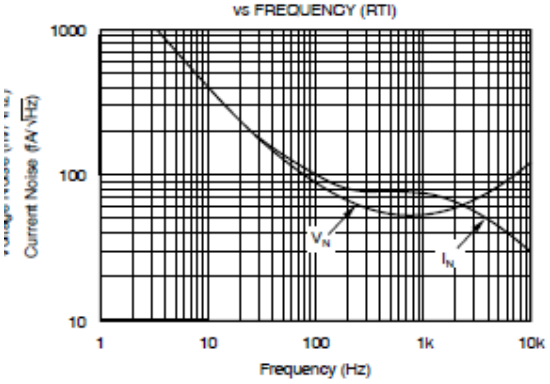

SETTLING TIME vs GAIN

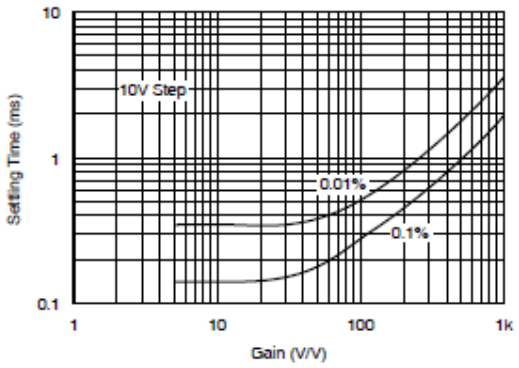

INPUT-REFERRED OFFSET VOLTAGE WARM-UP

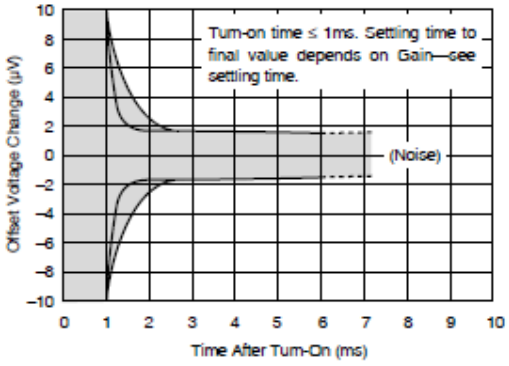

QUIESCENT CURRENT vs TEMPERATURE

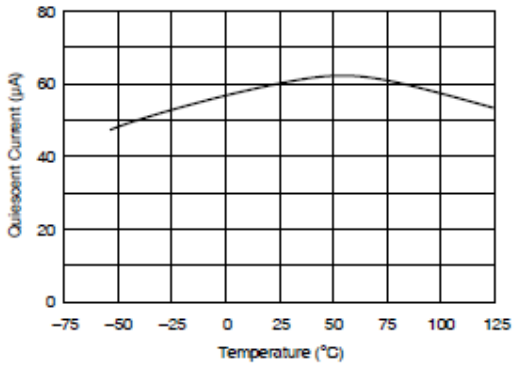

TOTAL HARMONIC DISTORTION+NOISE vs FREQUENCY

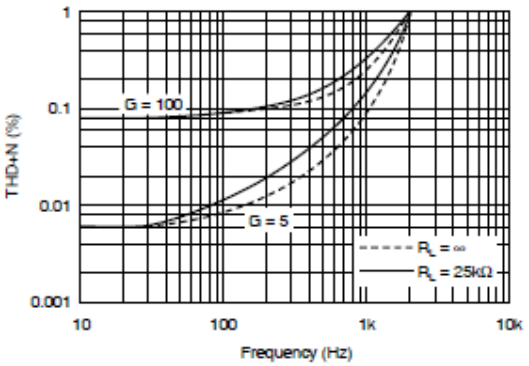

OUTPUT VOLTAGE SWING vs OUTPUT CURRENT

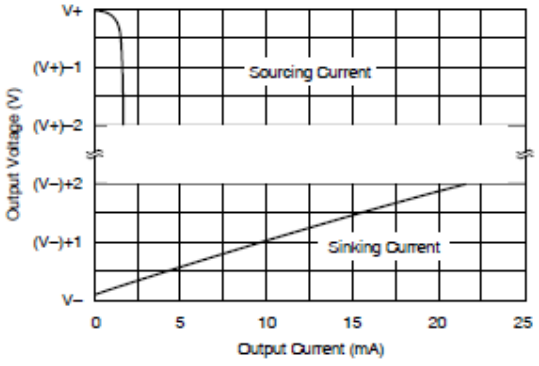

TYPICAL PERFORMANCE CURVES (CONT)

At T_A = +25°C and V_S = ±5V, unless otherwise noted.

SMALL-SIGNAL STEP RESPONSE
G = 5

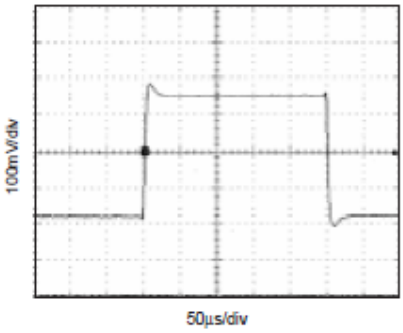

SMALL-SIGNAL STEP RESPONSE
G = 100

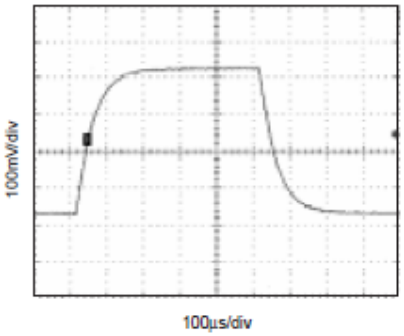

LARGE-SIGNAL STEP RESPONSE
G = 5

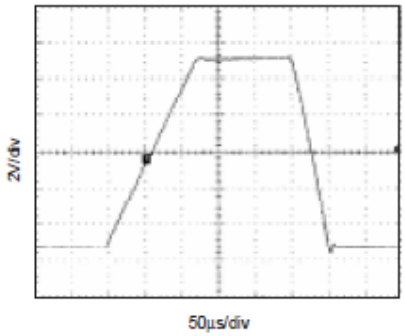

INPUT-REFERRED NOISE VOLTAGE
0.1Hz to 10Hz

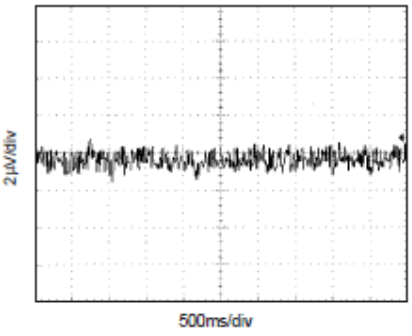

APPLICATION INFORMATION

Figure 1 shows the basic connections required for operation of the INA122. Applications with noisy or high impedance power supplies may require decoupling capacitors close to the device pins.

The output is referred to the output reference (Ref) terminal which is normally grounded. This must be a low-impedance connection to ensure good common-mode rejection. A resistance of 10Ω in series with the Ref pin will cause a typical device to degrade to approximately 80dB CMR.

SETTING THE GAIN

Gain of the INA122 is set by connecting a single external resistor, R_G, as shown:

$$G = 5 + \frac{200k\Omega}{R_G} \quad (1)$$

Commonly used gains and R_G resistor values are shown in Figure 1.

The 200kΩ term in equation 1 comes from the internal metal film resistors which are laser trimmed to accurate absolute values. The accuracy and temperature coefficient of these resistors are included in the gain accuracy and drift specifications of the INA122.

The stability and temperature drift of the external gain setting resistor, R_G, also affects gain. R_G's contribution to gain accuracy and drift can be directly inferred from the gain equation (1).

OFFSET TRIMMING

The INA122 is laser trimmed for low offset voltage and offset adjustment. Figure 2 shows an optional circuit for trimming the output offset voltage. The voltage applied to the Ref terminal is added to the output signal. An op amp buffer is used to provide low impedance at the Ref terminal to preserve good common-mode rejection.

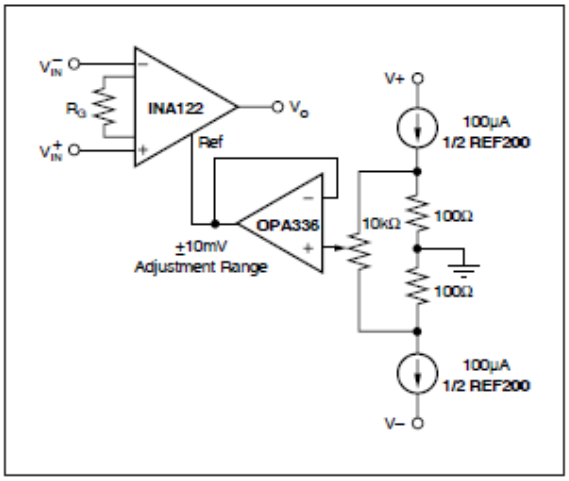

FIGURE 2. Optional Trimming of Output Offset Voltage.

INPUT BIAS CURRENT RETURN PATH

The input impedance of the INA122 is extremely high—approximately $10^{10}\Omega$. However, a path must be provided for the input bias current of both inputs. This input bias current is approximately −10nA (current flows out of the input terminals). High input impedance means that this input bias current changes very little with varying input voltage.

DESIRED GAIN (V/V)	R_G (Ω)	NEAREST 1% R_G VALUE
5	NC	NC
10	40k	40.2k
20	13.33k	13.3k
50	4444	4420
100	2105	2100
200	1026	1020
500	404	402
1000	201	200
2000	100.3	100
5000	40	40.2
10000	20	20

NC: No Connection.

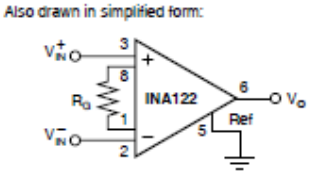

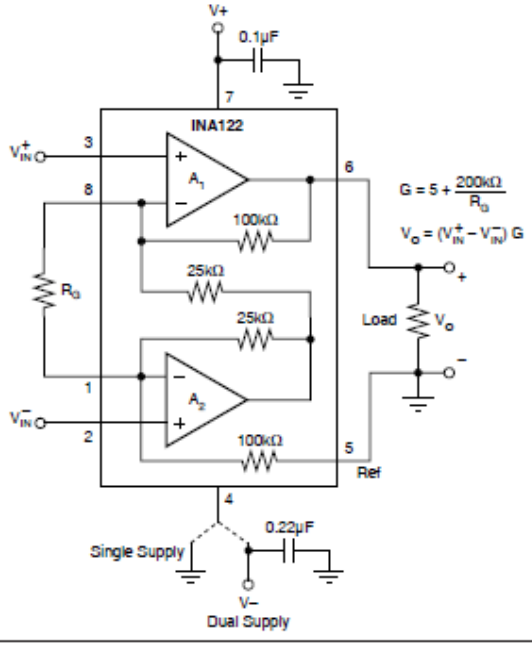

FIGURE 1. Basic Connections.

Input circuitry must provide a path for this input bias current for proper operation. Figure 3 shows various provisions for an input bias current path. Without a bias current path, the inputs will float to a potential which exceeds the common-mode range of the INA122 and the input amplifiers will saturate.

If the differential source resistance is low, the bias current return path can be connected to one input (see the thermocouple example in Figure 3). With higher source impedance, using two equal resistors provides a balanced input with possible advantages of lower input offset voltage due to bias current and better high-frequency common-mode rejection.

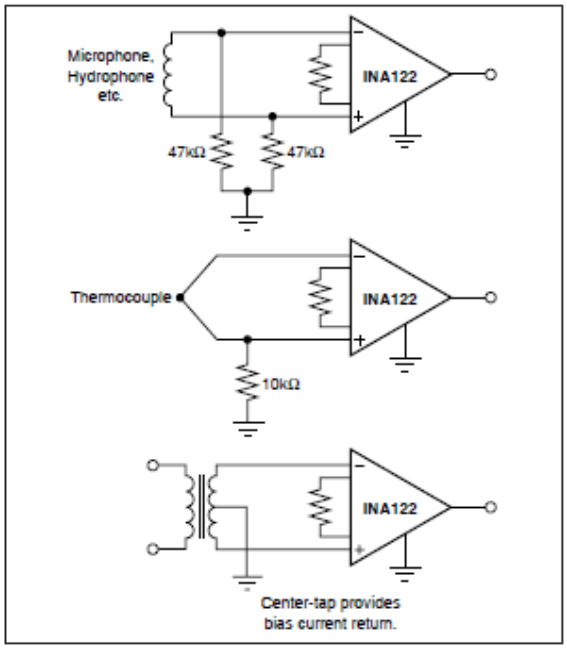

FIGURE 3. Providing an Input Common-Mode Current Path.

INPUT PROTECTION

The inputs of the INA122 are protected with internal diodes connected to the power supply rails (Figure 4). These diodes will clamp the applied signal to prevent it from damaging the input circuitry. If the input signal voltage can exceed the power supplies by more than 0.3V, the input signal current should be limited to less than 5mA to protect the internal clamp diodes. This can generally be done with a series input resistor. Some signal sources are inherently current-limited and do not require limiting resistors.

INPUT COMMON-MODE RANGE

The common-mode range for some common operating conditions is shown in the typical performance curves. The INA122 can operate over a wide range of power supply and V_{REF} configurations, making it impractical to provide a comprehensive guide to common-mode range limits for all possible conditions. The most commonly overlooked overload condition occurs by attempting to exceed the output swing of A_2, an internal circuit node that cannot be measured. Calculating the expected voltages at A_2's output (see equation in Figure 4) provides a check for the most common overload conditions.

The design of A_1 and A_2 are identical and their outputs can swing to within approximately 100mV of the power supply rails, depending on load conditions. When A_2's output is saturated, A_1 can still be in linear operation, responding to changes in the non-inverting input voltage. This may give the appearance of linear operation but the output voltage is invalid.

A single supply instrumentation amplifier has special design considerations. Using commonly available single-supply op amps to implement the two-op amp topology will not yield equivalent performance. For example, consider the condition where both inputs of common single-supply op amps are

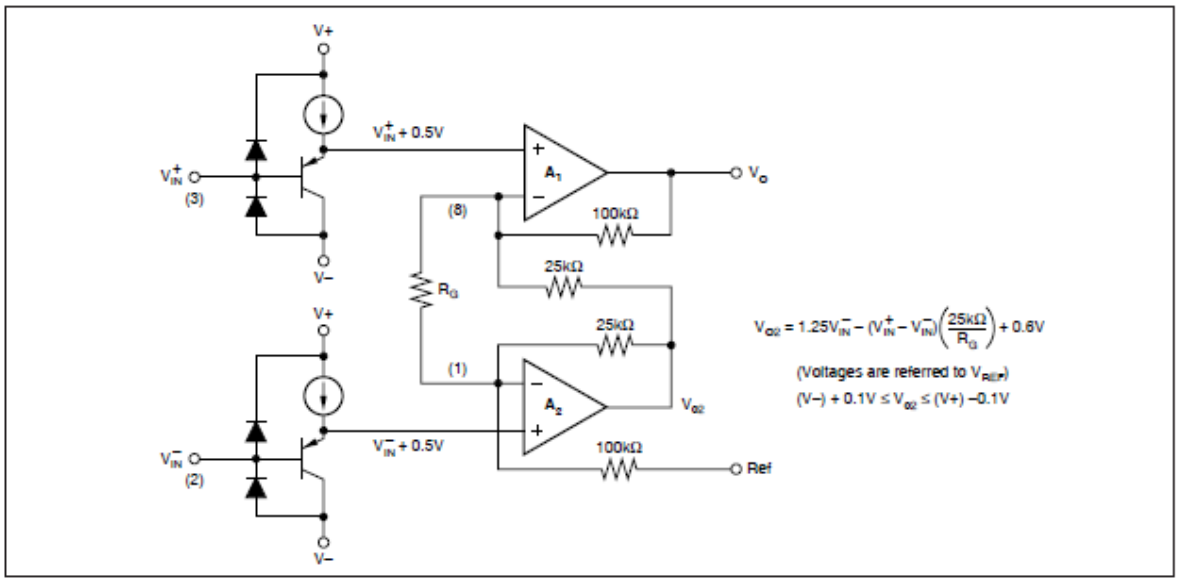

FIGURE 4. INA122 Simplified Circuit Diagram.

equal to 0V. The outputs of both A_1 and A_2 must be 0V. But any small positive voltage applied to V_{IN}^+ requires that A_2's output must swing below 0V, which is clearly impossible without a negative power supply.

To achieve common-mode range that extends to single-supply ground, the INA122 uses precision level-shifting buffers on its inputs. This shifts both inputs by approximately +0.5V, and through the feedback network, shifts A_2's output by approximately +0.6V. With both inputs and V_{REF} at single-supply, A_2's output is well within its linear range. A positive V_{IN}^+ causes A_2's output to swing below 0.6V.

As a result of this input level-shifting, the voltages at pin 1 and pin 8 are not equal to their respective input terminal voltages (pins 2 and 3). For most applications, this is not important since only the gain-setting resistor connects to these pins.

LOW VOLTAGE OPERATION

The INA122 can be operated on a single power supply as low as +2.2V (or a total of +2.2V on dual supplies). Performance remains excellent throughout the power supply range up to +36V (or ±18V). Most parameters vary only slightly throughout this supply voltage range—see typical performance curves.

Operation at very low supply voltage requires careful attention to ensure that the common-mode voltage remains within its linear range.

LOW QUIESCENT CURRENT OPERATION

The INA122 maintains its low quiescent current (60µA) while the output is within linear operation (up to 200mV from the supply rails). When the input creates a condition that overdrives the output into saturation, quiescent current increases. With V_O overdriven into the positive rail, the quiescent current increases to approximately 400µA. Likewise, with V_O overdriven into the negative rail (single supply ground) the quiescent current increases to approximately 200µA.

OUTPUT CURRENT RANGE

Output sourcing and sinking current values versus the output voltage ranges are shown in the typical performance curves. The positive and negative current limits are not equal. Positive output current sourcing will drive moderate to high load impedances. Battery operation normally requires the careful management of power consumption to keep load impedances very high throughout the design.

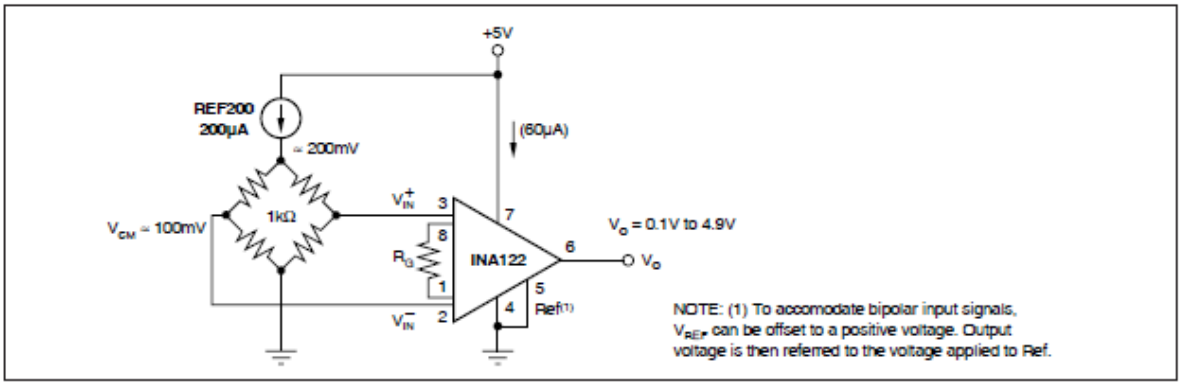

FIGURE 5. Micropower Single Supply Bridge Amplifier.

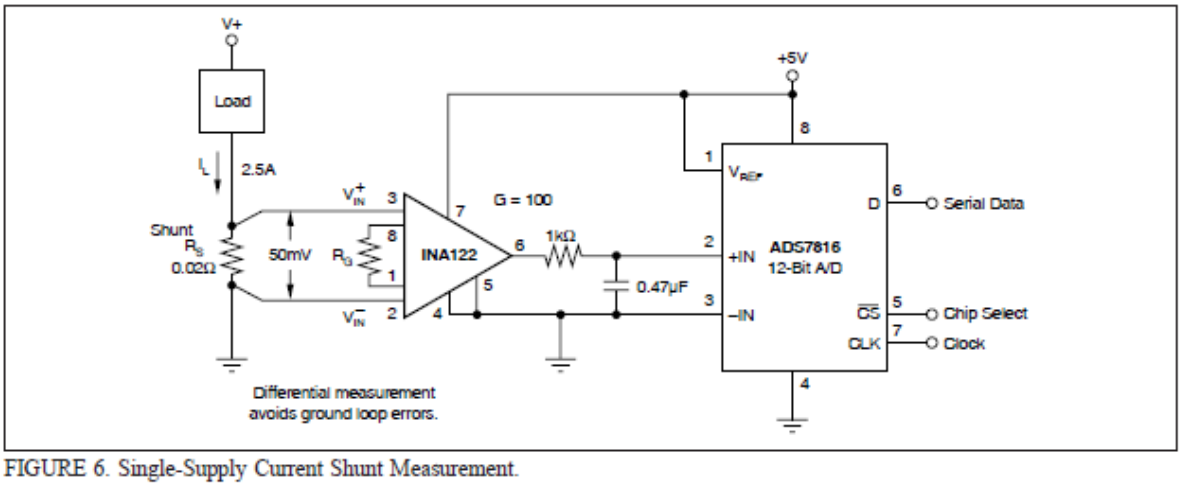

FIGURE 6. Single-Supply Current Shunt Measurement.

Datasheet TC9400 Frequency to Voltage Converter

MICROCHIP

TC9400/9401/9402

Voltage-to-Frequency/Frequency-to-Voltage Converters

Features

VOLTAGE-TO-FREQUENCY

- Choice of Linearity
  - TC9401: 0.01%
  - TC9400: 0.05%
  - TC9402: 0.25%
- DC to 100kHz (F/V) or 1Hz to 100kHz (V/F)
- Low Power Dissipation: 27mW (Typ.)
- Single/Dual Supply Operation
  - +8V to +15V or ±4V to ±7.5V
- Gain Temperature Stability: ±25 ppm/°C (Typ.)
- Programmable Scale Factor

FREQUENCY-TO-VOLTAGE

- Operation: DC to 100kHz
- Choice of Linearity
  - TC9401: 0.02%
  - TC9400: 0.05%
  - TC9402: 0.25%
- Programmable Scale Factor

Applications

- µP Data Acquisition
- 13-bit Analog-to-Digital Converters
- Analog Data Transmission and Recording
- Phase Locked Loops
- Frequency Meters/Tachometer
- Motor Control
- FM Demodulation

Device Selection Table

Part Number	Linearity (V/F)	Package	Temperature Range
TC9400COD	0.05%	14-Pin SOIC (Narrow)	0°C to +70°C
TC9400CPD	0.05%	14-Pin PDIP	0°C to +70°C
TC9400EJD	0.05%	14-Pin CerDIP	-40°C to +85°C
TC9401CPD	0.01%	14-Pin PDIP	0°C to +70°C
TC9401EJD	0.01%	14-Pin CerDIP	-40°C to +85°C
TC9402CPD	0.25%	14-Pin PDIP	0°C to +70°C
TC9402EJD	0.25%	14-Pin CerDIP	°C to +85°C

General Description

The TC9400/TC9401/TC9402 are low cost voltage-to-frequency (V/F) converters, utilizing low power CMOS technology. The converters accept a variable analog input signal and generate an output pulse train, whose frequency is linearly proportional to the input voltage.

The devices can also be used as highly accurate frequency-to-voltage (F/V) converters, accepting virtually any input frequency waveform and providing a linearly proportional voltage output.

A complete V/F or F/V system only requires the addition of two capacitors, three resistors, and reference voltage.

Package Type

14-Pin Plastic DIP/CERDIP

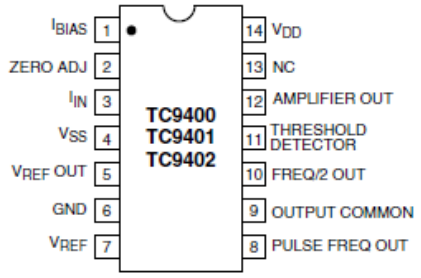

14-Pin SOIC

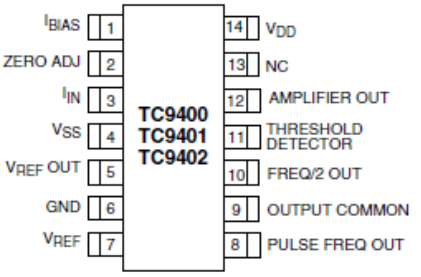

NC = No Internal Connection

TC9400/9401/9402

Functional Block Diagram

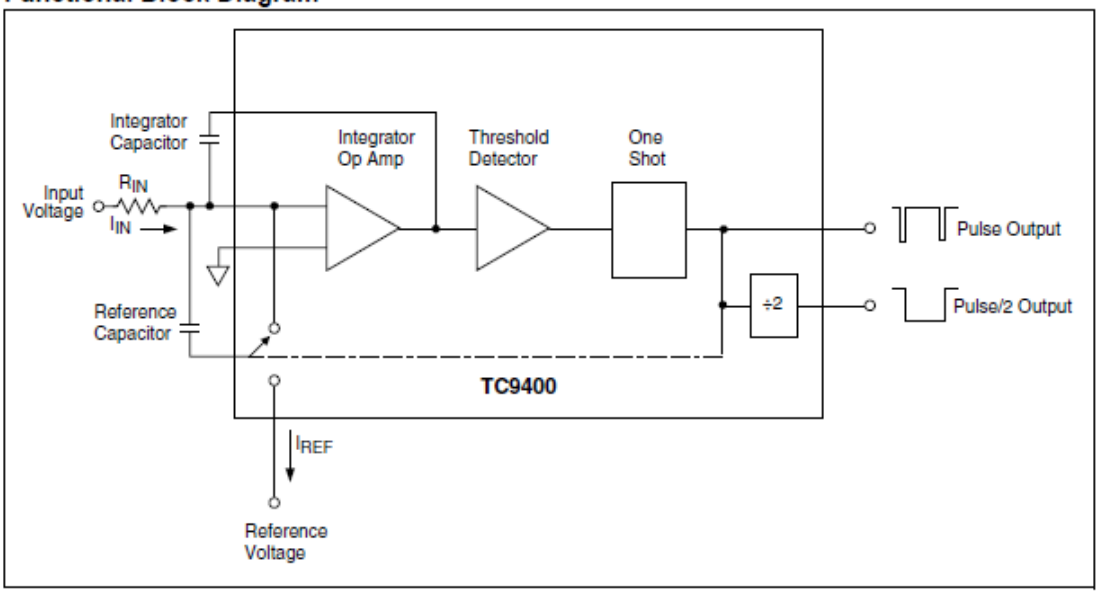

1.0 ELECTRICAL CHARACTERISTICS

Absolute Maximum Ratings*

$V_{DD} - V_{SS}$ ..... +18V
I_{IN} 10mA
$V_{OUTMAX} - V_{OUT}$ Common 23V
$V_{REF} - V_{SS}$ ..... -1.5V
Storage Temperature Range ..... -65°C to +150°C
Operating Temperature Range:
C Device ..... 0°C to +70°C
E Device ..... -40°C to +85°C
Package Dissipation ($T_A \leq 70°C$):
8-Pin CerDIP 800mW
8-Pin Plastic DIP 730mW
8-Pin SOIC 470mW

*Stresses above those listed under "Absolute Maximum Ratings" may cause permanent damage to the device. These are stress ratings only and functional operation of the device at these or any other conditions above those indicated in the operation sections of the specifications is not implied. Exposure to Absolute Maximum Rating conditions for extended periods may affect device reliability.

TC940X ELECTRICAL SPECIFICATIONS

Electrical Characteristics: V_{DD} = +5V, V_{SS} = -5V, V_{GND} = 0V, V_{REF} = -5V, R_{BIAS} = 100kΩ, Full Scale = 10kHz, unless otherwise specified. T_A = +25°C, unless temperature range is specified (-40°C to +85°C for E device, 0°C to +70°C for C device).

Parameter	Min	Typ	Max	Min	Typ	Max	Min	Typ	Max	Units	Test Conditions
Voltage-to-Frequency											
Accuracy		**TC9400**			**TC9401**			**TC9402**			
Linearity 10kHz	—	0.01	0.05	—	0.004	0.01	—	0.05	0.25	% Full Scale	Output Deviation from Straight Line Between Normalized Zero and Full Scale Input
Linearity 100kHz	—	0.1	0.25	—	0.04	0.08	—	0.25	0.5	% Full Scale	Output Deviation from Straight Line Between Normalized Zero Reading and Full Scale Input
Gain Temperature Drift **(Note 1)**	—	±25	±40	—	±25	±40	—	±50	±100	ppm/°C Full Scale	Variation in Gain A due to Temperature Change
Gain Variance	—	±10	—	—	±10	—	—	±10	—	% of Nominal	Variation from Ideal Accuracy
Zero Offset **(Note 2)**	—	±10	±50	—	±10	±50	—	±20	±100	mV	Correction at Zero Adjust for Zero Output when Input is Zero
Zero Temperature Drift **(Note 1)**	—	±25	±50	—	±25	±50	—	±50	±100	µV/°C	Variation in Zero Offset Due to Temperature Change

Note 1: Full temperature range; not tested.
2: I_{IN} = 0.
3: Full temperature range, I_{OUT} = 10mA.
4: I_{OUT} = 10µA.
5: Threshold Detect = 5V, Amp Out = 0V, full temperature range.
6: 10Hz to 100kHz; not tested.
7: 5µsec minimum positive pulse width and 0.5µsec minimum negative pulse width.
8: $t_R = t_F$ = 20nsec.
9: $R_L \geq 2k\Omega$, tested @ 10kΩ.
10: Full temperature range, V_{IN} = -0.1V.

TC9400/9401/9402

TC940X ELECTRICAL SPECIFICATIONS (CONTINUED)

Electrical Characteristics: V_{DD} = +5V, V_{SS} = -5V, V_{GND} = 0V, V_{REF} = -5V, R_{BIAS} = 100kΩ, Full Scale = 10kHz, unless otherwise specified. T_A = +25°C, unless temperature range is specified (-40°C to +85°C for E device, 0°C to +70°C for C device).

Parameter	Min	Typ	Max	Min	Typ	Max	Min	Typ	Max	Units	Test Conditions
Analog Input											
I_{IN} Full Scale	—	10	—	—	10	—	—	10	—	µA	Full Scale Analog Input Current to achieve Specified Accuracy
I_{IN} Over Range	—	—	50	—	—	50	—	—	50	µA	Over Range Current
Response Time	—	2	—	—	2	—	—	2	—	Cycle	Settling Time to 0.1% Full Scale
Digital Section		**TC9400**			**TC9401**			**TC9402**			
V_{SAT} @ I_{OL} = 10mA	—	0.2	0.4	—	0.2	0.4	—	0.2	0.4	V	Logic "0" Output Voltage **(Note 3)**
V_{OUTMAX} – V_{OUT} Common **(Note 4)**	—	—	18	—	—	18	—	—	18	V	Voltage Range Between Output and Common
Pulse Frequency Output Width	—	3	—	—	3	—	—	3	—	µsec	
Frequency-to-Voltage											
Supply Current											
I_{DD} Quiescent **(Note 5)**	—	1.5	6	—	1.5	6	—	3	10	mA	Current Required from Positive Supply during Operation
I_{SS} Quiescent **(Note 5)**	—	-1.5	-6	—	-1.5	-6	—	-3	-10	mA	Current Required from Negative Supply during Operation
V_{DD} Supply	4	—	7.5	4	—	7.5	4	—	7.5	V	Operating Range of Positive Supply
V_{SS} Supply	-4	—	-7.5	-4	—	-7.5	-4	—	-7.5	V	Operating Range of Negative Supply
Reference Voltage											
V_{REF} – V_{SS}	-2.5	—	—	-2.5	—	—	-2.5	—	—	V	Range of Voltage Reference Input
Accuracy											
Non-Linearity **(Note 10)**	—	0.02	0.05	—	0.01	0.02	—	0.05	0.25	% Full Scale	Deviation from ideal Transfer Function as a Percentage Full Scale Voltage
Input Frequency Range **(Notes 7 and 8)**	10	—	100k	10	—	100k	10	—	100k	Hz	Frequency Range for Specified Non-Linearity

Note 1: Full temperature range; not tested.
2: I_{IN} = 0.
3: Full temperature range, I_{OUT} = 10mA.
4: I_{OUT} = 10µA.
5: Threshold Detect = 5V, Amp Out = 0V, full temperature range.
6: 10Hz to 100kHz; not tested.
7: 5µsec minimum positive pulse width and 0.5µsec minimum negative pulse width.
8: $t_R = t_F$ = 20nsec.
9: $R_L \geq 2k\Omega$, tested @ 10kΩ.
10: Full temperature range, V_{IN} = -0.1V.

TC940X ELECTRICAL SPECIFICATIONS (CONTINUED)

Electrical Characteristics: V_{DD} = +5V, V_{SS} = -5V, V_{GND} = 0V, V_{REF} = -5V, R_{BIAS} = 100kΩ, Full Scale = 10kHz, unless otherwise specified. T_A = +25°C, unless temperature range is specified (-40°C to +85°C for E device, 0°C to +70°C for C device).

Parameter	Min	Typ	Max	Min	Typ	Max	Min	Typ	Max	Units	Test Conditions
Frequency Input											
Positive Excursion	0.4	—	V_{DD}	0.4	—	V_{DD}	0.4	—	V_{DD}	V	Voltage Required to Turn Threshold Detector On
Negative Excursion	-0.4		-2	-0.4	—	-2	-0.4	—	-2	V	Voltage Required to Turn Threshold Detector Off
Minimum Positive Pulse Width **(Note 8)**	—	5	—	—	5	—	—	5	—	µsec	Time between Threshold Crossings
Minimum Negative Pulse Width **(Note 8)**	—	0.5	—	—	0.5	—	—	0.5	—	µsec	Time Between Threshold Crossings
Input Impedance	—	10	—	—	10	—		—	10	MΩ	
Analog Outputs		**TC9400**			**TC9401**			**TC9402**			
Output Voltage **(Note 9)**	—	V_{DD} – 1	—	—	V_{DD} – 1	—	—	V_{DD} – 1	—	V	Voltage Range of Op Amp Output for Specified Non-Linearity
Output Loading	2	—	—	2	—	—	2	—	—	kΩ	Resistive Loading at Output of Op Amp
Supply Current		**TC9400**			**TC9401**			**TC9402**			
I_{DD} Quiescent **(Note 10)**	—	1.5	6	—	1.5	6	—	3	10	mA	Current Required from Positive Supply During Operation
I_{SS} Quiescent **(Note 10)**	—	-1.5	-6		-1.5	-6	—	-3	-10	mA	Current Required from Negative Supply During Operation
V_{DD} Supply	4	—	7.5	4	—	7.5	4	—	7.5	V	Operating Range of Positive Supply
V_{SS} Supply	-4	—	-7.5	-4	—	-7.5	-4	—	-7.5	V	Operating Range of Negative Supply
Reference Voltage											
$V_{REF} - V_{SS}$	-2.5	—	—	-2.5	—	—	-2.5	—	—	V	Range of Voltage Reference Input

Note 1: Full temperature range; not tested.
2: I_{IN} = 0.
3: Full temperature range, I_{OUT} = 10mA.
4: I_{OUT} = 10µA.
5: Threshold Detect = 5V, Amp Out = 0V, full temperature range.
6: 10Hz to 100kHz; not tested.
7: 5µsec minimum positive pulse width and 0.5µsec minimum negative pulse width.
8: $t_R = t_F$ = 20nsec.
9: $R_L \geq 2k\Omega$, tested @ 10kΩ.
10: Full temperature range, V_{IN} = -0.1V.

TC9400/9401/9402

2.0 PIN DESCRIPTIONS

The descriptions of the pins are listed in Table 2-1.

TABLE 2-1: PIN FUNCTION TABLE

Pin No. 14-Pin PDIP/CERDIP 14-Pin SOIC (Narrow)	Symbol	Description
1	I_{BIAS}	This pin sets bias current in the TC9400. Connect to V_{SS} through a 100kΩ resistor.
2	ZERO ADJ	Low frequency adjustment input.
3	I_{IN}	Input current connection for the V/F converter.
4	V_{SS}	Negative power supply voltage connection, typically -5V.
5	V_{REF} OUT	Reference capacitor connection.
6	GND	Analog ground.
7	V_{REF}	Voltage reference input, typically -5V.
8	PULSE FREQ OUT	Frequency output. This open drain output will pulse LOW each time the Freq. Threshold Detector limit is reached. The pulse rate is proportional to input voltage.
9	OUTPUT COMMON	Source connection for the open drain output FETs.
10	FREQ/2 OUT	This open drain output is a square wave at one-half the frequency of the pulse output (Pin 8). Output transitions of this pin occur on the rising edge of Pin 8.
11	THRESHOLD DETECTOR	Input to the Threshold Detector. This pin is the frequency input during F/V operation.
12	AMPLIFIER OUT	Output of the integrator amplifier.
13	NC	No internal connection.
14	V_{DD}	Positive power supply connection, typically +5V.

3.0 DETAILED DESCRIPTION

3.1 Voltage-to-Frequency (V/F) Circuit Description

The TC9400 V/F converter operates on the principal of charge balancing. The operation of the TC9400 is easily understood by referring to Figure 3-1. The input voltage (V_{IN}) is converted to a current (I_{IN}) by the input resistor. This current is then converted to a charge on the integrating capacitor and shows up as a linearly decreasing voltage at the output of the Op Amp. The lower limit of the output swing is set by the threshold detector, which causes the reference voltage to be applied to the reference capacitor for a time period long enough to charge the capacitor to the reference voltage. This action reduces the charge on the integrating capacitor by a fixed amount ($q = C_{REF} \times V_{REF}$), causing the Op Amp output to step up a finite amount.

At the end of the charging period, C_{REF} is shorted out. This dissipates the charge stored on the reference capacitor, so that when the output again crosses zero, the system is ready to recycle. In this manner, the continued discharging of the integrating capacitor by the input is balanced out by fixed charges from the reference voltage. As the input voltage is increased, the number of reference pulses required to maintain balance increases, which causes the output frequency to also increase. Since each charge increment is fixed, the increase in frequency with voltage is linear. In addition, the accuracy of the output pulse width does not directly affect the linearity of the V/F. The pulse must simply be long enough for full charge transfer to take place.

The TC9400 contains a "self-start" circuit to ensure the V/F converter always operates properly when power is first applied. In the event that, during power-on, the Op Amp output is below the threshold and C_{REF} is already charged, a positive voltage step will not occur. The Op Amp output will continue to decrease until it crosses the -3.0V threshold of the "self-start" comparator. When this happens, an internal resistor is connected to the Op Amp input, which forces the output to go positive until the TC9400 is in its Normal Operating mode.

The TC9400 utilizes low power CMOS processing for low input bias and offset currents, with very low power dissipation. The open drain N-channel output FETs provide high voltage and high current sink capability.

FIGURE 3-1: 10Hz TO 10kHz V/F CONVERTER

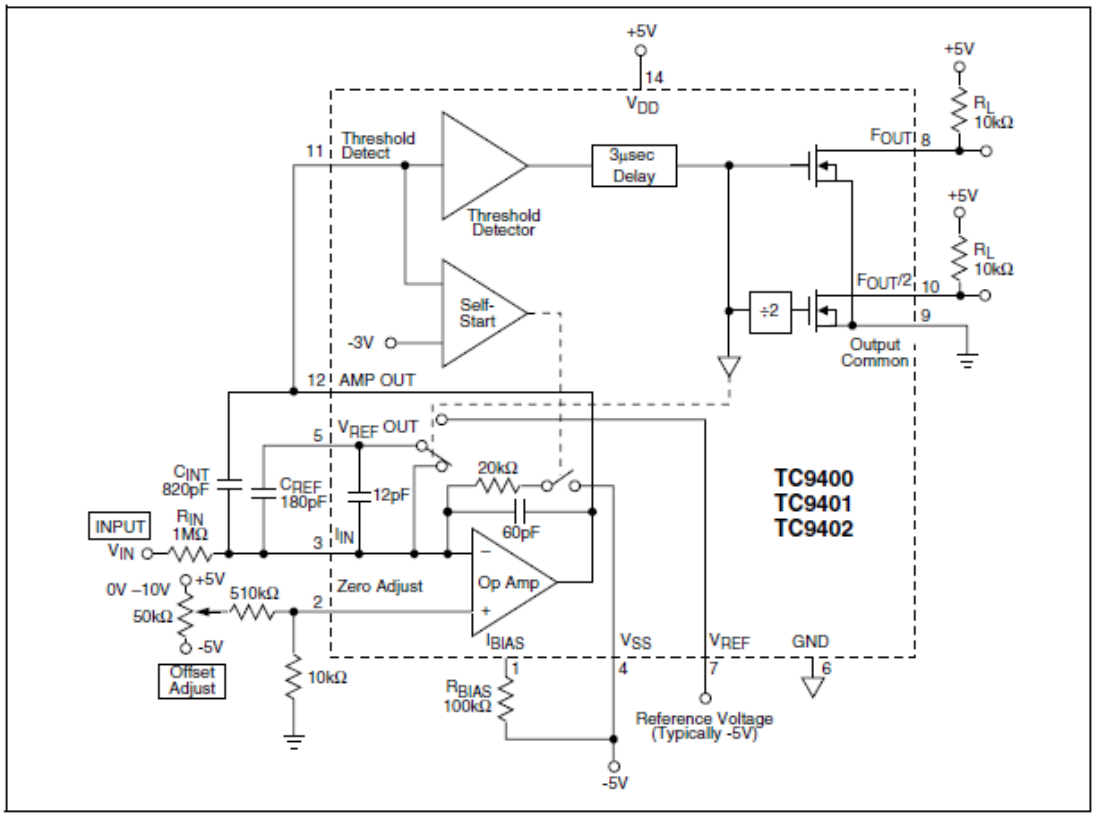

3.2 Voltage-to-Time Measurements

The TC9400 output can be measured in the time domain as well as the frequency domain. Some microcomputers, for example, have extensive timing capability, but limited counter capability. Also, the response time of a time domain measurement is only the period between two output pulses, while the frequency measurement must accumulate pulses during the entire counter time-base period.

Time measurements can be made from either the TC9400's PULSE FREQ OUT output, or from the FREQ/2 OUT output. The FREQ/2 OUT output changes state on the rising edge of PULSE FREQ OUT, so FREQ/2 OUT is a symmetrical square wave at one-half the pulse output frequency. Timing measurements can, therefore, be made between successive PULSE FREQ OUT pulses, or while FREQ/2 OUT is high (or low).

4.0 PIN FUNCTIONS

4.1 Threshold Detector Input

In the V/F mode, this input is connected to the AMPLIFIER OUT output (Pin 12) and triggers a 3µsec pulse when the input voltage passes through its threshold. In the F/V mode, the input frequency is applied to this input.

The nominal threshold of the detector is half way between the power supplies, or $(V_{DD} + V_{SS})/2 \pm 400mV$. The TC9400's charge balancing V/F technique is not dependent on a precision comparator threshold, because the threshold only sets the lower limit of the Op Amp output. The Op Amp's peak-to-peak output swing, which determines the frequency, is only influenced by external capacitors and by V_{REF}.

4.2 Pulse Freq Out

This output is an open drain N-channel FET, which provides a pulse waveform whose frequency is proportional to the input voltage. This output requires a pull-up resistor and interfaces directly with MOS, CMOS, and TTL logic (see Figure 4-1).

FIGURE 4-1: OUTPUT WAVEFORMS

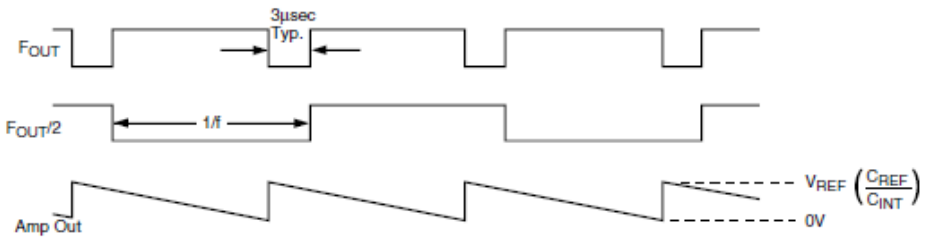

Notes:
1. To adjust F_{MIN}, set V_{IN} = 10mV and adjust the 50kΩ offset for 10Hz output.
2. To adjust F_{MAX}, set V_{IN} = 10V and adjust R_{IN} or V_{REF} for 10kHz output.
3. To increase F_{OUTMAX} to 100kHz, change C_{REF} to 2pF and C_{INT} to 75pF.
4. For high performance applications, use high stability components for R_{IN}, C_{REF}, V_{REF} (metal film resistors and glass capacitors). Also, separate output ground (Pin 9) from input ground (Pin 6).

4.3 Freq/2 Out

This output is an open drain N-channel FET, which provides a square wave one-half the frequency of the pulse frequency output. The FREQ/2 OUT output will change state on the rising edge of PULSE FREQ OUT. This output requires a pull-up resistor and interfaces directly with MOS, CMOS, and TTL logic.

4.4 Output Common

The sources of both the FREQ/2 OUT and the PULSE FREQ OUT are connected to this pin. An output level swing from the drain voltage to ground, or to the V_{SS} supply, may be obtained by connecting this pin to the appropriate point.

4.5 R_{BIAS}

An external resistor, connected to V_{SS}, sets the bias point for the TC9400. Specifications for the TC9400 are based on R_{BIAS} = 100kΩ ±10%, unless otherwise noted.

Increasing the maximum frequency of the TC9400 beyond 100kHz is limited by the pulse width of the pulse output (typically 3µsec). Reducing R_{BIAS} will decrease the pulse width and increase the maximum operating frequency, but linearity errors will also increase. R_{BIAS} can be reduced to 20kΩ, which will typically produce a maximum full scale frequency of 500kHz.

4.6 Amplifier Out

This pin is the output stage of the operational amplifier. During V/F operation, a negative going ramp signal is available at this pin. In the F/V mode, a voltage proportional to the frequency input is generated.

4.7 Zero Adjust

This pin is the non-inverting input of the operational amplifier. The low frequency set point is determined by adjusting the voltage at this pin.

4.8 I_{IN}

The inverting input of the operational amplifier and the summing junction when connected in the V/F mode. An input current of 10µA is specified, but an over range current up to 50µA can be used without detrimental effect to the circuit operation. I_{IN} connects the summing junction of an operational amplifier. Voltage sources cannot be attached directly, but must be buffered by external resistors.

4.9 V_{REF}

A reference voltage from either a precision source, or the V_{SS} supply is applied to this pin. Accuracy of the TC9400 is dependent on the voltage regulation and temperature characteristics of the reference circuitry.

Since the TC9400 is a charge balancing V/F converter, the reference current will be equal to the input current. For this reason, the DC impedance of the reference voltage source must be kept low enough to prevent linearity errors. For linearity of 0.01%, a reference impedance of 200W or less is recommended. A 0.1µF bypass capacitor should be connected from V_{REF} to ground.

4.10 V_{REF} Out

The charging current for C_{REF} is supplied through this pin. When the Op Amp output reaches the threshold level, this pin is internally connected to the reference voltage and a charge, equal to V_{REF} x C_{REF}, is removed from the integrator capacitor. After about 3µsec, this pin is internally connected to the summing junction of the Op Amp to discharge C_{REF}. Break-before-make switching ensures that the reference voltage is not directly applied to the summing junction.

5.0 VOLTAGE-TO-FREQUENCY (V/F) CONVERTER DESIGN INFORMATION

5.1 Input/Output Relationships

The output frequency (F_{OUT}) is related to the analog input voltage (V_{IN}) by the transfer equation:

EQUATION 5-1:

$$\text{Frequency Out} = \frac{V_{IN}}{R_{IN}} \times \frac{1}{(V_{REF})(V_{REF})}$$

5.2 External Component Selection

5.2.1 R_{IN}

The value of this component is chosen to give a full scale input current of approximately 10µA:

EQUATION 5-2:

$$R_{IN} \cong \frac{V_{IN\ FULLSCALE}}{10\mu A}$$

EQUATION 5-3:

$$R_{IN} \cong \frac{10V}{10\mu A} = 1M\Omega$$

Note that the value is an approximation and the exact relationship is defined by the transfer equation. In practice, the value of R_{IN} typically would be trimmed to obtain full scale frequency at V_{IN} full scale (see Section 5.3, Adjustment Procedure). Metal film resistors with 1% tolerance or better are recommended for high accuracy applications because of their thermal stability and low noise generation.

5.2.2 C_{INT}

The exact value is not critical but is related to C_{REF} by the relationship:

$$3C_{REF} \le C_{INT} \le 10C_{REF}$$

Improved stability and linearity are obtained when $C_{INT} \le 4C_{REF}$. Low leakage types are recommended, although mica and ceramic devices can be used in applications where their temperature limits are not exceeded. Locate as close as possible to Pins 12 and 13.

5.2.3 C_{REF}

The exact value is not critical and may be used to trim the full scale frequency (see Section 7.1, Input/Output Relationships). Glass film or air trimmer capacitors are recommended because of their stability and low leakage. Locate as close as possible to Pins 5 and 3 (see Figure 5-1).

FIGURE 5-1: RECOMMENDED C_{REF} VS. V_{REF}

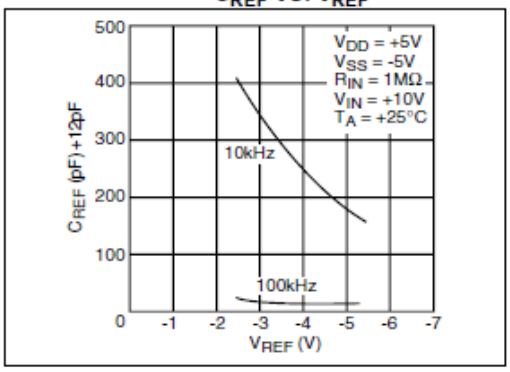

5.2.4 V_{DD}, V_{SS}

Power supplies of ±5V are recommended. For high accuracy requirements, 0.05% line and load regulation and 0.1µF disc decoupling capacitors, located near the pins, are recommended.

5.3 Adjustment Procedure

Figure 3-1 shows a circuit for trimming the zero location. Full scale may be trimmed by adjusting R_{IN}, V_{REF}, or C_{REF}. Recommended procedure for a 10kHz full scale frequency is as follows:

1. Set V_{IN} to 10mV and trim the zero adjust circuit to obtain a 10Hz output frequency.
2. Set V_{IN} to 10V and trim either R_{IN}, V_{REF}, or C_{REF} to obtain a 10kHz output frequency.

If adjustments are performed in this order, there should be no interaction and they should not have to be repeated.

5.4 Improved Single Supply V/F Converter Operation

A TC9400, which operates from a single 12 to 15V variable power source, is shown in Figure 5-2. This circuit uses two Zener diodes to set stable biasing levels for the TC9400. The Zener diodes also provide the reference voltage, so the output impedance and temperature coefficient of the Zeners will directly affect power supply rejection and temperature performance. Full scale adjustment is accomplished by trimming the input current. Trimming the reference voltage is not recommended for high accuracy applications unless an Op Amp is used as a buffer, because the TC9400 requires a low impedance reference (see Section 4.9, V_{REF} pin description, for more information).

The circuit of Figure 5-2 will directly interface with CMOS logic operating at 12V to 15V. TTL or 5V CMOS logic can be accommodated by connecting the output pull-up resistors to the +5V supply. An optoisolator can also be used if an isolated output is required; also, see Figure 5-3.

FIGURE 5-2: VOLTAGE TO FREQUENCY

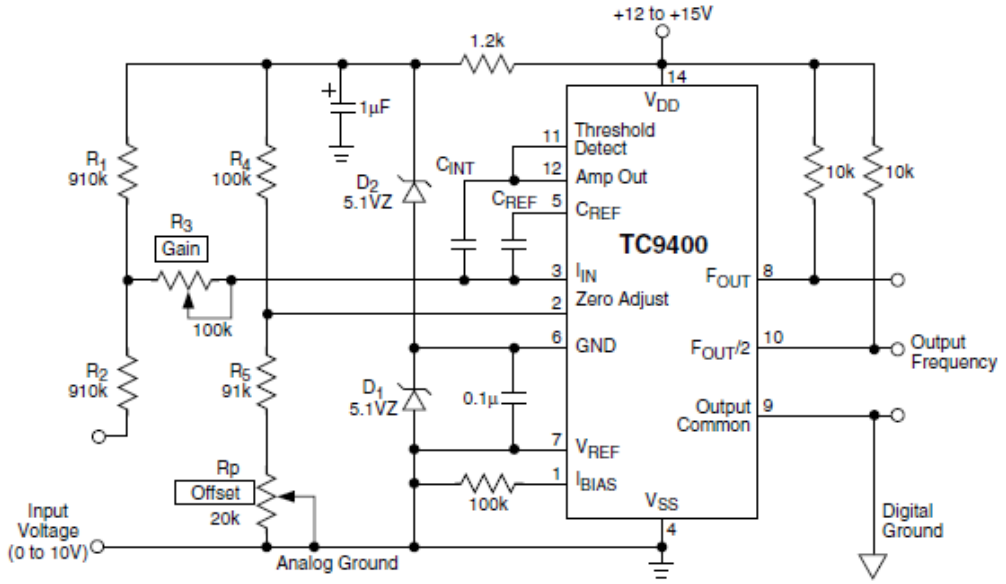

Component Selection

F/S FREQ.	C_{REF}	C_{INT}
1kHz	2200pF	4700pF
10kHz	180pF	470pF
100kHz	27pF	75pF

FIGURE 5-3: FIXED VOLTAGE - SINGLE SUPPLY OPERATION

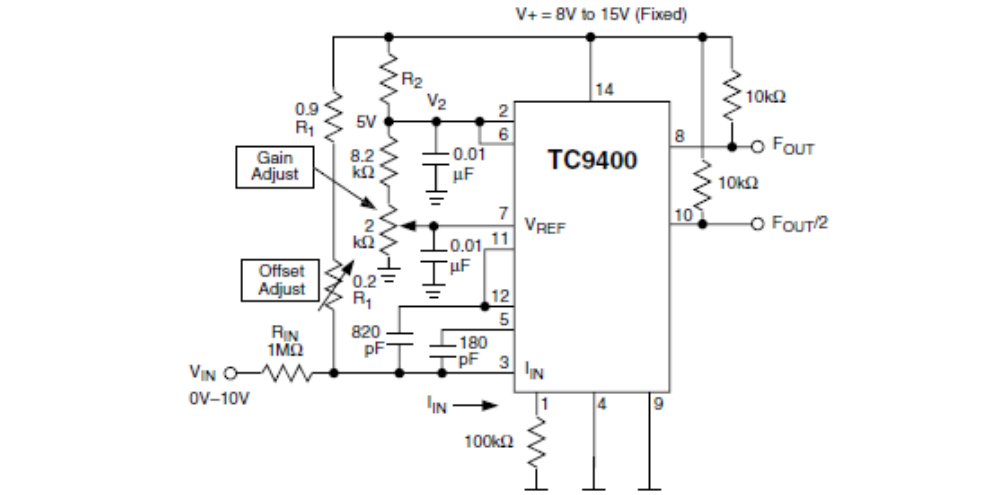

V+	R_1	R_2
10V	1MΩ	10kΩ
12V	1.4MΩ	14kΩ
15V	2MΩ	20kΩ

$$F_{OUT} = I_{IN} = \frac{1}{(V_2 - V_7)(C_{REF})}$$

$$I_{IN} = \frac{(V_{IN} - V_2)}{R_{IN}} + \frac{(V+ - V_2)}{(0.9R_1 + 0.2R_1)}$$

6.0 FREQUENCY-TO-VOLTAGE (F/V) CIRCUIT DESCRIPTION

When used as an F/V converter, the TC9400 generates an output voltage linearly proportional to the input frequency waveform.

Each zero crossing at the threshold detector's input causes a precise amount of charge ($q = C_{REF} \infty V_{REF}$) to be dispensed into the Op Amp's summing junction. This charge, in turn, flows through the feedback resistor, generating voltage pulses at the output of the Op Amp. A capacitor (C_{INT}) across R_{INT} averages these pulses into a DC voltage, which is linearly proportional to the input frequency.

7.0 F/V CONVERTER DESIGN INFORMATION

7.1 Input/Output Relationships

The output voltage is related to the input frequency (F_{IN}) by the transfer equation:

EQUATION 7-1:

$$V_{OUT} = [V_{REF} C_{REF} R_{INT}] F_{IN}$$

The response time to a change in F_{IN} is equal to (R_{INT} C_{INT}). The amount of ripple on V_{OUT} is inversely proportional to C_{INT} and the input frequency.

C_{INT} can be increased to lower the ripple. Values of 1µF to 100µF are perfectly acceptable for low frequencies.

When the TC9400 is used in the Single Supply mode, V_{REF} is defined as the voltage difference between Pin 7 and Pin 2.

7.2 Input Voltage Levels

The input frequency is applied to the Threshold Detector input (Pin 11). As discussed in the V/F circuit section of this data sheet, the threshold of Pin 11 is approximately (V_{DD} + V_{SS})/2 ±400mV. Pin 11's input voltage range extends from V_{DD} to about 2.5V below the threshold. If the voltage on Pin 11 goes more than 2.5 volts below the threshold, the V/F mode start-up comparator will turn on and corrupt the output voltage. The Threshold Detector input has about 200mV of hysteresis.

In ±5V applications, the input voltage levels for the TC9400 are ±400mV, minimum. If the frequency source being measured is unipolar, such as TTL or CMOS operating from a +5V source, then an AC coupled level shifter should be used. One such circuit is shown in Figure 7-1(a).

The level shifter circuit in Figure 7-1(b) can be used in single supply F/V applications. The resistor divider ensures that the input threshold will track the supply voltages. The diode clamp prevents the input from going far enough in the negative direction to turn on the start-up comparator. The diode's forward voltage decreases by 2.1mV/°C, so for high ambient temperature operation, two diodes in series are recommended; also, see Figure 7-2.

FIGURE 7-1: FREQUENCY INPUT LEVEL SHIFTER

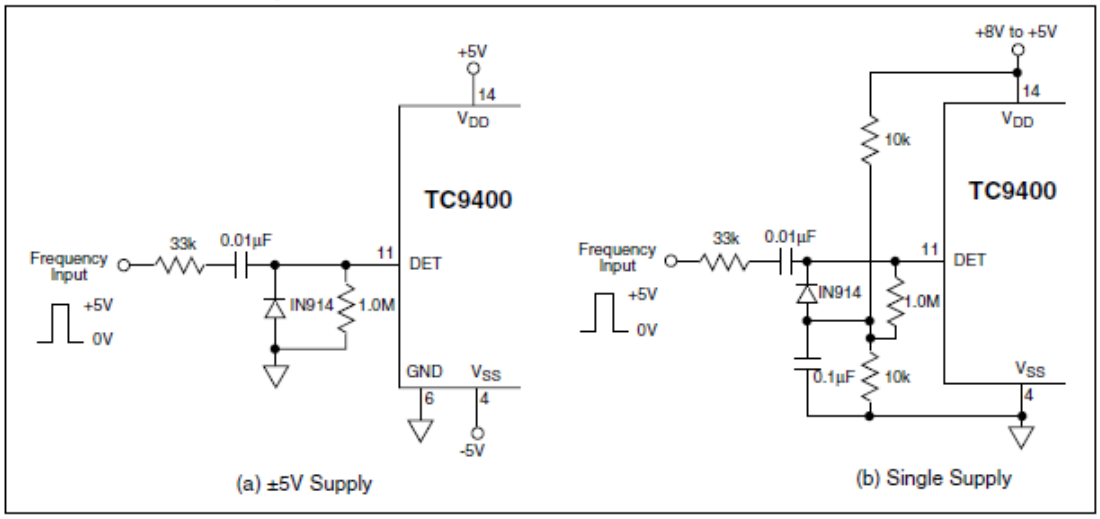

FIGURE 7-2: F/V SINGLE SUPPLY F/V CONVERTER

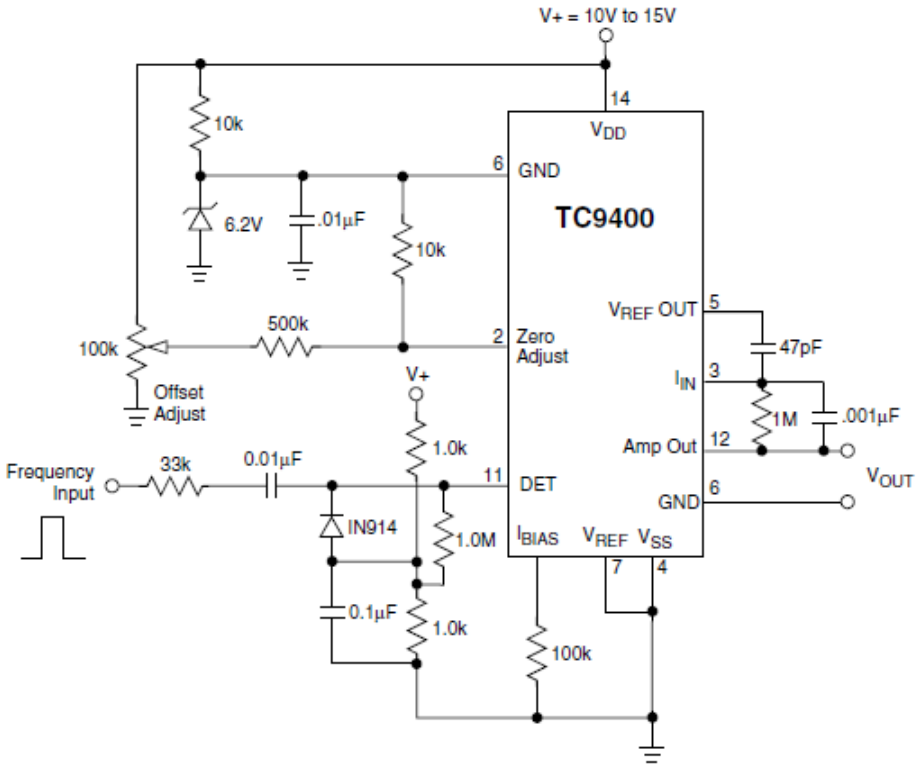

Note: The output is referenced to Pin 6, which is at 6.2V (Vz). For frequency meter applications, a 1mA meter with a series scaling resistor can be placed across Pins 6 and 12.

7.3 Input Buffer

F_{OUT} and $F_{OUT}/2$ are not used in the F/V mode. However, these outputs may be useful for some applications, such as a buffer to feed additional circuitry. Then, F_{OUT} will follow the input frequency waveform, except that F_{OUT} will go high 3µsec after F_{IN} goes high; $F_{OUT}/2$ will be square wave with a frequency of one-half F_{OUT}.

If these outputs are not used, Pins 8, 9 and 10 should be connected to ground (see Figure 7-3 and Figure 7-4).

FIGURE 7-3: F/V DIGITAL OUTPUTS

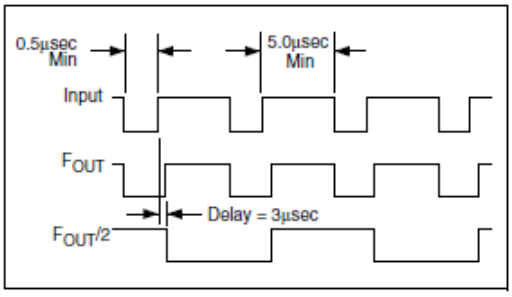

FIGURE 7-4: DC - 10kHz CONVERTER

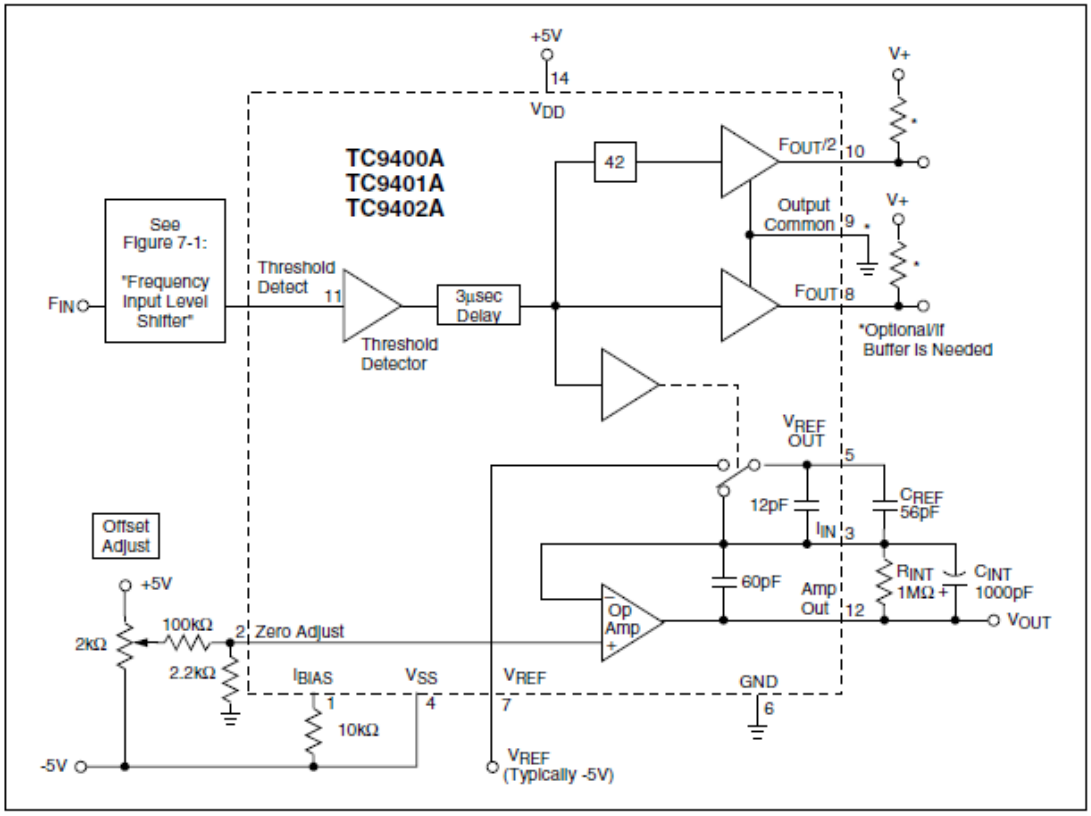

7.4 Output Filtering

The output of the TC9400 has a sawtooth ripple superimposed on a DC level. The ripple will be rejected if the TC9400 output is converted to a digital value by an integrating analog-to-digital converter, such as the TC7107 or TC7109. The ripple can also be reduced by increasing the value of the integrating capacitor, although this will reduce the response time of the F/V converter.

The sawtooth ripple on the output of an F/V can be eliminated without affecting the F/V's response time by using the circuit in Figure 7-5. The circuit is a capacitance multiplier, where the output coupling capacitor is multiplied by the AC gain of the Op Amp. A moderately fast Op Amp, such as the TL071, should be used.

FIGURE 7-5: RIPPLE FILTER

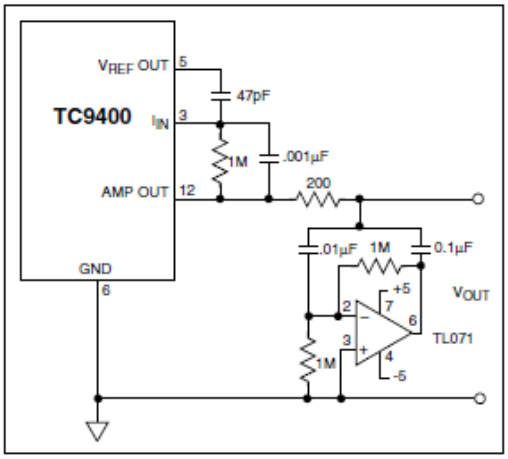

8.0 F/V POWER-ON RESET

In F/V mode, the TC9400 output voltage will occasionally be at its maximum value when power is first applied. This condition remains until the first pulse is applied to F_{IN}. In most frequency measurement applications, this is not a problem because proper operation begins as soon as the frequency input is applied.

In some cases, however, the TC9400 output must be zero at power-on without a frequency input. In such cases, a capacitor connected from Pin 11 to V_{DD} will usually be sufficient to pulse the TC9400 and provide a Power-on Reset (see Figure 8-1 (a) and (b)). Where predictable power-on operation is critical, a more complicated circuit, such as Figure 8-1 (b), may be required.

FIGURE 8-1: POWER-ON OPERATION/RESET

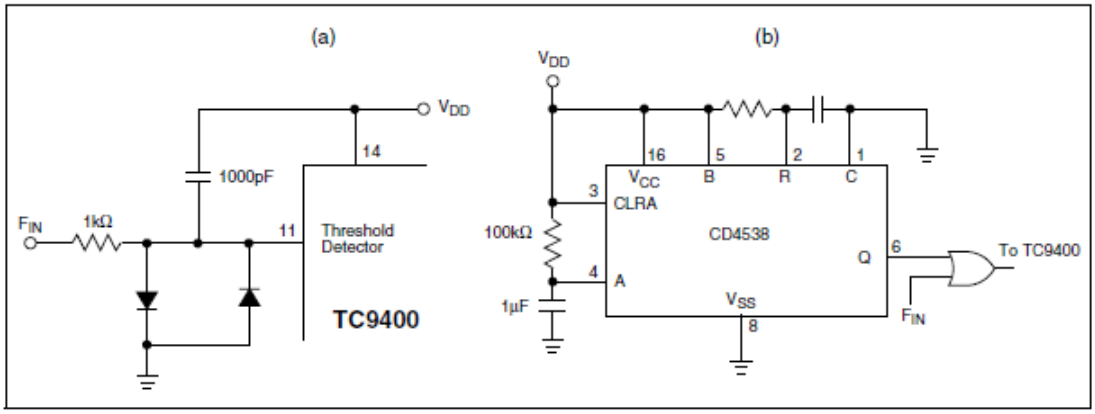

TC9400/9401/9402

9.0 PACKAGE INFORMATION

9.1 Package Marking Information

Package marking data is not available at this time.

9.2 Taping Form

Component Taping Orientation for 14-Pin SOIC (Narrow) Devices

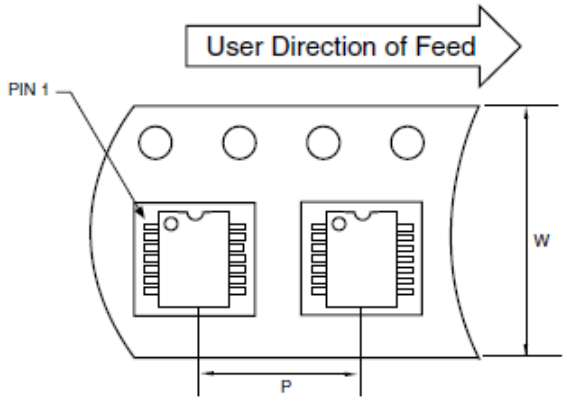

Standard Reel Component Orientation
for TR Suffix Device

Carrier Tape, Reel Size, and Number of Components Per Reel

Package	Carrier Width (W)	Pitch (P)	Part Per Full Reel	Reel Size
14-Pin SOIC (N)	12 mm	8 mm	2500	13 in

9.3 Package Dimensions

14-Pin CDIP (Narrow)

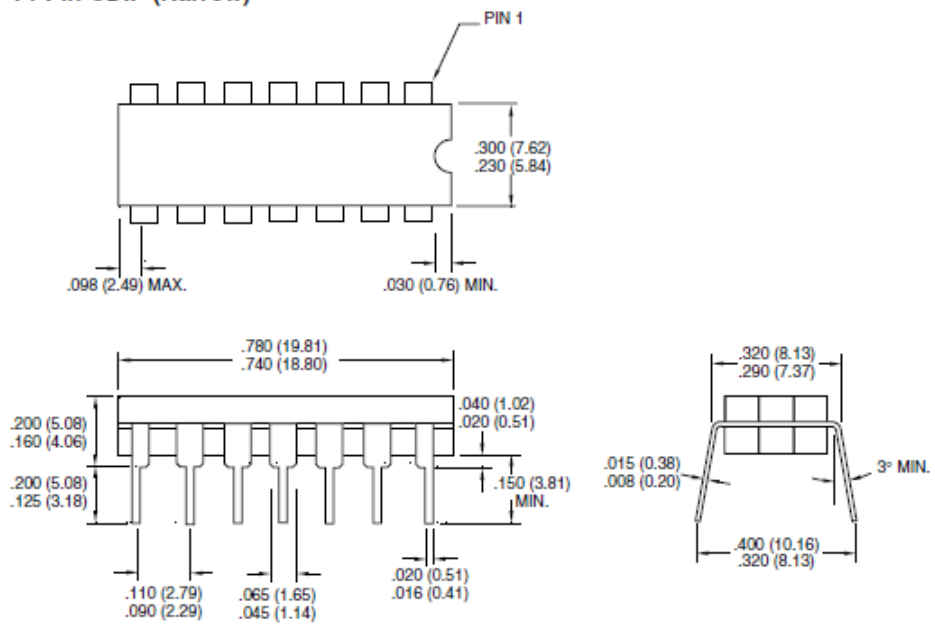

Dimensions: inches (mm)

9.3 Package Dimensions (Continued)

14-Pin PDIP (Narrow)

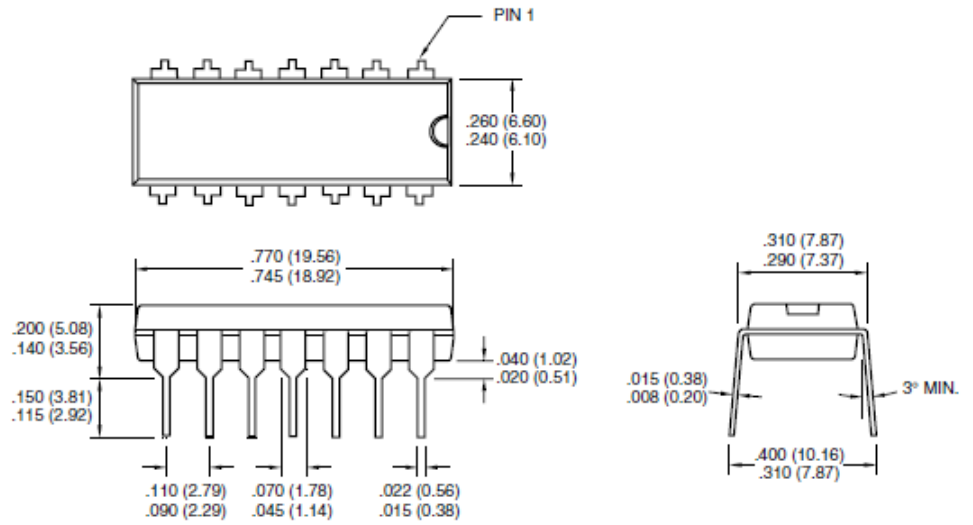

14-Pin SOIC (Narrow)

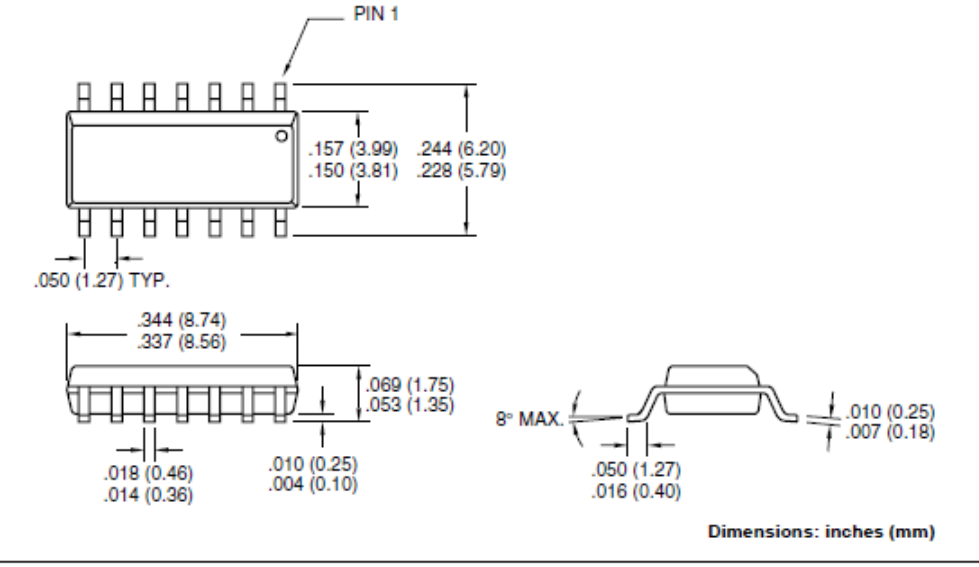

Datasheet Swoop

ATmega32 processor, serial programming and J TAG interfaces are provided for the ATmega32 processor

Sensors

- Up to four Wheatstone bridges with strain gauges, amplified with onboard INA122 instrumentation amplifiers and connected with terminal blocks, with optional gain and offset adjustment potentiometers.
- Other analog sensors connected via a terminal block.
- Other digital sensors connected via a different terminal block; digital pins on this block include a serial port TXD/RXD, digital interrupt pin INT2, and a counter input to 16-bit timer/counter 1.

Saving Data

SD card adapter on back side of board

- An FT232RL USB-serial interface chip and mini-USB connector can be mounted on the board and used to communicate directly with a host computer.

- The board can use power, such as from a battery, connected to a terminal block. It can use USB power instead, either 5V directly from the USB power line or 3.3V from the regulator in the FT232RL chip.

Power connector, located at the bottom of the board, just to the left of the microcontroller:
Pins, from left side:

-	Negative supply input (ground)
+	Positive supply input, normally +6V to +12V (or check specifications on whichever voltage regulators are used on a given board)

Digital connector, located at the bottom of the board, just to the right of the microcontroller:
Pins, from left side:

TXD	Transmitted data for serial port 1, or Port D pin 3*
RXD	Received data for serial port 1, or Port D pin 2*
INT2	External interrupt pin 2, or Port B pin 2
B1	Port B pin 1, or the input to Timer/Counter 1 in pulse counter mode
D7	Port D pin 7, or Timer/Counter 2 output capture for PWM or waveform generation
D6	Port D pin 6, or Timer/Counter 1 input capture trigger

Vcc	Supply pin for +5V or +3.3V power; use only for low current (<~20mA) external devices
GND	Ground for digital signals (do not use as ground for analog signals)

Wheatstone bridge connectors, located along the right edge of the board:
There are two connectors. Each one connects two Wheatstone bridges to two instrumentation amplifiers. Bridges are activated in pairs; to turn on bridges 0 and 1, send a logic 1 to Port C pin 0, and to turn on bridges 2 and 3, send a logic 1 to Port C pin 1. When the bridges are deactivated, the control pins should be left as outputs and set to logic 0.

Pins for the lower bridge, from the bottom of the board upward (or left to right as you look at the terminal block from the outside of the board):

EX	Excitation voltage, normally +5V from the analog voltage regulator or USB power, shared by both bridges
-	Negative input for Wheatstone bridge 3
1	Positive input for Wheatstone bridge 3
+	Negative input for Wheatstone bridge 2
0	Positive input for Wheatstone bridge 2
G	Ground for Wheatstone bridges 2 and 3, shared by both bridges; note ground is switched off when bridges are deactivated to save power, and the whole bridge floats up to the excitation voltage

Pins for the upper bridge, from the bottom of the board upward (or left to right as you look at the terminal block from the outside of the board):

EX	Excitation voltage, normally +5V from the analog voltage regulator or USB power, shared by both bridges
-	Negative input for Wheatstone bridge 1
1	Positive input for Wheatstone bridge 1
+	Negative input for Wheatstone bridge 0
0	Positive input for Wheatstone bridge 0
G	Ground for Wheatstone bridges 0 and 1, shared by both bridges; note ground is switched off when bridges are deactivated to save power, and the whole bridge floats up to the excitation voltage

Analog Connector, at the top of the board, just above the microcontroller and accelerometer pad:
Pins are shown from right to left looking at the board with the connector at the top, or left to right when holding the board so you look directly into the terminal block:

G	Ground for analog signals; do not use this ground for digital signals or

	Wheatstone bridges
	ADC4, channel 4 of analog to digital converter
	ADC5, channel 5 of analog to digital converter (shared with accelerometer Z axis)
	ADC6, channel 6 of analog to digital converter (shared with accelerometer Y axis)
	ADC7, channel 7 of analog to digital converter (shared with accelerometer X axis)
	Analog supply voltage; use only to power low current devices

Schematic

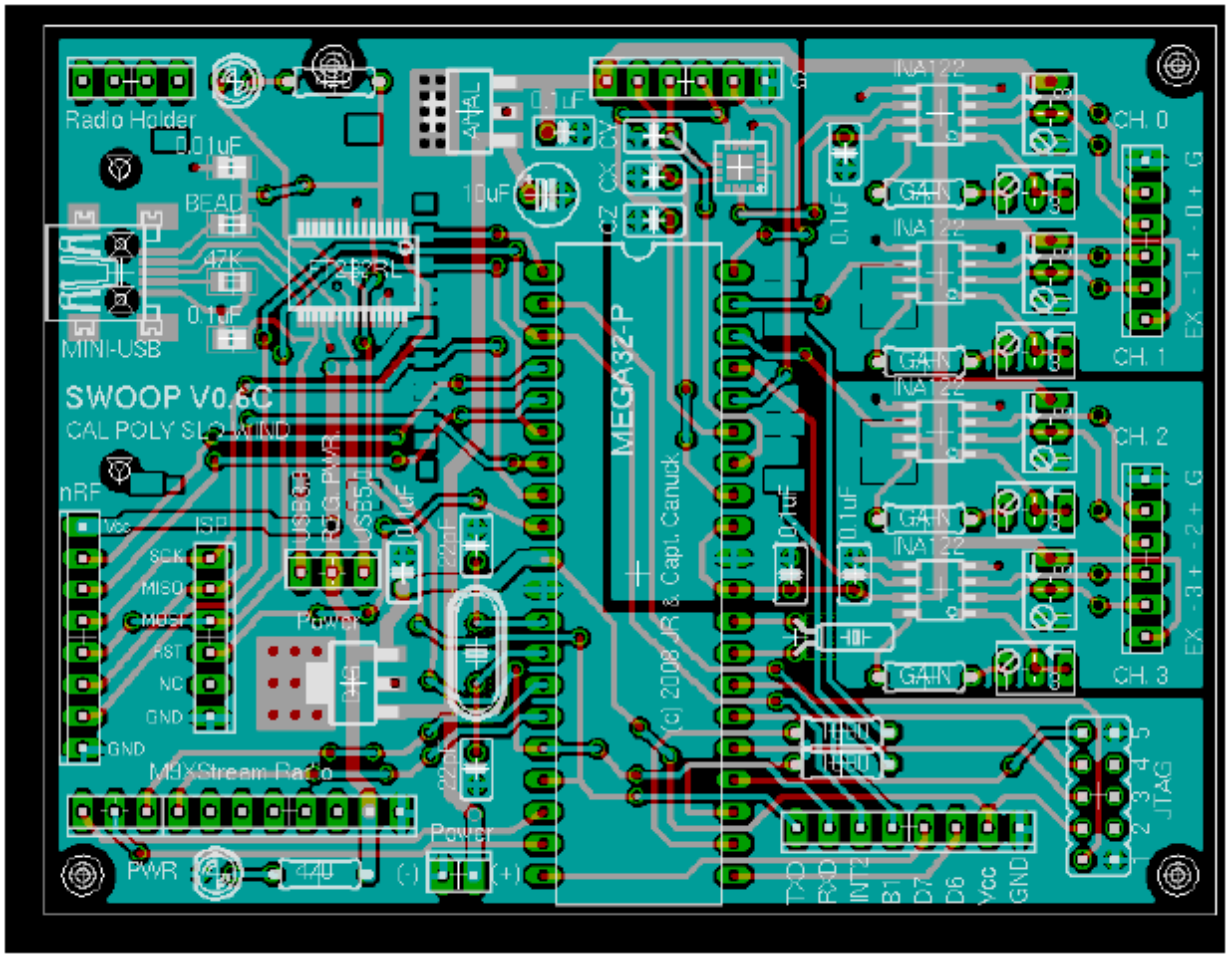

Datasheet SparkFun Logomatic V2

Overview

The Logomatic is new and improved, with a microSD card replacing the full-size SD, USB with universal mass storage, and charge circuitry with overcharge protection to charge a lithium polymer battery through the USB connection. It also has new hardware and firmware, but the same versatile features as the Logomatic V1.0.

- Modes of operation: auto UART, character triggered UART, ADC
- Configurable baud rates in UART modes of 1200, 2400, 4800, 9600, 19200, 38400, 57600, and 115200 baud
- Triggered UART mode has a configurable frame length of up to 510 characters (including trigger character)
- Triggered UART frames are delimited with carriage return and line feed characters for easy reading
- 8 ADC channels, all selectable as on or off
- ADC logging in ASCII or binary format
- ASCII logging delimited by tabs between measurements, delimited between frames by carriage return and line feed characters
- Variable frequency for ADC mode
- Frequency "safeties" to ensure that the file doesn't try to overwrite itself, maximum of 1500Hz for one channel and 187 Hz for all eight channels (ASCII logging mode)
- For the brave of heart you can turn the safety off!

The basic layout of the Logomatic V2.0 can be seen in Figure 1.

1. Power switch
2. V_{in} jack
3. Reset button
4. Status LEDs
5. UART0/Programming port
6. Stop logging button
7. Push-push microSD card socket
8. ADC ports
9. USB Mini-B jack

The Logomatic has an LDO (low dropout) 3.3V regulator. The maximum power dissipation of the voltage regulator is about

Figure 1

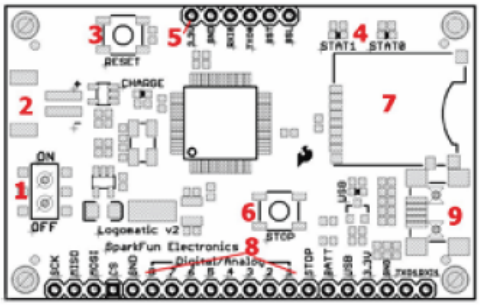

Theory of Operation

The Logomatic saves data to a microSD in a two-stage process. Data is first saved to one of two 512-byte data buffers. As each buffer is filled, it is logged to the SD card and logging continues on the other buffer.

The limiting factor on the speed of the Logomatic is the write process to the SD card. The longest write cycle is approximately 42.5mS, which means the shortest time allowed to log data to one of the buffers is also 42.5mS. If logging occurs faster than this, the buffer that's currently being written to the SD card will be overwritten by new input during the write process to the SD.

In UART modes, this could possibly become an issue at a baud rate of 115200 (1 start bit, 1 stop bit, 8 data bits). If streaming at this rate without any breaks, 512 bytes are filled in 44.4mS. Lower data rates should not show any difficulty.

In ADC mode, safety margins are imposed to alleviate buffer overwriting. Sample rates are capped depending on how many channels you have active, though this is only imposed when logging in ASCII format. The frequency caps are:

1 channel active, 1500 Hz maximum
2 channels active, 750 Hz maximum
3 channels active, 500 Hz maximum
4 channels active, 375 Hz maximum
5 channels active, 300 Hz maximum
6 channels active, 250 Hz maximum

resulting file. To get the faster data rates, just change the "Safety On" option from "Y" to "N" and set the "Frequency" number to whatever you want. The parser that reads the configuration file reads up to 4 digits, so you can set it as high as 9999Hz (though it will likely stop running at that speed).

First Power-up and Configuration File

Before you power up your Logomatic for the first time, put your microSD card into your card reader and format it in FAT16. Then install the card into your Logomatic and turn it on. The LEDs will blink reassuringly and then go quiet. Now, turn the unit off, plug a USB (connector type B-mini) into the unit, and power back on. The unit will mount as a drive on your computer (alternatively, you can remove the card and use a card reader to read it). You will now find two files on your card, LOGCON.TXT and LOG0.TXT. The first is the configuration file, the second is the first logged file (empty). Open up the configuration file and you will see this:

MODE = 0
ASCII = Y
Baud = 4
Frequency = 100
Trigger Character = $
Text Frame = 100
AD1.3 = N
AD0.3 = N
AD0.2 = N
AD0.1 = N
AD1.2 = N
AD0.4 = N
AD1.7 = N
AD1.6 = N
Safety On = Y

Mode

There are 3 mode settings: "0" for automatic UART logging, "1" for triggered UART logging, and "2" for ADC logging.

Mode 0 logs everything that comes in on UART0, provided that it's the right UART configuration (8 data bits, one stop bit, no parity

The "ASCII" field only applies to ADC mode (mode 2). It specifies whether the unit will log in ASCII format ("ASCII = Y") or binary format ("ASCII = N").

Baud

The "Baud" field sets the baud rate for the UART logging modes. The available rates are as follows:

"1" = 1200
"2" = 2400
"3" = 4800
"4" = 9600
"5" = 19200
"6" = 38400
"7" = 57600
"8" = 115200

Frequency

The "Frequency" field only applies to ADC logging mode and is responsible for setting the sampling rate of the Logomatic. The number shown (100 in this case) is in hertz and can be set from 1 to 9999. However, if the frequency safeties are active, the maximum values will be imposed as indicated in an earlier section.

Trigger Character

The "Trigger Character" field only applies to the triggered UART mode (mode 1). This is the character that the device waits for to begin logging a specified number of characters.

Text Frame

The "Text Frame" field specifies the number of characters to be logged with the trigger character when the Logomatic is running in mode 1. The reader should be aware that the first character in the logged text frame will be the trigger character, so if you wish to log 100 characters after the trigger you should set the text frame to 101. **Note:** This mode of operation is slightly different than the other modes in that each text frame has its own dedicated 512 byte buffer. When the end of the text frame is reached, the buffer will be logged and any new data coming in will be routed to the

one of the two UART modes.

Safety On

The last field in the configuration file is the "Safety On" field. This sets the frequency caps for ADC mode on with a "Y" or off with an "N." The values for those caps are mentioned in an earlier section.

The ADC values in the configuration files correspond to the outputs on the board as follows:

1 = AD 0.3

2 = AD 0.2

3 = AD 0.1

4 = AD 0.4

5 = AD 1.7

6 = AD 1.6

7 = AD 1.2

8 = AD 1.3

There is also a hardware test function that can be accessed through this parameter. Instead of a "Y" or an "N," setting it to "T" will put the unit in hardware test mode, you can watch the ADC lines slowly polled over the serial UART lines at 9600 baud. Note: this mode is not intended for normal operation. It is only intended for determining hardware failures.

Output Formats

The formats of the text files produced by the Logomatic will be a little different in each mode.

For mode 0 (automatic UART), any ASCII characters that come in on the UART will be sent to the SD card. Nothing is omitted and nothing is added.

For mode 1 (triggered UART), anything after and including the trigger character will be logged, including white space characters, up to the end of the specified data frame. Each data frame is delimited with a carriage return and a line feed character to make it easier to distinguish between the frames.

frames are delimited by the characters "$$".

USB Universal Mass Storage Features

The Logomatic 2.0 SD card can easily be accessed through a USB connection. To access the card in this manner, connect the Logomatic to a computer using a USB cable with a type B-mini connector. Then power the unit on. The unit will mount as a new drive (as a standard flash drive would). Now you can edit, create, or delete files. When you are finished, power the unit off and remove the USB cable.

Stop Button

The stop button will halt the Logomatic. All logging will stop, and any partially-filled buffer will be automatically logged to the SD card. Turning off the Logomatic or removing its power source will also stop the unit from logging (and keep the log file intact), but if there is a partially filled buffer it will not be logged. When the unit is stopped with the stop button, the LEDs will blink continuously until the unit is power-cycled.

Charging

If the unit is powered by a lithium polymer battery, it can be charged using the USB port. Any time the battery is attached and the unit is connected to a USB port, the battery will charge until it is fully charged. When the battery is full, the unit will stop charging it until the battery voltage drops below a certain level again. Note: The unit does not need to be powered on to charge.

Operation

Now that you know how the Logomatic works and what all of the settings do, it's time to power it up. Set your configuration however you like, make sure the SD card is fully inserted in the SD slot, and turn the unit on. The two status LEDs will blink at you rather quickly during the initialization, then the unit will go to work with the settings you chose. The only further indication of operation that you will see is when one of the two data buffers logs to the SD card, STAT0 for buffer #1 and STAT1 for buffer #2. These will be very quick "blips" because the LEDs are only on during the write process, between 20 and 40 mS.

When you are done logging, press the STOP button before shutting of the unit to be sure that any unfilled buffers are logged to the SD

Appendix E – Matlab Code

Initial Braking vs. Suspension Analysis

```
%Written by Nik Goodell

%5-20-2011
%Will take data array from the Swoop file and generate braking torque and
%suspension data
%time on column 1, Braking on column 2, Suspension on column 3

clc
hold off

tstep=CurrentArray(4,1)-CurrentArray(3,1);
a = size(CurrentArray);
asize = a(1);
CurrentArray(1:asize,4) = (CurrentArray(1:asize,2)-630)*0.39636; %Braking Torque.
Conversion factor based on calibration tests. (Bits to Nm)
CurrentArray(1:asize,5) = CurrentArray(1:asize,3)*-0.1999+105.8; %Amount Suspension is
Compressed. Conversion factor based on calibration tests. (Bits to mm)
%plot(CurrentArray(1:asize,1),CurrentArray(1:asize,4),CurrentArray(1:asize,1),CurrentA
rray(1:asize,5));

for n=1:(asize-1) %Adds a column for change in suspension to CurrentArray
ifCurrentArray(n,4)>2 %ignores suspension movement when the brakes are below 2 Nm
SuspChange = (CurrentArray(n+1,5)-CurrentArray(n,5))/tstep; %Rate of Change of
Suspension position (mm/s)
else
SuspChange=nan;
end
ifSuspChange>0
CurrentArray(n,7)=SuspChange; %Rate of Change of Suspension position (mm/s)
else
CurrentArray(n,7)=-1*SuspChange; %Rate of Change of Suspension position (mm/s)
end
end

for n=1:(asize-1) %Adds a column for suspension position to CurrentArray
ifCurrentArray(n,4)>0 %ignores suspension position when the brakes are below 0 Nm
SuspPos = CurrentArray(n,5); %Suspension position (mm)
else
SuspPos=nan;
end
CurrentArray(n,6)=SuspPos; %Rate of Change of Suspension position (mm/s)
End

PlotStart=round(0/tstep); %time in seconds that you want the plot to start
ifPlotStart<0.5
PlotStart=1;
end
PlotEnd=round(asize); %time to end the plot ('time'/tstep) OR leave equal to asize

%This plot is for time series of braking and suspension on the same plot
%use PlotStart for range to plot
plot(CurrentArray(PlotStart:PlotEnd,1),CurrentArray(PlotStart:PlotEnd,4),'r',CurrentAr
ray(PlotStart:PlotEnd,1),CurrentArray(PlotStart:PlotEnd,5),'b');
xlabel('Time (s)','FontSize',20);
ylabel('Braking Torque (Nm)','FontSize',20);
title('Suspension and Braking vs. Time','FontSize',24);
```

```
%This plot is for a scatter of shock compression position vs. Braking Torque
scatter(CurrentArray(PlotStart:PlotEnd,4),CurrentArray(PlotStart:PlotEnd,5),'.');
xlabel('Braking Torque (N-m)','FontSize',20);
ylabel('Suspension Compression (mm)','FontSize',20);
title('Suspension Position vs. Braking Torque','FontSize',24);

%This plot is for a scatter of shock compression rate vs. Braking Torque
scatter(CurrentArray(PlotStart:PlotEnd,4),CurrentArray(PlotStart:PlotEnd,7),'.');
xlabel('Braking Torque (N-m)','FontSize',20);
ylabel('Suspension Movement (mm/s)','FontSize',20);
title('Suspension Rate vs. Braking Torque','FontSize',24);


%%%%%%%%Statistic Values Array%%%%%%%%%%%%%%%%%%%%%%%%%%%%%%%%%%%%%%%%%%%%%%%%

%Binning the data so it can be averaged
d=0;
Bin=0;
BinSize=2;
AvgArray(200/BinSize,4)=zeros;
BinArray(200,asize)=zeros;
% BinArray(1:200,1:asize)=nan;
while Bin<200
avgNum=0;
    d=d+1;
    Bin=Bin+BinSize;
count(Bin,1)=0;
for n=1:(asize-1) %A
if Bin<CurrentArray(n,4)
ifCurrentArray(n,4)<Bin+BinSize
count(Bin,1)=count(Bin,1)+1;
BinArray(Bin,count(Bin,1))=CurrentArray(n,7);
avgNum=CurrentArray(n,7)+avgNum;
end
end
end


AvgArray(d,1)=Bin;
AvgArray(d,2)=(avgNum/count(Bin,1)); %Returns the average of each bin
AvgArray(d,3)=std(BinArray(Bin,1:count(Bin,1)));
if count(Bin,1)>10
AvgArray(d,4)=AvgArray(d,2)+3*AvgArray(d,3);
else
AvgArray(d,4)=nan;
end

holdon
scatter(AvgArray(1:40,1),AvgArray(1:40,4));


end
%%%%%%%%%%%%%%%%%%%%%%%%%%%%%%%%%%%%%%%%%%%%%%%%%%%%%%%%%%%%%%%%%%%%%%%%%%%%%%%

holdoff

for n=1:200 % This will total up the number of samples in each bin
if count(n,1)<5
count(n,1)=nan;
end
end
scatter(1:200,count(1:200,1));
```

```
%This plot is for the averages after the data is binned
scatter(AvgArray(1:200/round(BinSize),1),AvgArray(1:200/round(BinSize),2));
xlabel('Braking Torque (N-m)','FontSize',20);
ylabel('Suspension Movement (mm/s)','FontSize',20);
title('Suspension Compression Rate vs. Braking Torque','FontSize',24)
```

Pedaling Forces vs. Suspension

```
% 12/03/11
%Kathleen Kramer, NikGoodell

clc
clear

%http://www.mathworks.com/help/techdoc/learn_matlab/bq45sar.html for
%bins/outliers

%% parameters
%fSwoop=24.502; %frequency of data collection swoop (24.5Hz nominal) - Adjust if final spikes do
not align - Experimentally determined (the 0.002 is fine tuning)
fLogo=100;  %frequency of data collection Logomatic (Hz) - Assumed accurate


%% Read data - Enter the filename you want to read in here
rawSwoop = csvread('DATA_001.csv');   %first row meaningless, C1=-, C2=brakes, C3= rear wheel
speed, C4 = front wheel speed, C5 = suspension
rawPedal = csvread('Log10.txt');      %reading in the pedal data. Enter the filename
swoopSize= size(rawSwoop);                  %the number of data points in the swoop board
logoSize = size(rawPedal);                  %the number of data points in the logomatic board
rawSwoop = rawSwoop(3:(swoopSize(1)-2),:);  %trimming the first and last two points from the data
series
rawPedal = rawPedal(3:(logoSize(1)-2),:);   %trimming the first and last two points from the data
series
swoopSize= size(rawSwoop);                  %redefined rawSwoop size
logoSize = size(rawPedal);                  %redefined rawPedal size


%% Setting the zero values for correcting bias - Always allow the system to start at zero
brakeZero=mean([rawSwoop(25:100,2)]);   %taking the zero from the beginning of the run
rearMPHzero=mean([rawSwoop(10:25,3)]);  %taking the zero from the beginning of the run
frontMPHzero=mean([rawSwoop(10:25,4)]); %taking the zero from the beginning of the run
shockZero=mean([rawSwoop(25:100,5)]);   %taking the zero from the beginning of the run
pedalZero=mean([rawPedal(25:125)]);     %taking the zero from the beginning of the run

%% Trimming the data series to the sync spikes

%Pedal Board
n=1;
whilerawPedal(n)<300       %finds the point where the first spike begins
pStart=n;
    n=n+1;
end
pMax=0;
for n=pStart:(pStart+50)    %finds the peak of the first spike
ifrawPedal(n)>pMax
pMax=rawPedal(n);
pStart=n;
end
end
n=logoSize(1);
whilerawPedal(n)<300
pEnd=n;
    n=n-1;
end
pMax=0;
for n=(pEnd-50):pEnd%finds the peak of the first spike
ifrawPedal(n)>pMax
pMax=rawPedal(n);
pEnd=n;
end
    n=n+1;
end

%Swoop Board
```

```
n=1;
whilerawSwoop(n,2)>brakeZero-50    %finds the point where the first spike begins
sStart=n;
    n=n+1;
end
sMin=1000;
for n=sStart:(sStart+10)            %finds the peak of the first spike
ifrawSwoop(n,2)<sMin
sMin=rawSwoop(n,2);
sStart=n;
end
end
n=swoopSize(1);
whilerawSwoop(n,2)>brakeZero-50    %finds the point where the first spike begins
sEnd=n;
    n=n-1;
end
sMin=1000;
for n=sEnd-10:sEnd                  %finds the peak of the first spike
ifrawSwoop(n,2)<sMin
sMin=rawSwoop(n,2);
sEnd=n;
end
end
rawPedal=rawPedal(pStart:pEnd,:);   %redefine the logo to start and end at the sync marks
rawSwoop=rawSwoop(sStart:sEnd,:);   %redefine raw swoop to start and end at the sync marks
swoopSize=size(rawSwoop);           %redefined rawSwoop size
logoSize=size(rawPedal);            %redefined rawPedal size

%% Setting the frequency for the Swoop based on the Logomatic and the three sync spikes
fSwoop=swoopSize(1)/logoSize(1)*fLogo;              %Based on the time(s) being equal between the
spikes

%% Convert each signal to meaninful units
%brakeTorquenf=(rawSwoop(:,2)-brakeZero)*-5;         %in N-m
brakeTorquenf=(rawSwoop(:,2)-brakeZero)*-0.396872644;         %in N-m
rearMPHnf=(rawSwoop(:,3)-rearMPHzero)*.0335;        %in mph
frontMPHnf = (rawSwoop(:,4)-frontMPHzero)*.036171;  %in mph
shockMMnf=(rawSwoop(:,5)-shockZero)*-.23889;        %in mm
pedalTorque=(rawPedal(:)-pedalZero)*0.161545669;        %in N-m


%% define time arrays based on # of data points and sampling rate
tSwoopRow=[0:1:(swoopSize(1)-1)]/fSwoop;
tSwoop=tSwoopRow';
tLogoRow=[0:1:(logoSize(1)-1)]/fLogo;
tLogo=tLogoRow';
time=tLogoRow(logoSize(1)-1);             %

%% Wheelspeed filter
%Running the wheel speed data through a first order filter forward and
%backward. There is zero phase shift in the data.
h=fdesign.lowpass('Fp,Fst,Ap,Ast',0.01,.22,.2,1);
d=design(h,'equiripple'); %Lowpass FIR filter
frontMPH=filtfilt(d.Numerator,1,frontMPHnf); %zero-phase filtering
rearMPH=filtfilt(d.Numerator,1,rearMPHnf); %zero-phase filtering

%% Suspension filter
h=fdesign.lowpass('Fp,Fst,Ap,Ast',0.01,.9,.1,1);
d=design(h,'equiripple'); %Lowpass FIR filter
shockMM=filtfilt(d.Numerator,1,shockMMnf); %zero-phase filtering

%% Brake filter
h=fdesign.lowpass('Fp,Fst,Ap,Ast',0.01,.8,.1,1);
d=design(h,'equiripple'); %Lowpass FIR filter
brakeTorque=filtfilt(d.Numerator,1,brakeTorquenf); %zero-phase filtering

%% Time Series Plots
speedMax=max(frontMPH); %Used for axis limits
```

```
pedalMax=max(pedalTorque); %Used for axis limits
shockMax=max(shockMM); %Used for axis limits
brakeMax=max(brakeTorque); %Used for axis limits
brakeColor=[0.6 0 0]; %Set plot color here
pedalColor=[0 0.6 0.2]; %Set plot color here
fSpeedColor=[0 0.4 1]; %Set plot color here
%rSpeedColor=[0.8 0.2 0.4]; %Set plot color here. Used when rear wheel speed is working
rSpeedColor=fSpeedColor;    %Used when rear wheel speed data is not being plotted
suspColor='k'; %Set plot color here
axesFont=14; %Set axis title font size here

figure
subplot(2,1,1) %Plot 1
[haxes,hline1,hline2]=plotyy(tSwoop,shockMM,tLogo,pedalTorque);
xlabel ('Time (s)','FontSize',axesFont)
%Primary Axis
xlim([0 time])
axes (haxes(1))
ylim([0 shockMax*1.2])
set(gca,'YColor',suspColor)
ylabel ('Suspension Movement (mm)','Color',suspColor,'FontSize',axesFont)
%Secondary Axis
axes (haxes(2))
xlim([0 time])
ylim([0 pedalMax*1.2])
set(gca,'YColor',pedalColor)
ylabel ('Pedaling Torque (N-m)','Color',pedalColor,'FontSize',axesFont)
set(hline1,'Color',suspColor)
set(hline2,'Color',pedalColor)

subplot(2,1,2) %Plot 2
[haxes,hline1,hline2]=plotyy(tSwoop, frontMPH, tSwoop, rearMPH);
xlabel ('Time (s)','FontSize',axesFont)
%Primary Axis
xlim([0 time])
axes(haxes(1))
ylim([0 speedMax*1.2])
set(gca,'YColor',fSpeedColor)
ylabel ('Front Wheel Speed (mph)','Color',fSpeedColor,'FontSize',axesFont)
%Secondary Axis
axes (haxes(2))
xlim([0 time])
ylim([0 speedMax*1.2])
set(gca,'YColor',rSpeedColor)
%ylabel ('Rear Wheel Speed(mph)','Color',rSpeedColor,'FontSize',axesFont)   %turned off since
rear wheel is not working
set(hline1,'Color',fSpeedColor)
set(hline2,'Color',rSpeedColor,'LineStyle','none')  %Disappears the rear wheel line since it is
not working

figure (2)
subplot(2,1,1)
[haxes,hline1,hline2]=plotyy(tSwoop,shockMM,tSwoop,brakeTorque);
xlabel ('Time (s)','FontSize',axesFont)
%Primary Axis
xlim([0 time])
axes (haxes(1))
ylim([0 shockMax*1.2])
set(gca,'YColor',suspColor)
ylabel ('Suspension Movement (mm)','Color',suspColor,'FontSize',axesFont)
%Secondary Axis
axes (haxes(2))
xlim([0 time])
ylim([0 brakeMax*1.2])
set(gca,'YColor',brakeColor)
ylabel ('Brake Torque (N-m)','Color',brakeColor,'FontSize',axesFont)
set(hline1,'Color',suspColor)
set(hline2,'Color',brakeColor)

subplot(2,1,2)
```

```
[haxes,hline1,hline2]=plotyy(tSwoop, frontMPH, tSwoop, rearMPH);
xlabel ('Time (s)','FontSize',axesFont)
%Primary Axis
xlim([0 time])
axes (haxes(1))
ylim([0 speedMax*1.2])
set(gca,'YColor',fSpeedColor)
ylabel ('Front Wheel Speed (mph)','Color',fSpeedColor,'FontSize',axesFont)
%Secondary Axis
axes (haxes(2))
xlim([0 time])
ylim([0 speedMax*1.2])
set(gca,'YColor',rSpeedColor)
%ylabel ('Rear Wheel Speed(mph)','Color',rSpeedColor,'FontSize',axesFont)   %turned off since
rear wheel is not working
set(hline1,'Color',fSpeedColor)
set(hline2,'Color',rSpeedColor,'LineStyle','none')  %Disappears the rear wheel line since it is
not working

%% Suspension Velocity and Acceleration
%Numerical Derivatives
dx=diff(shockMM);                                   %Difference between elements in the shockMM array
dt=diff(tSwoop);                                    %Difference between elements in the tSwoop array
(time step)
for n=2:swoopSize(1)-1                              %Derivative of shock position to get velocity
shockMM_snf(n,1)=(dx(n-1)+dx(n))/(2*dt(n));         %Three point finite difference method gives zero
phase shift in the array
    n=n+1;
shockMM_snf(n,1)=0;
end
dv=diff(shockMM_snf);                               %Difference between elements of the shock
velocity array
for n=2:swoopSize(1)-1                              %Derivative of shock velocity to get acceleration
    shockMM_s2nf(n,1)=(dv(n-1)+dv(n))/(2*dt(n));    %Three point finite difference method gives
zero phase shift in the array
    n=n+1;
    shockMM_s2nf(n,1)=0;
end
h=fdesign.lowpass('Fp,Fst,Ap,Ast',0.01,.9,.1,1);%filtering the velocity data
d=design(h,'equiripple'); %Lowpass FIR filter
shockMM_s=filtfilt(d.Numerator,1,shockMM_snf); %zero-phase filtering
h=fdesign.lowpass('Fp,Fst,Ap,Ast',0.01,.9,.1,1);%filtering the acceleration data
d=design(h,'equiripple'); %Lowpass FIR filter
shockMM_s2=filtfilt(d.Numerator,1,shockMM_s2nf); %zero-phase filtering

%% Making a pedal force array that is the same length as the suspension arrays
for n=20:(swoopSize(1))
    t=round(n*fLogo/fSwoop);
if t>=logoSize
pedalShorter(n,1)=pedalShorter(n-1,1);
else
pedalShorter(n,1)=mean([pedalTorque(t-1,1):pedalTorque(t+1,1)]);
end
    n=n+1;
end

%% Pedal VS Suspension Plots
% %This plot is for a scatter of shock compression vs. Pedal Torque
% figure(3)
% scatter(pedalShorter,shockMM,'.');
% xlabel('Pedal Torque (N-m)','FontSize',20);
% ylabel('Suspension Position (mm)','FontSize',20);
% title('Suspension Position vs. Pedal Torque (N-m)','FontSize',24);
%
% %This plot is for a scatter of shock compression rate vs. Pedal Torque
% figure(4)
% scatter(pedalShorter,shockMM_s,'.');
% xlabel('Pedal Torque (N-m)','FontSize',20);
% ylabel('Suspension Movement (mm/s)','FontSize',20);
% title('Suspension Rate vs. Pedal Torque (N-m)','FontSize',24);
```

```
% %This plot is for a scatter of shock compression accvs. Pedal Torque
% figure(5)
% scatter(pedalShorter,shockMM_s2,'.');
% xlabel('Pedal Torque (N-m)','FontSize',20);
% ylabel('Suspension Acceleration (mm/s^2)','FontSize',20);
% title('Suspension Acceleration vs. Pedal Torque (N-m)','FontSize',24);
%
% figure (6)
% velMax=max(shockMM_s); %Used for axis limits
% [haxes,hline1,hline2]=plotyy(tSwoop,shockMM,tSwoop,shockMM_s);
% xlabel ('Time (s)','FontSize',axesFont)
% %Primary Axis
% xlim([0 time])
% axes (haxes(1))
% ylim([0 shockMax*1.2])
% set(gca,'YColor',suspColor)
% ylabel ('Suspension Position (mm)','Color',suspColor,'FontSize',axesFont)
% %Secondary Axis
% axes (haxes(2))
% xlim([0 time])
% ylim([0 velMax*1.2])
% set(gca,'YColor',brakeColor)
% ylabel ('Suspension Rate (mm/s)','Color',brakeColor,'FontSize',axesFont)
% set(hline1,'Color',suspColor)
% set(hline2,'Color',brakeColor)


%% We will now look into finding the trends in the data...
%Binning the pedal force data so it can be averaged
d=0;                                    %counter variable (n is being used)
Bin=0;                                  %initializing Bin; the pedalTorque range
BinSize=15;                             %width of each Bin (Nm)
numBins=round(600/BinSize);
shockMMBin(1:numBins,1)=nan;
shockMM_sBin(1:numBins,1)=nan;
while Bin<600
posSum=0;                               %initializing
velSum=0;                               %initializing
accSum=0;                               %initializing
    d=d+1;                                  %incrementing loop counter
binCount(d,1)=0;                        %initializing
for n=1:swoopSize(1)-1                  %goes through the susp data one by one
iffrontMPH(n)>1                        %only if the bike is in motion
if Bin<pedalShorter(n)                  %is the torque over the bin lower limit?
ifpedalShorter(n)<Bin+BinSize%is the torque under the bin upper limit?
binCount(d,1)=binCount(d,1)+1;          %count of all the susp points in this bin range
posSum=shockMM(n)+posSum;               %sum of all the pos points in this bin range
velSum=shockMM_s(n)+velSum;             %sum of all the vel points in this bin range
accSum=shockMM_s2(n)+accSum;            %sum of all the acc points in this bin range
end
end
end
end
ifbinCount(d,1)<50                         %is the number of samples in the bin enough to make it
useful?
shockMMBin(d,1)=nan;                        %if no then shock pos for that bin is nan
shockMM_sBin(d,1)=nan;                      %if no then shock vel for that bin is nan
        shockMM_s2Bin(d,1)=nan;                     %if no then shock acc for that bin is nan
else
shockMMBin(d,1)=posSum/binCount(d,1);       %if yes then shock pos for that bin is the average of
the data points in that range
shockMM_sBin(d,1)=velSum/binCount(d,1);     %if yes then shock vel for that bin is the average of
the data points in that range
        shockMM_s2Bin(d,1)=accSum/binCount(d,1);     %if yes then shock acc for that bin is the
average of the data points in that range
end
torqueBins(d,1)=Bin+0.5*BinSize;            %the center of each torque bin range
    Bin=Bin+BinSize;                            %setting the next bin
end
```

```
%% Now we plot and look for the trends
%hold on
%scatter(torqueBins(1:d,1),shockMM_s2Bin(1:d,1));       %Used to plot a scatter of the binned
data for either shockMMBin, shockMM_sBin or shockMM_s2Bin
%hold on
%scatter(torqueBins(1:d,1),binCount(1:d,1)); %just a scatter of the count in each bin; a metric
for statistical significance
%hold off


%to do: find meaningful relationships, remove text from data files
%write code to spit out formatted plots of Torque to shock pos/vel/acc
%use plots on line 248-288 and line 331
```

Appendix F – Test Parameters and Results

Controlled Tests: Changing One Independent Variable (Section 7.1.1)

Table F.1 - Description of each test trial completed in front of Kathleen's house.

Trial	Comments
1	Smooth pavement, no brakes
2	Smooth pavement, constant light braking on slope
3	Smooth pavement, braking on level ground
4	Smooth pavement, intermittent light braking on slope
5	Smooth pavement, intermittent heavy braking on slope
6	Smooth pavement, heavy braking on slope
7	Off curb, no brakes
8	Off curb, no brakes
9	Off curb, no brakes
10	Messed up, forgot to brake
11	Went off curb in wrong location (Missing Data)
12	Off curb, constant braking, extra braking for car passing
13	Off curb, constant braking
14	Off curb, constant braking
15	Off curb, constant braking
16	Off curb, constant braking
17	Off curb, constant braking

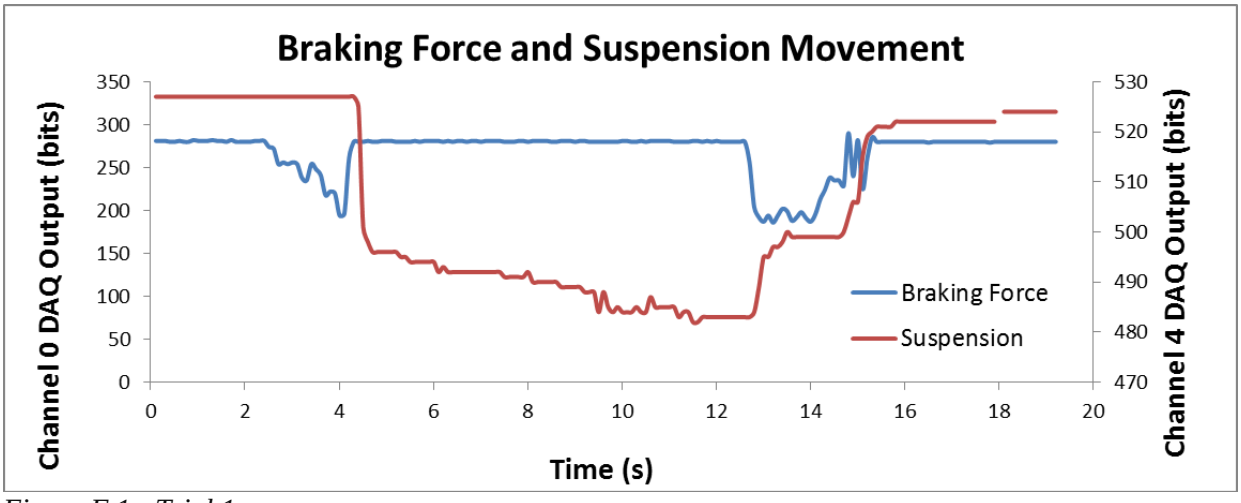

Figure F.1 - Trial 1

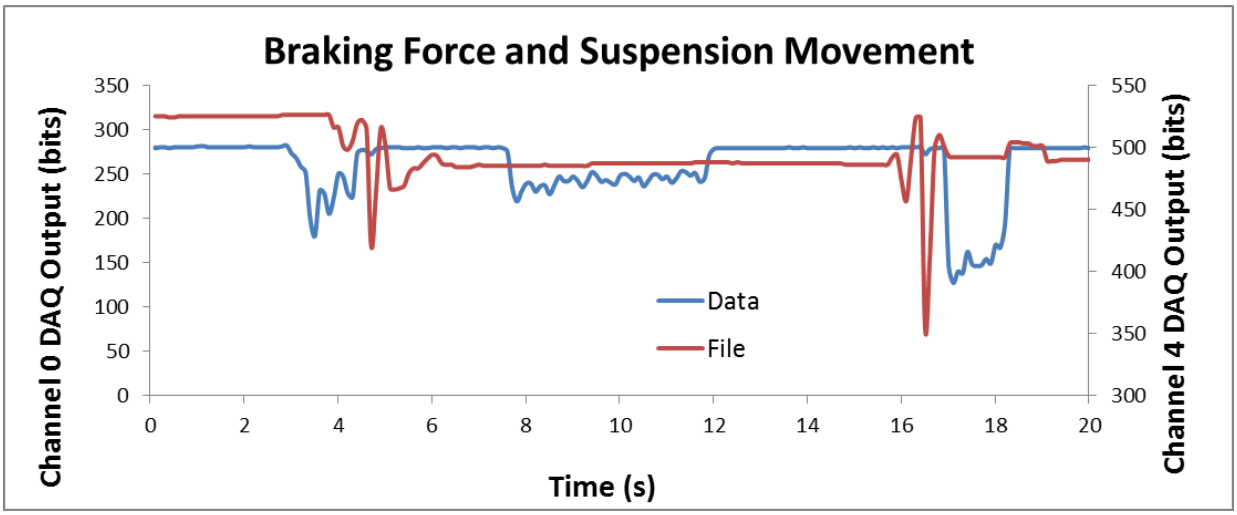

Figure F.2 - Trial 2

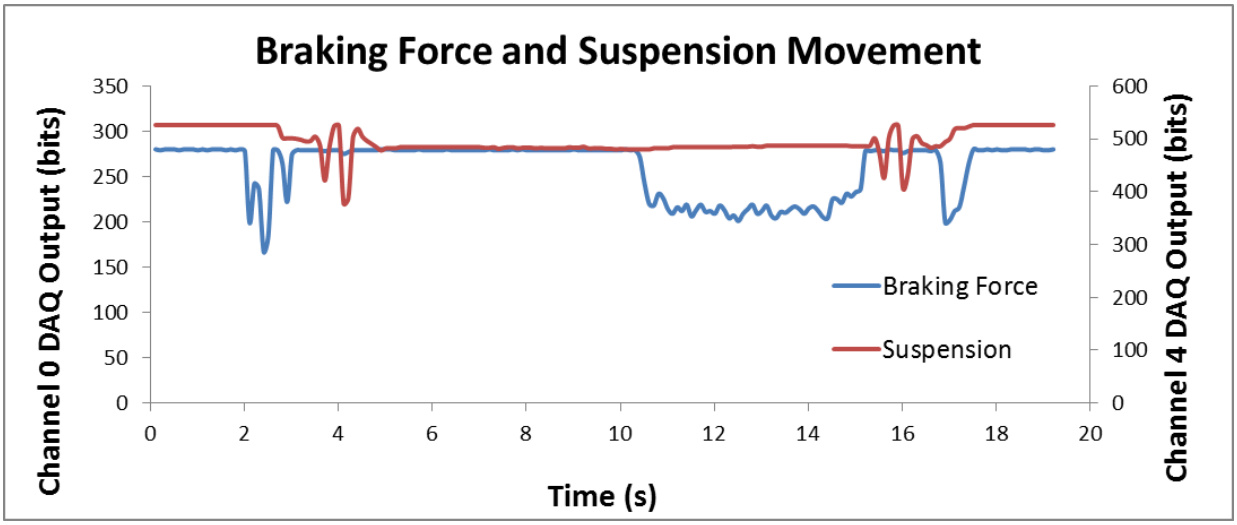

Figure F.3 - Trial 3

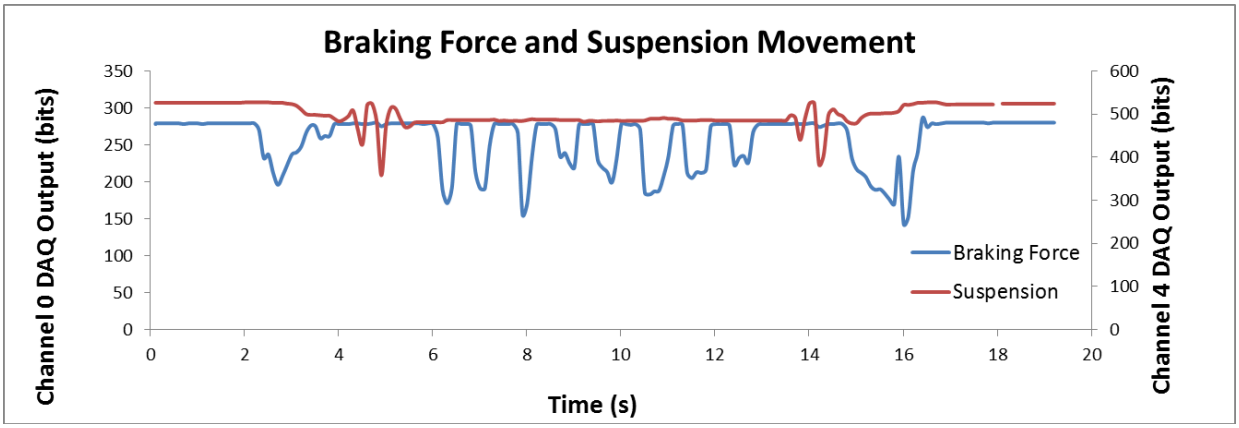

Figure F.4 - Trial 4

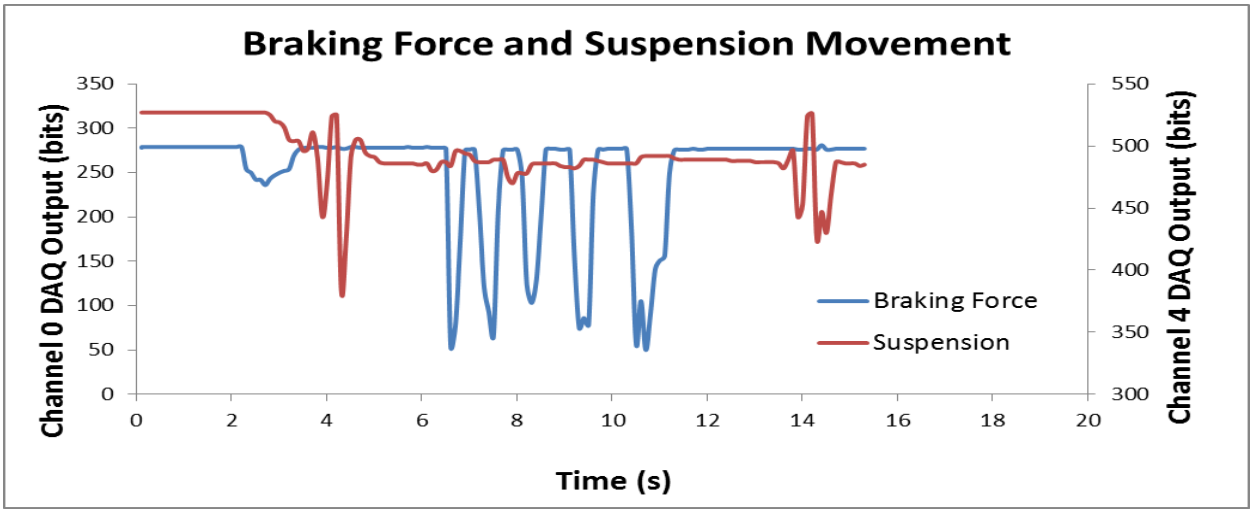

Figure F.5 - Trial 5

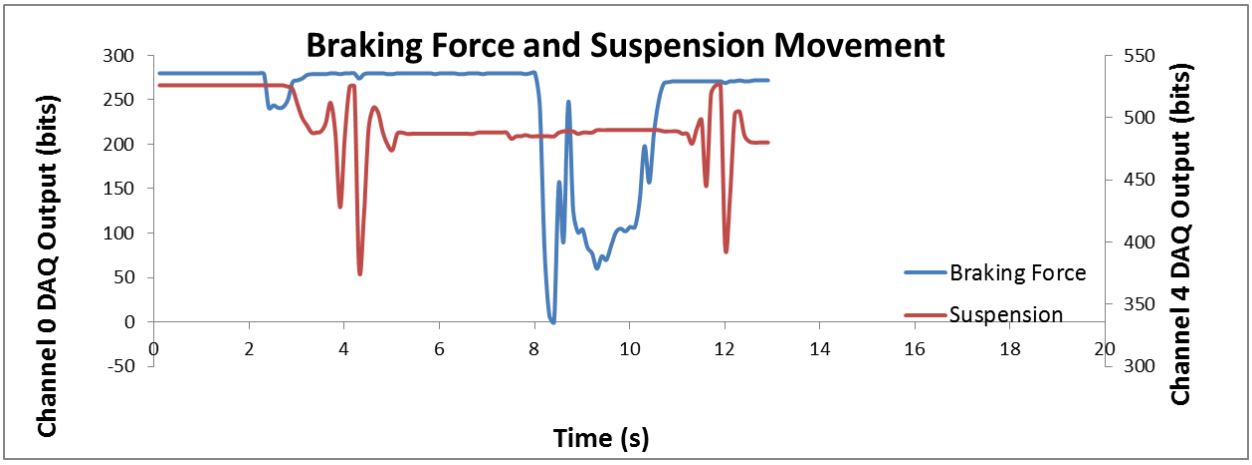

Figure F.6 - Trial 6

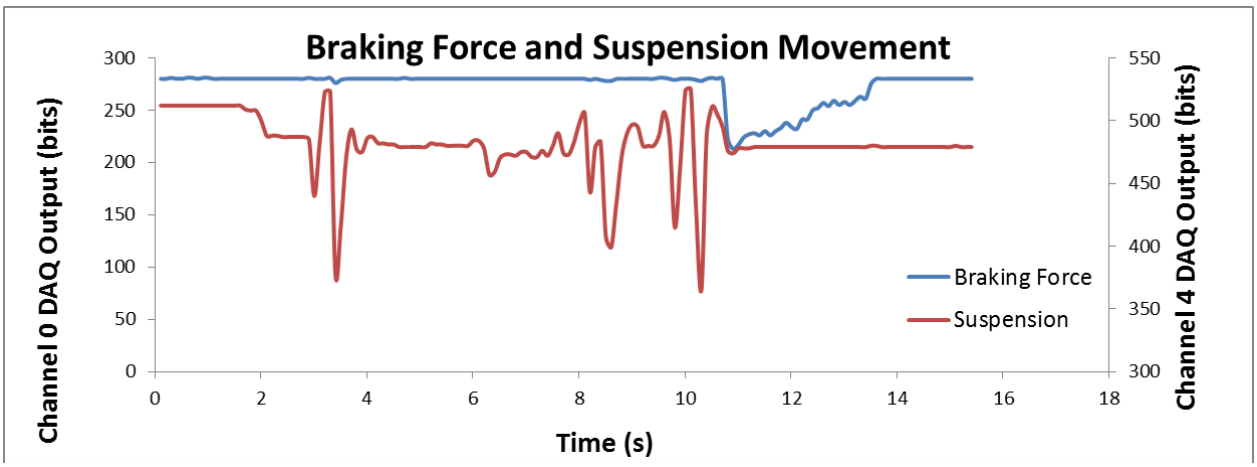

Figure F.7 - Trial 7

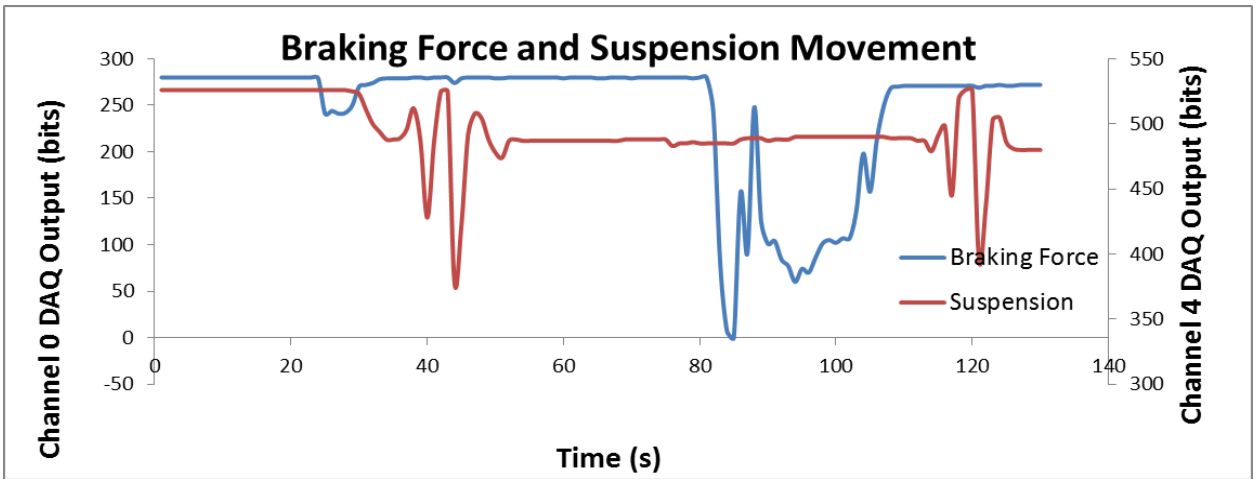

Figure F.8 - Trial 8

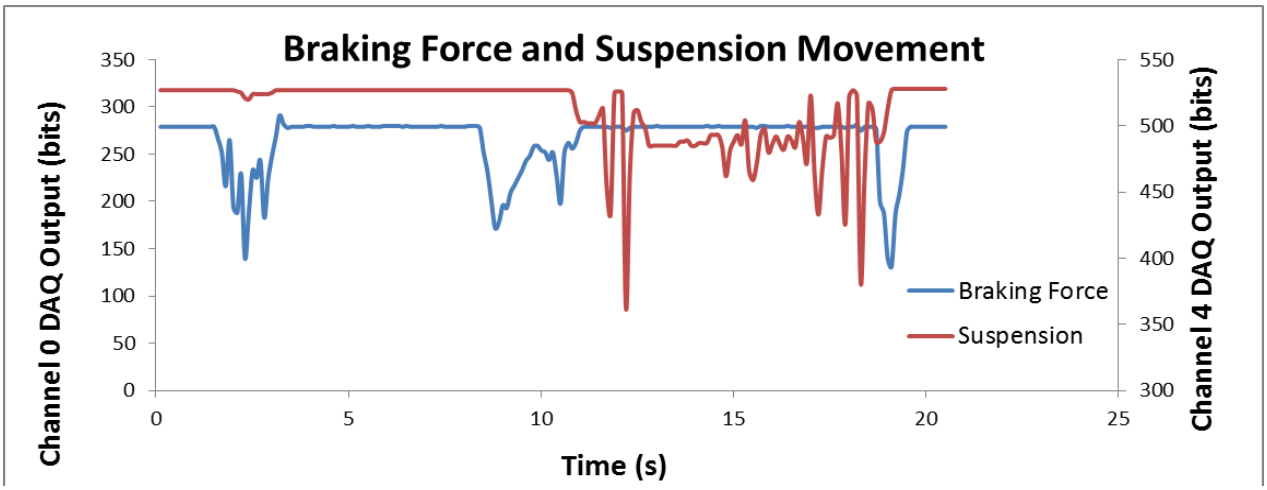

Figure F.9 - Trial 9

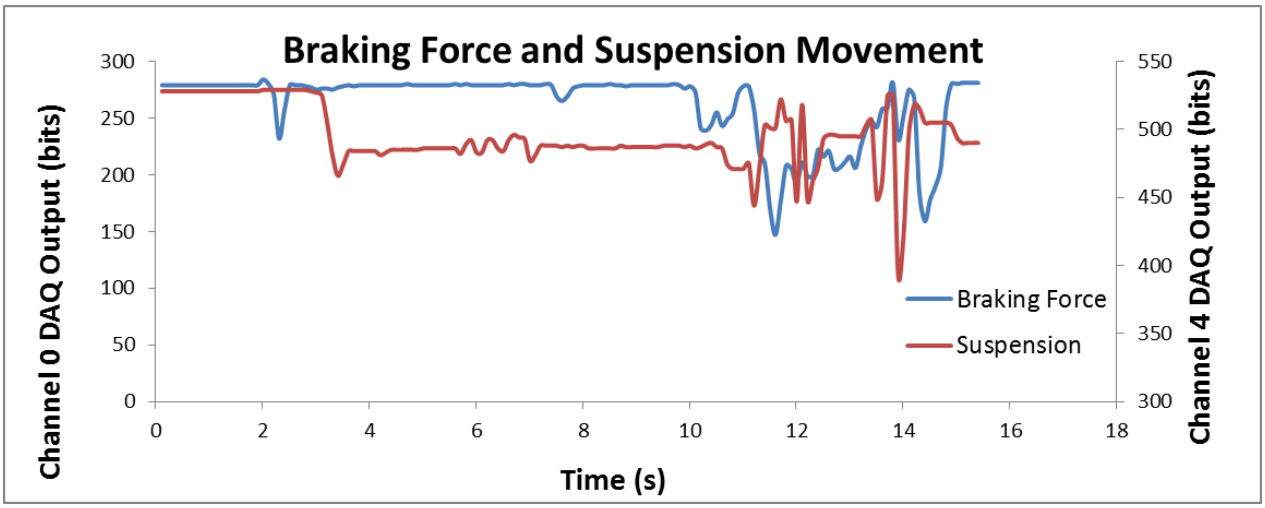

Figure F.10 - Trial 10

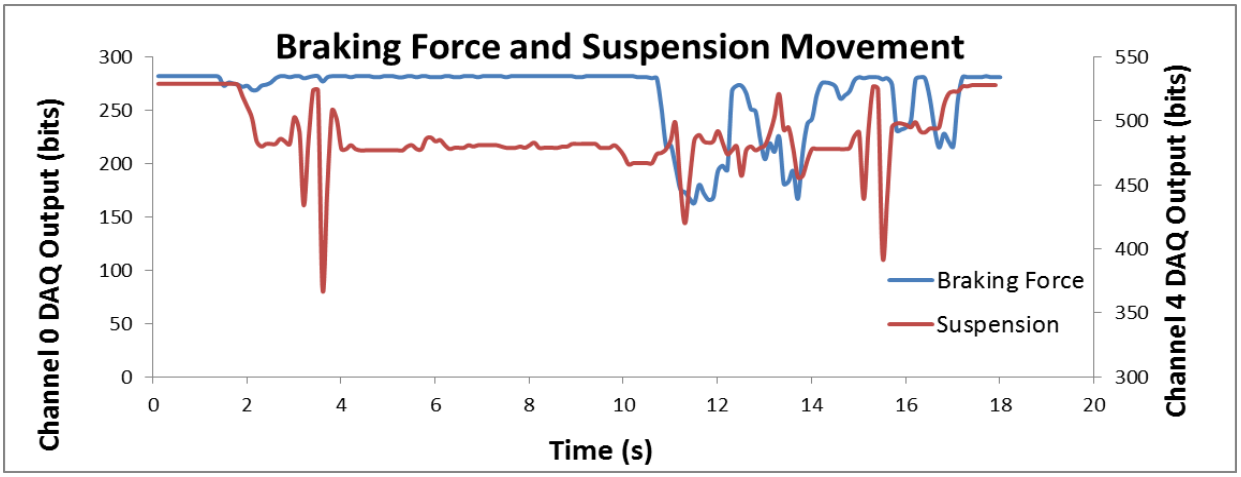

Figure F.11 - Trial 11

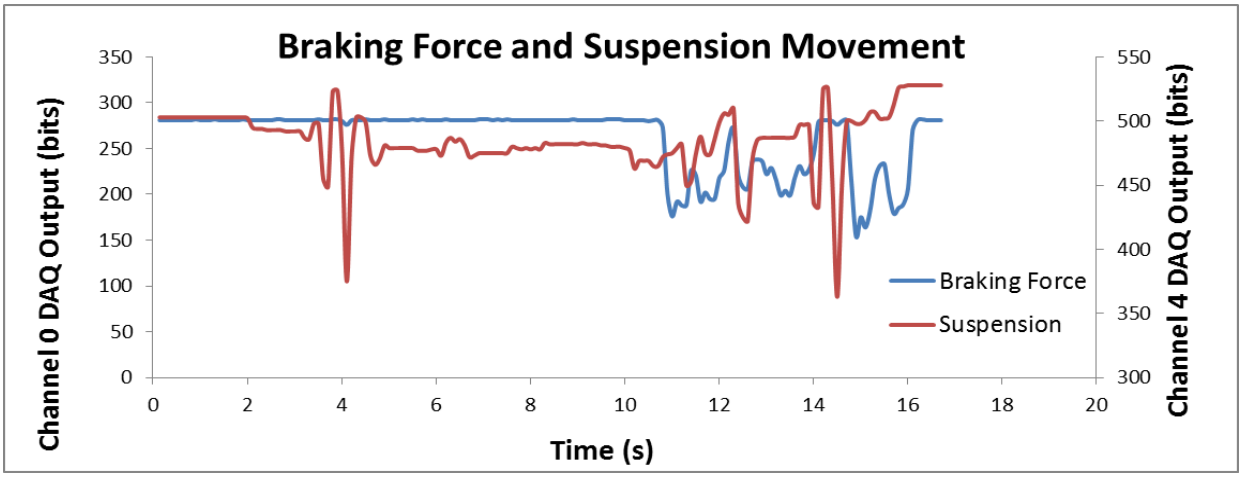

Figure F.12 - Trial 13

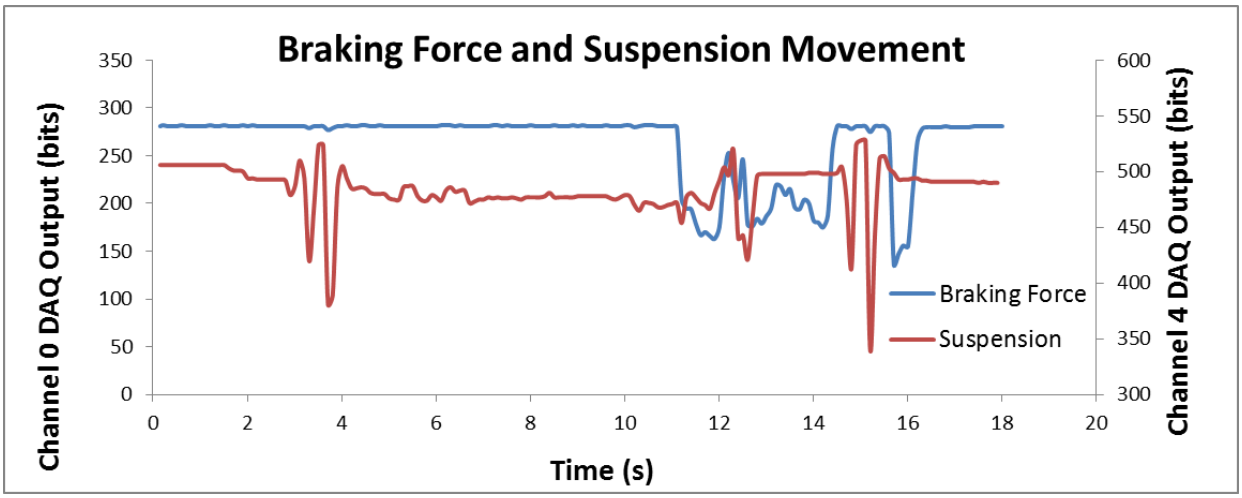

Figure F.13 - Trial 14

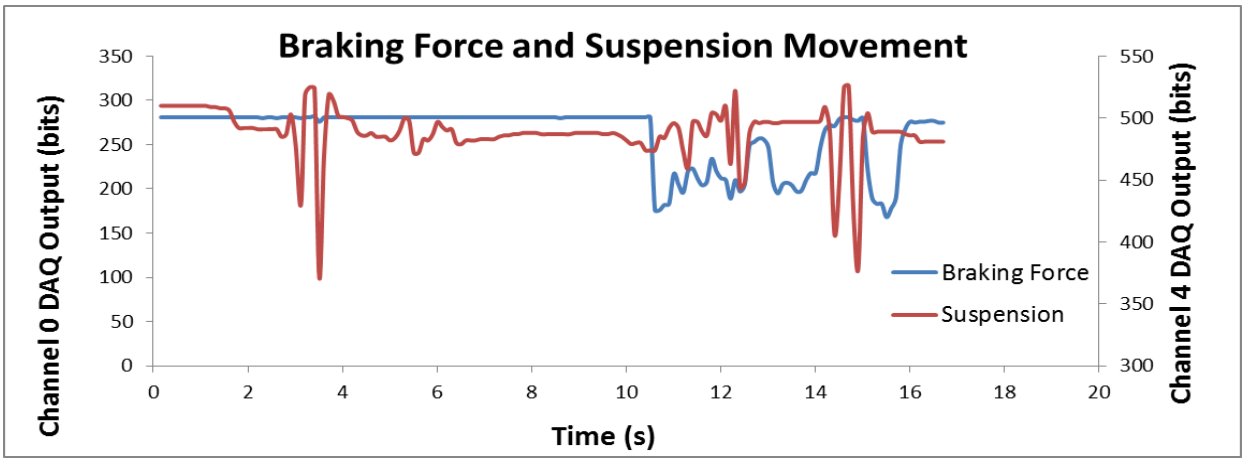

Figure F.14 - Trial 15

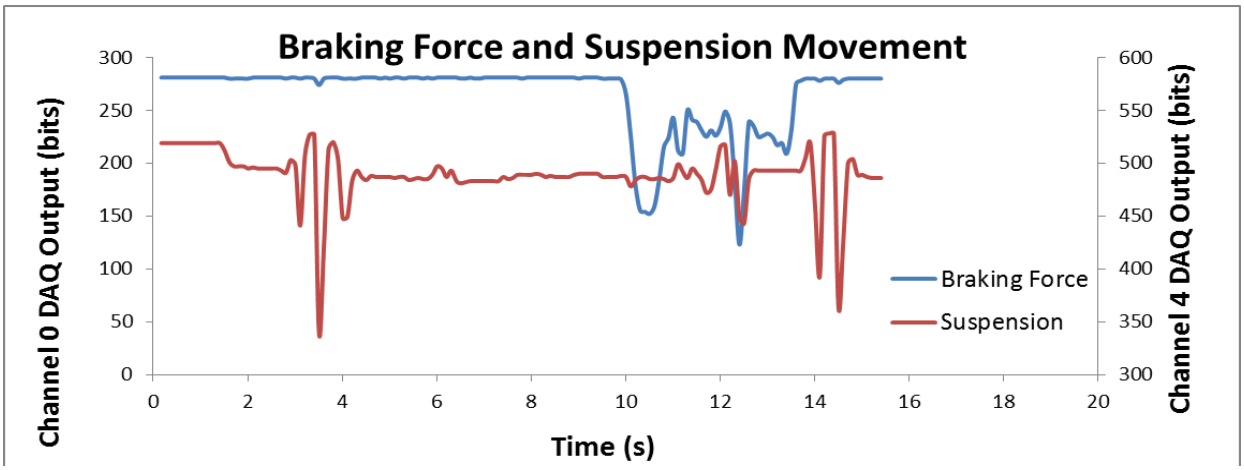

Figure F.15 - Trial 16

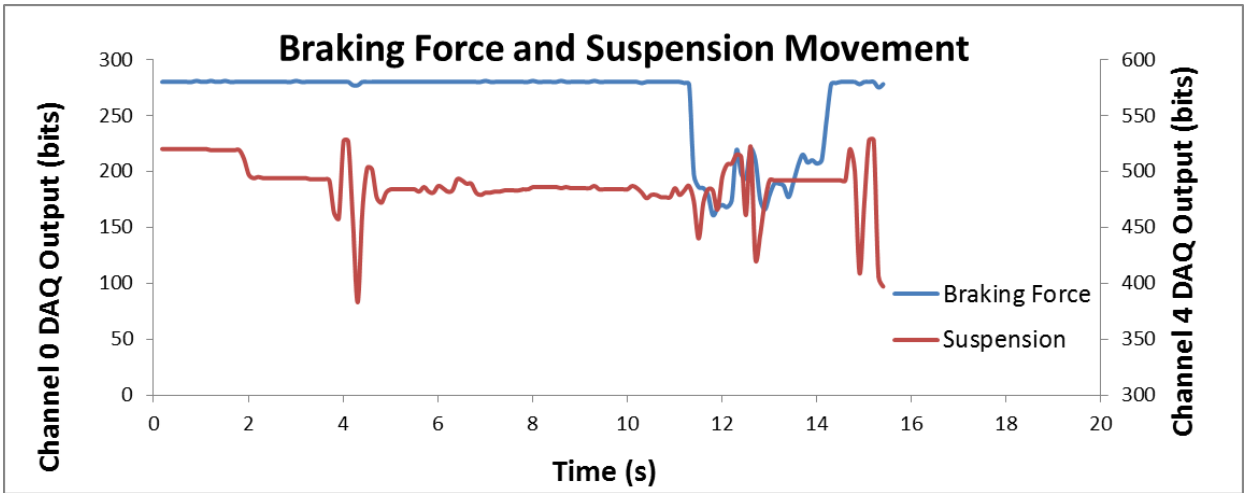

Figure F.16 - Trial 17

Trail Tests: Collecting a Large Quantity of Data (Section 7.1.2)

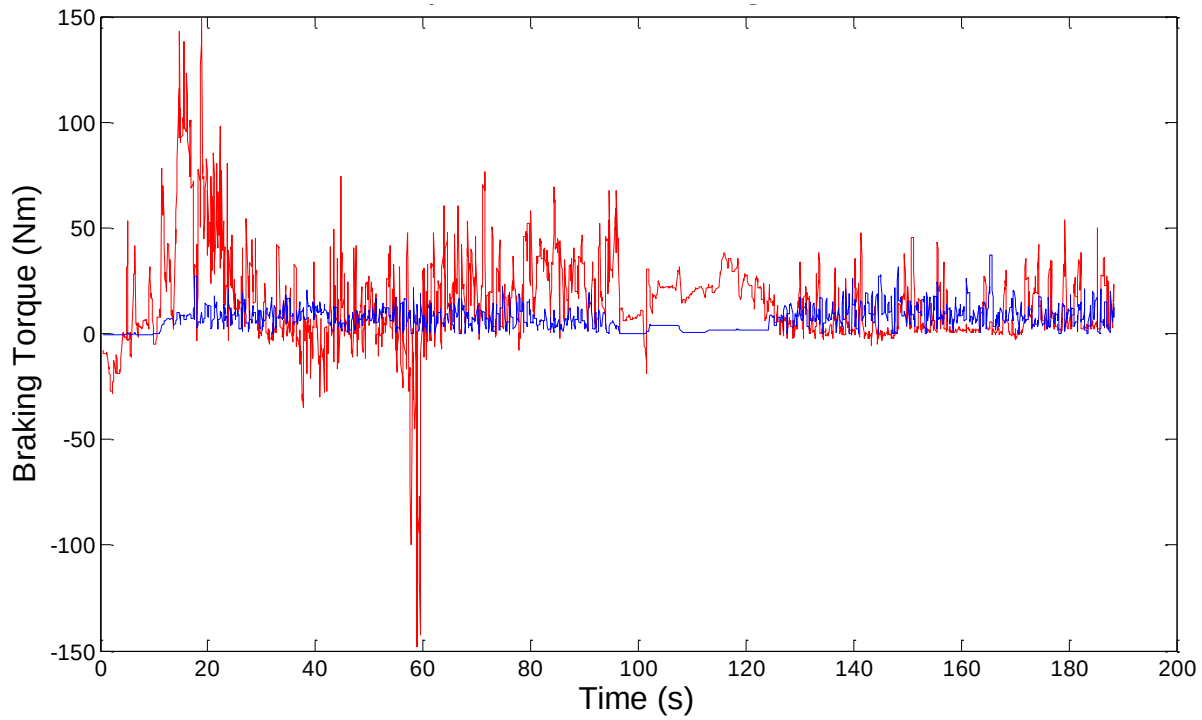

Figure F.17 - Time series for the entire Morning Glory run used for braking testing.

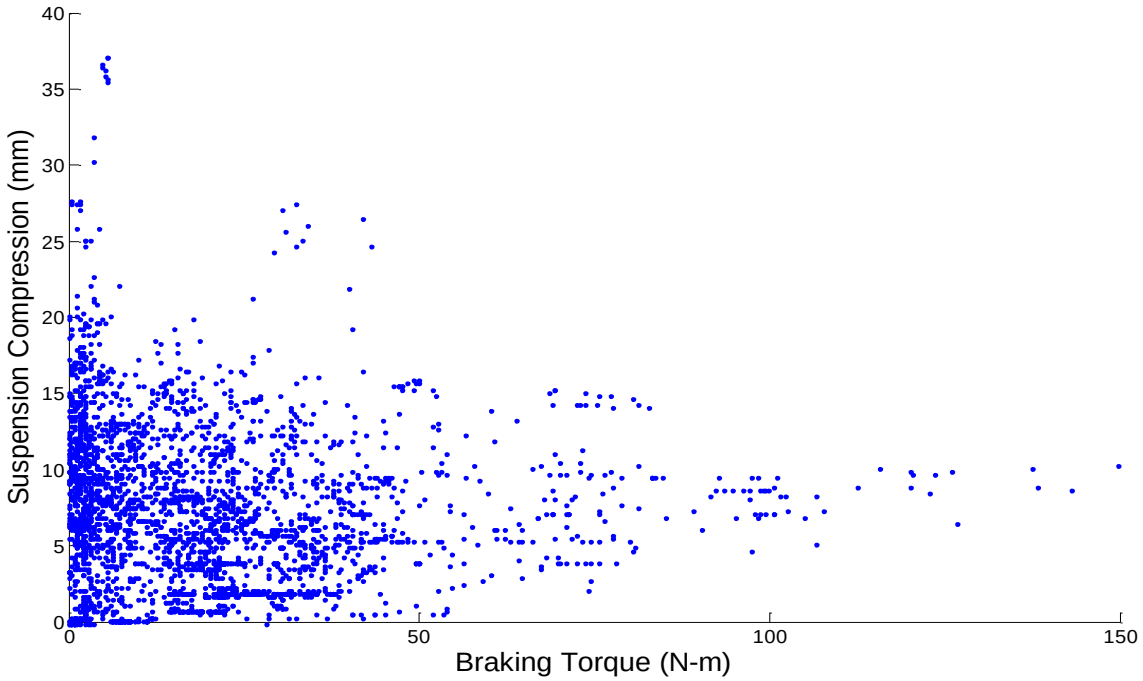

Figure F.18 - Scatter of all the data points collected during the Morning Glory run.

Flat Pavement Testing in Various Gears (Section 7.2.1)

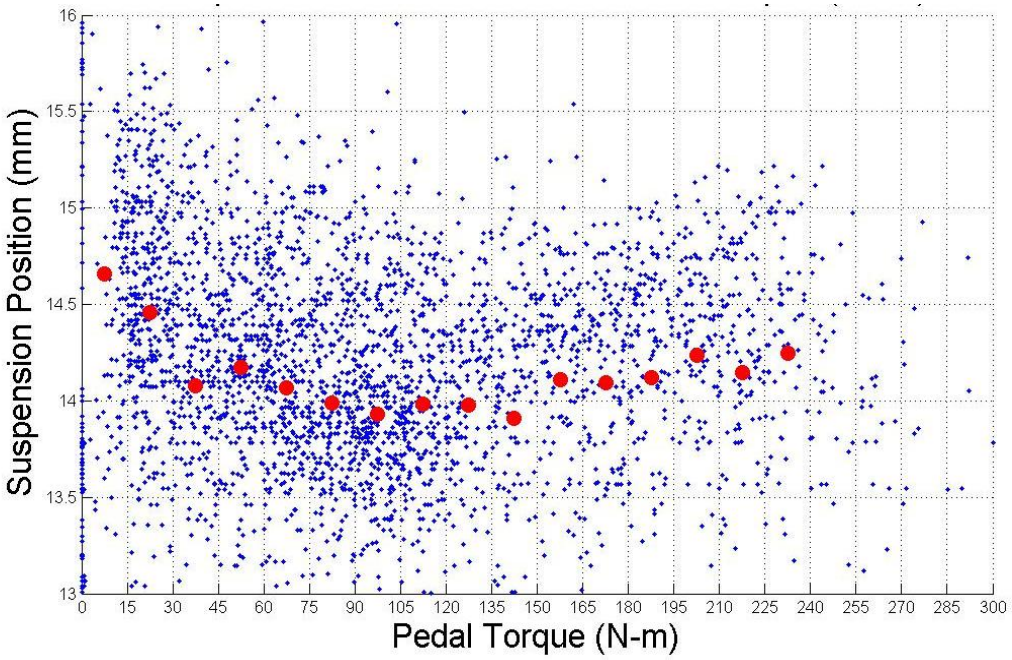

Figure F.19 – Suspension Position vs Pedaling Torque in Gear 3

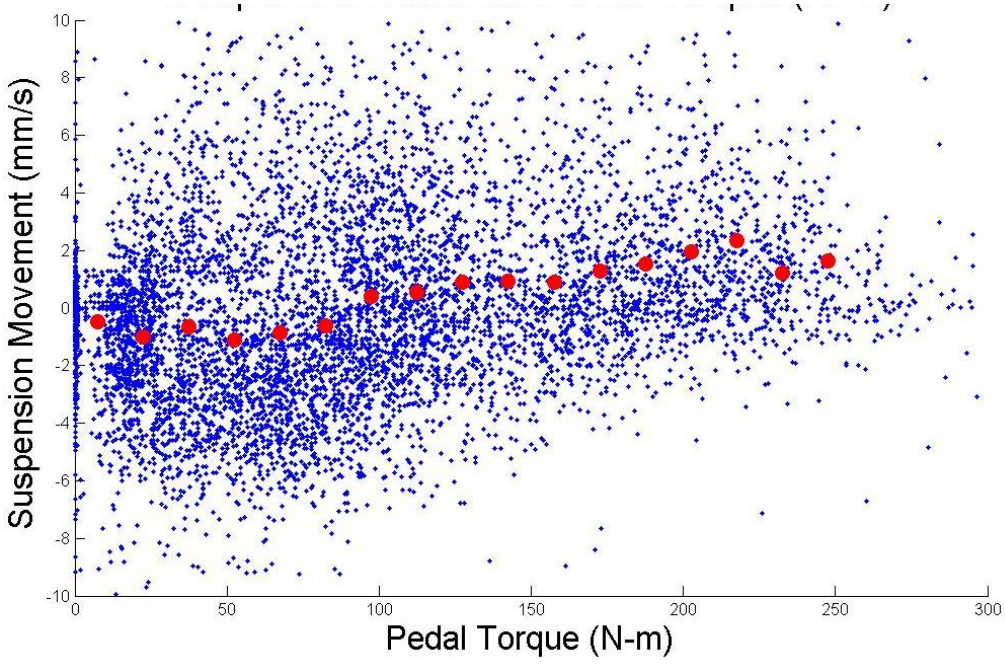

Figure F.20 – Suspension Velocity vs. Pedaling Torque in Gear 3

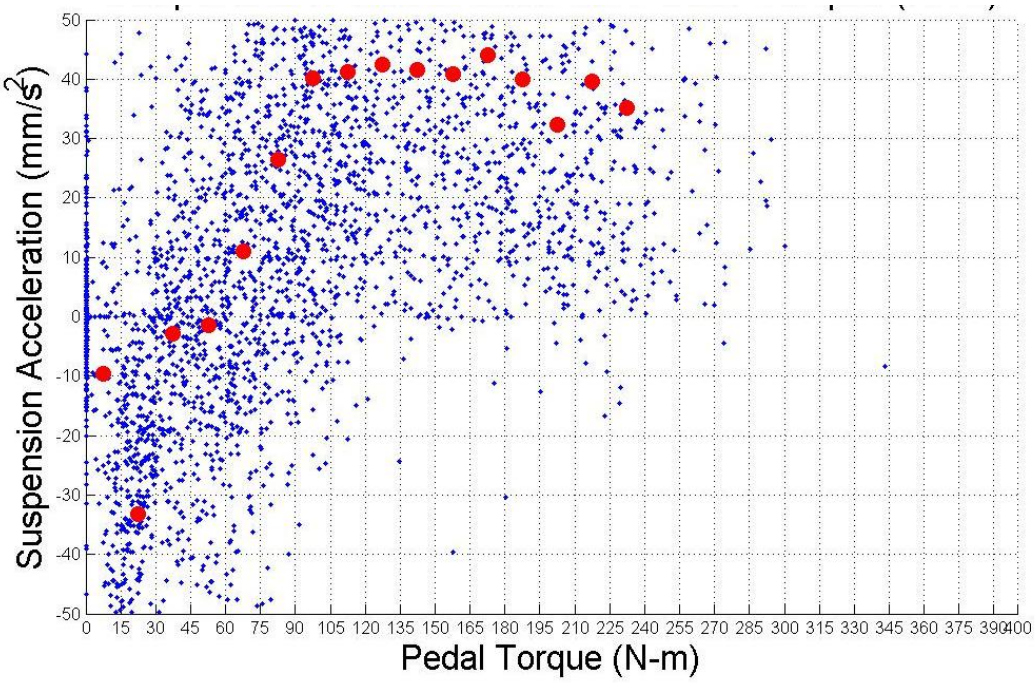

Figure F.21 – Suspension Acceleration vs. Pedaling Torque in Gear 3

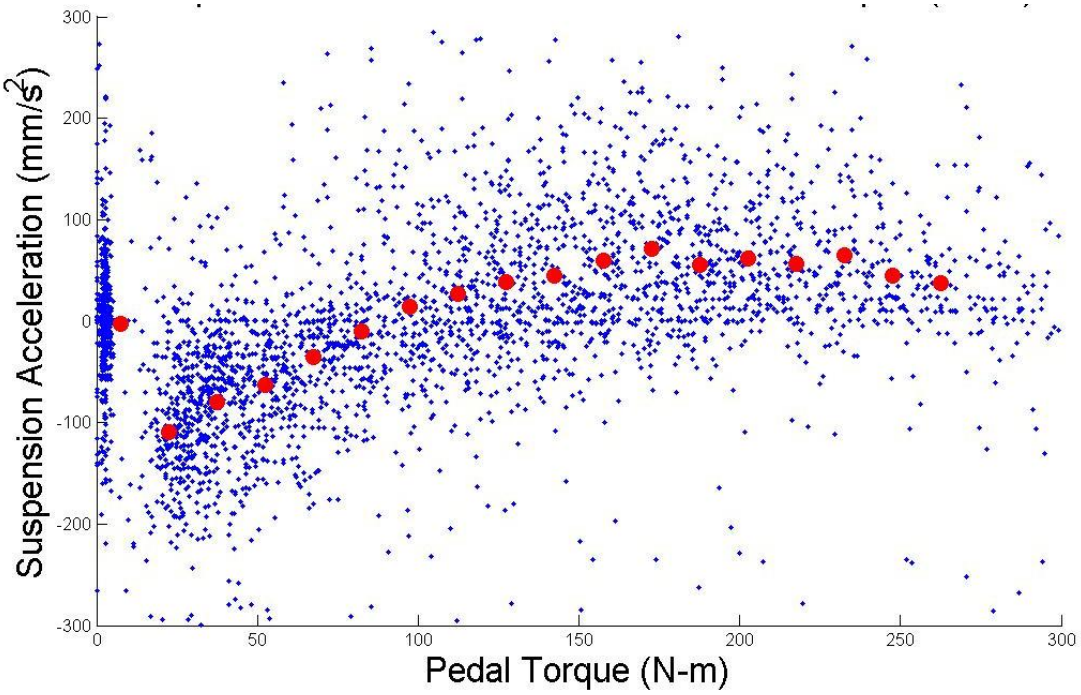

Figure F.22 - Suspension Acceleration vs. Pedaling Torque in Gear 8

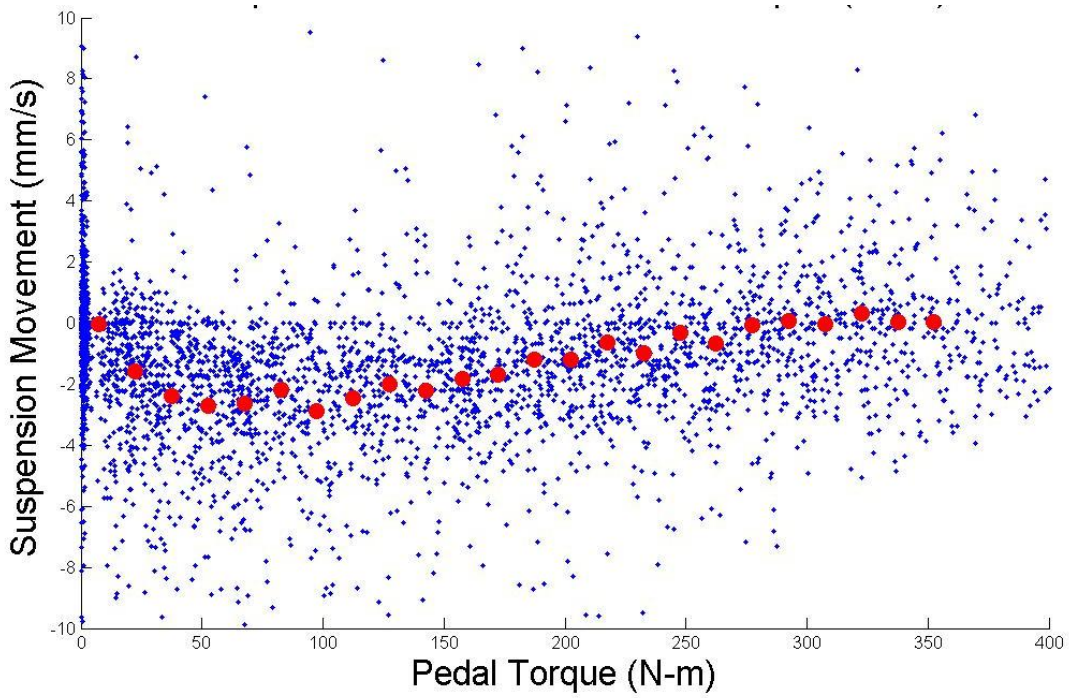

Figure F.23 - Suspension Velocity vs. Pedaling Torque in Gear 10

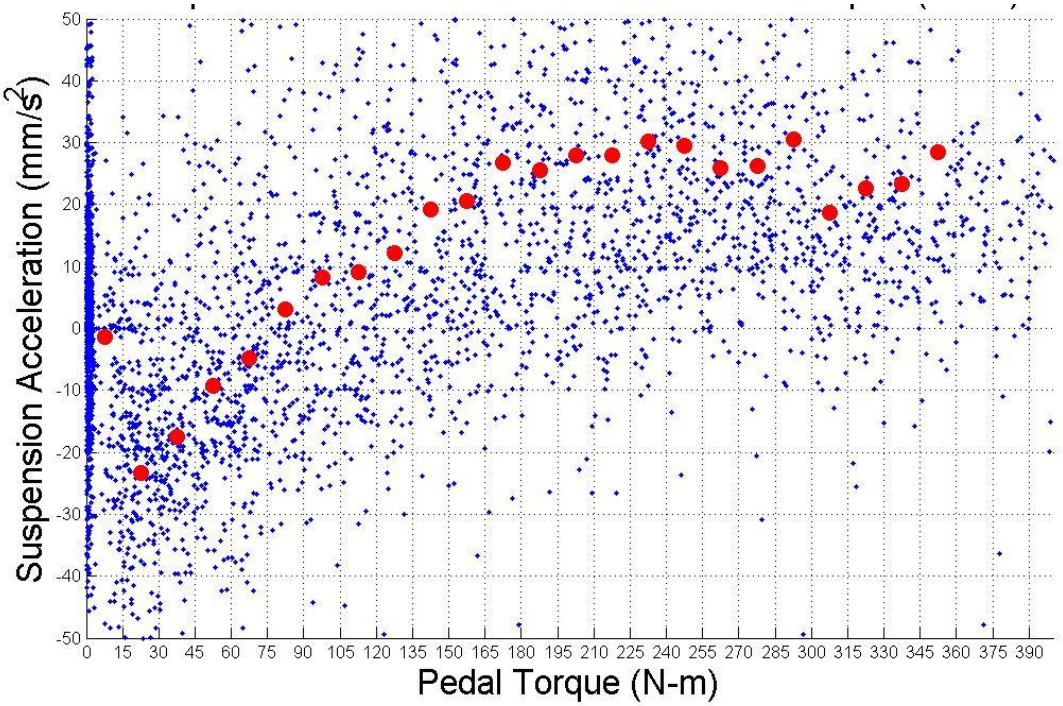

Figure F.24 - Suspension Acceleration vs. Pedaling Torque in Gear 10

Uphill Pavement Pedaling in Various Gears (Section 7.2.2)

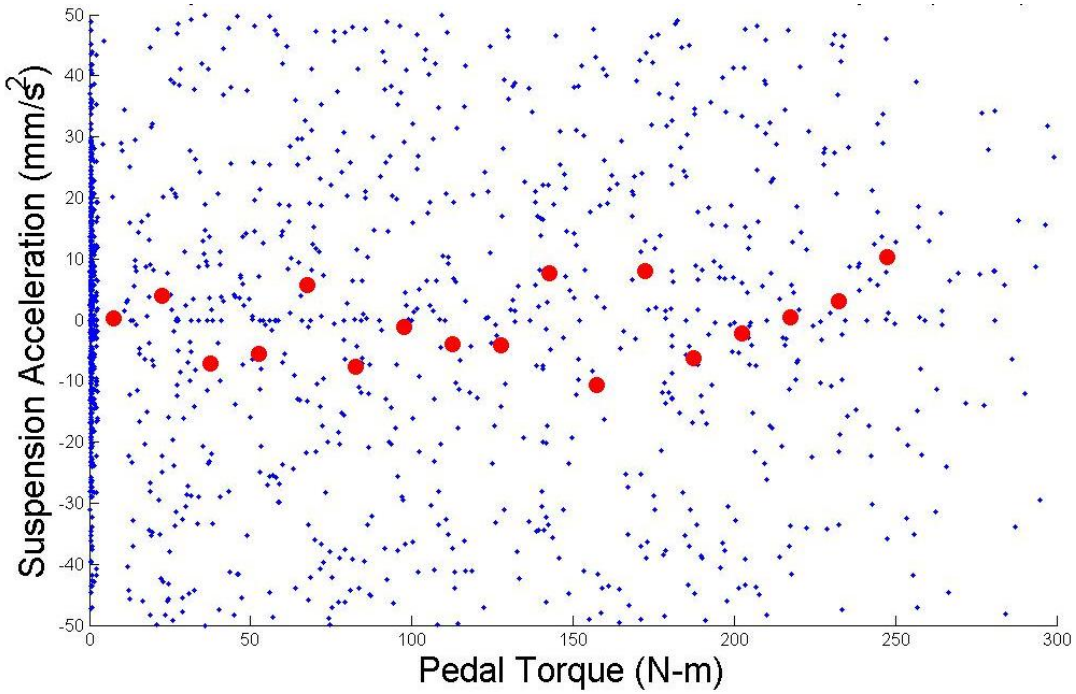

Figure F.25 - Suspension Acceleration vs. Pedaling Torque in Gear 4

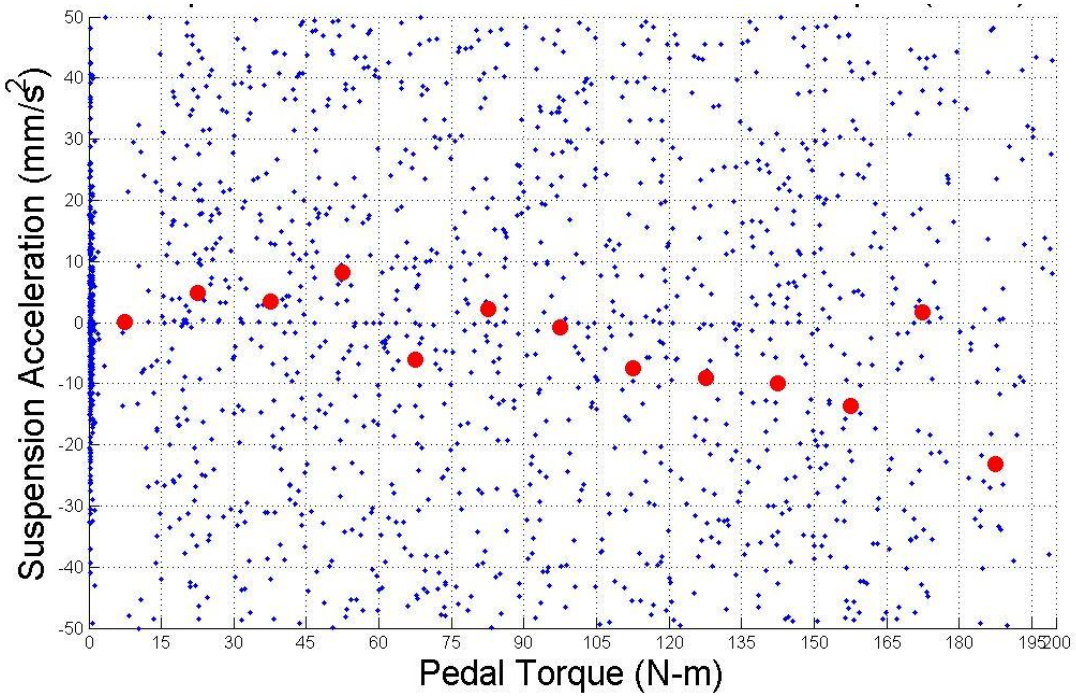

Figure F.26 - Suspension Acceleration vs. Pedaling Torque in Gear 5